

This dissertation has been
microfilmed exactly as received 69-2495

FAJEN, Fredric E., 1936-
ELECTRON IMPACT EXCITATION OF THE
HYDROGEN MOLECULE.

The University of Oklahoma, Ph.D., 1968
Physics, spectroscopy

University Microfilms, Inc., Ann Arbor, Michigan

THE UNIVERSITY OF OKLAHOMA

GRADUATE COLLEGE

ELECTRON IMPACT EXCITATION OF THE HYDROGEN MOLECULE

A DISSERTATION

SUBMITTED TO THE GRADUATE FACULTY

in partial fulfillment of the requirements for the

degree of

DOCTOR OF PHILOSOPHY

BY

FREDRIC E. FAJEN

Norman, Oklahoma

1968

ELECTRON IMPACT EXCITATION OF THE HYDROGEN MOLECULE

APPROVED BY

COH.

J. M. Confield

S. E. Babby, Jr.

Robert M. St. John

Arthur Bernhart

DISSERTATION COMMITTEE

ACKNOWLEDGEMENT

The author wishes to express his gratitude to Dr. Chun C. Lin for suggesting this problem, and for his encouragement, criticism, and advice throughout the course of this study. The financial and technical support provided by the Advanced Study Program of the Los Alamos Scientific Laboratory, is also gratefully acknowledged. The author wishes also to thank Dr. H. W. Hoerlin for his encouragement and substantial support of this work.

TABLE OF CONTENTS

	Page
LIST OF TABLES.....	v
LIST OF ILLUSTRATIONS.....	vi
Chapter	
I. Introduction.....	1
II. Wave Functions.....	5
III. Formulation of the Born Approximation.....	28
IV. Formulation of the Close Coupling Theory.....	41
V. Application of the Close Coupling Theory to Excitation of H_2	51
VI. Close Coupling with Vibration Included.....	80
VII. Conclusions.....	93
Bibliography.....	95
Appendix I Numerical Procedures.....	97
Appendix II Some Transition Probabilities and Born Cross Sections of Ne.....	107

LIST OF TABLES

Table	Page
1. Basis functions and configurations for the C state.....	7
2. Basis functions for the B and E states.....	16
3. Experimental and computed energy differences.....	25
4. Computed energies of the vibrational levels.....	26
5. Born cross sections for excitation to the various vibrational levels.....	39
6. Partial cross sections found by the close coupling approximation with $L = 5$	61
7. Partial cross sections found by the close coupling approximation with $L = 3$	62
8. Born partial cross sections.....	63
9. Some partial cross sections for the B and C states.....	64
10. Total cross sections for excitation to the B state.....	65
11. Some partial cross sections for the E state.....	67
12. Some partial cross sections for the C state.....	70
13. Total cross sections for excitation to the $n = 2$ electronic states.....	71
14. Results of the numerical experiment for an electron energy of 15 eV.....	76
15. Results of the numerical experiment for an electron energy of 25 eV.....	77
16. Results of the numerical experiment for an electron energy of 50 eV.....	78
17. Cross sections for excitation of the first four vibrational levels of the B state.....	84
18. Cross sections for excitation of the first four vibrational levels of the E state.....	86
19. Results of the close coupling calculation including some vibrational levels of the X, C, and E states.....	88
20. The cross sections for the first few vibrational levels of the B, C, and E states.....	92

LIST OF FIGURES

Figures	Page
1. Electronic energies for the B state.....	17
2. Electronic energies for the E state.....	19
3. Potential curve.....	22
4. $G_n(q)$ vs q for the C, B, and E states.....	35
5. Born cross sections for the C, B, and E states.....	36
6. Born cross section for the E state.....	37
7. Electronic energy level diagram.....	58
8. Total cross sections for the E state.....	72
9. Total cross sections for the C state.....	73
10. Total cross sections for the B state.....	74

ELECTRON IMPACT EXCITATION OF THE HYDROGEN MOLECULE

CHAPTER I

INTRODUCTION

Although considerable theoretical work has been done on electron impact excitation of atoms¹, comparatively little has been done in the area of electron excitation of molecules, owing primarily to the lack of accurate wave functions for the excited states of molecules, and to the added complication of the multi-center force field in which the electronic motion takes place.

The earliest work of this type was done in 1932 by Massey and Mohr², who applied the Born approximation to the excitation of the B $2p\sigma$ ${}^1\Sigma_u^+$ state of molecular hydrogen. They used two center variational wave functions for both the ground state and the B state. In 1941, Roscoe³ considered the excitation of the C $2p\pi$ ${}^1\Pi_u$, D $3p\pi$ ${}^1\Pi_u$, and E $2s\sigma$ ${}^1\Sigma_g^+$ states as well as the B state, also using the Born approximation. MacDonald's excited state wave functions were used, in which the inner electron is described by a $1s\sigma_g$ ${}^1F_2^+$ orbital, while the excited electron is considered to be in a hydrogenic (atomic) orbital centered about the molecular midpoint. Even with these relatively simple wave functions, approximations were used to evaluate the integrals.

More recently, Khare⁵ has calculated the cross sections for

excitation to the B and C states, using as wave functions the one-center expansions of Hyzina⁶ for both the ground state and the excited states. The use of these one center functions allows the Born integrals to be evaluated exactly.

All of the above calculations have been carried out for a single internuclear separation, relying on the Franck-Condon factors to give the probabilities for excitation to the different vibrational levels. Roscoe, however, expressed doubt about the validity of this procedure. The correct procedure is to evaluate the electronic scattering amplitude as a function of internuclear distance and then find the matrix elements of this quantity between the initial and final vibrational levels.

Although it is generally accepted that the Born approximation is correct at very high energies, it may be seriously in error in the low to medium energy range (threshold to about 100 eV), owing to its neglect of the distortion of the incoming wave, the effects of coupling between the various states of the target molecule, and the effects of exchange between the incoming electron and the molecular electrons. The close coupling approximation, even without exchange effects included, has been shown to give much better agreement with experiment in some cases of electron excitation of atoms⁷.

Recently, accurate two-center wave functions^{8,9,10} have become available for several of the excited states of the H₂ molecule. Also, with the computational speed and capacity of modern electronic computers, it is now possible to perform cross section calculations with accuracy and sophistication which is comparable to some of the more

recent work on electron-atom collisions. To this end, the "numerical machinery" has been developed to calculate cross sections by (a) the Born approximation, taking into account the variation of the scattering amplitude with internuclear separation, and (b) the close coupling approximation, including not only the initial state-final state coupling, but also the coupling between the different excited states.

During the progress of this work, a paper appeared by K. J. Miller and M. Krauss¹¹, in which Born approximation cross sections were presented for some of the H₂ excited states, including the B and C states. Variational two-center wave functions were employed, and full account was taken of the variation of the scattering amplitude with internuclear distance. Although the numerical results presented herein for the Born cross sections are not significantly different from those of Miller and Krauss, there is a slight difference in the conclusions which are drawn from these results. This difference is discussed in the text. The rather minor overlap between the work presented here and that published by Miller and Krauss does not detract from the value of this dissertation, since the major effort here is to show in what respects the close coupling results differ from the Born results, and to obtain cross sections which are valid in the medium energy range as well as at high energies.

In Chapter II, the electronic wave functions are discussed, and a method for finding the vibrational wave functions is presented. The Born approximation theory is formulated in Chapter III, and is applied to the excitation of the B, C, and E states. Chapter IV gives the formulation of the close coupling theory, Chapter V describes the application

of this theory to the electronic excitation of the H_2 molecule, and the extension of the theory to include vibrational effects is given in Chapter VI. The results are summarized qualitatively in Chapter VII.

Some of the numerical procedures are discussed in Appendix I. In addition to this work on electron excitation of H_2 , the excitation functions have been calculated for all transitions from the ground state of Ne to the $(2p)^5 3p$ configuration. The Born-Ochkur approximation was used, and intermediate coupling wave functions were used for the various states of the $(2p)^5 3p$ configuration. The results of these calculations are included as Appendix II.

CHAPTER II

WAVE FUNCTIONS

Electronic Wave Functions

For the ground state $X \ ^1\Sigma_g^+$, and for the excited state $C \ ^1\Pi_u$, the wave functions used were those calculated by E. R. Davidson.^a These wave functions are expressed in the form

$$\psi(1,2) = \sum_{K=1}^N C_K \varphi_K(1,2) \quad . \quad N \sim 50 \text{ for most cases. (1)}$$

Each $\varphi_K(1,2)$ is called a "configuration", and is composed of symmetrized products of one-electron functions called "basis functions". The coefficients C_K are determined by the solution of the secular equation which results from application of the linear variation method. The basis functions are defined by

$$f_i = (n_i j_i m_i \alpha_i \beta_i)$$

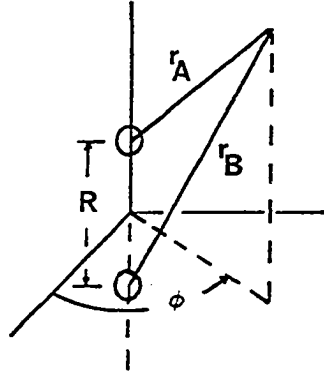
$$(n j m \alpha \beta) \equiv \left(\frac{2}{R} \right)^{3/2} \xi^{n_j} \eta^j \left[(\xi^2 - 1)(1 - \eta^2) \right]^{\frac{|m|}{2}} e^{-\alpha \xi + \beta \eta} \frac{e^{i m \varphi}}{\sqrt{2\pi}}, \quad (2)$$

where ξ , η , φ are the usual elliptic coordinates,

^a E. R. Davidson, Chemistry Dept., University of Washington, private communication. For a discussion of these wave functions, see S. Rothenberg and E. R. Davidson, *Natural Orbitals for Hydrogen Molecule Excited States*, J. Chem. Phys. 45, 2560 (1966). For a discussion of the E electronic state, see E. R. Davidson, J. Chem. Phys. 35, 1189 (1961). Also see Prof. Davidson's Ph. D. dissertation, which is published as Air Force Office of Scientific Research report no. AFOSR-485.

$$\xi = \frac{r_A + r_B}{R},$$

$$\eta = \frac{r_A - r_B}{R},$$



and R is the internuclear distance. Some relationships between spherical polar coordinates with the origin at the molecular midpoint and these elliptic coordinates are given here for future reference. If r, θ, φ are the spherical polar coordinates, one can write

$$r = \frac{R}{2} [\xi^2 + \eta^2 - 1]^{1/2},$$

$$r \sin \theta = \frac{R}{2} [(\xi^2 - 1)(1 - \eta^2)]^{1/2},$$

$$r \cos \theta = -\frac{R}{2} \xi \eta, \text{ and}$$

$$r^2 \sin \theta dr d\theta d\varphi = \left(\frac{R}{2}\right)^3 (\xi^2 - \eta^2) d\xi d\eta d\varphi.$$

(3)

The first few basis functions used by Davidson for the $C^1\Pi_u$ state at $R = 1.0$ are given in Table 1. The "configurations" are defined by a pair of integers specifying the basis functions to be used.

$$(i j) \equiv \frac{1}{2} [f_i(1)f_j(2) + f_j(1)f_i(2)].$$

The first few configurations for the C state at $R = 1.0a_0$ are also given in Table 1.

Table 1. Basis functions and configurations for the C state. The basis function $(n_j m_j \alpha \beta)$ is defined as $(2/R)^{3/2} \xi^{n_i} \eta^{j_i} \left[(\xi^2 - 1 (1 - \eta^2)) \right]^{m_i} e^{-\alpha \xi + \beta \eta} \frac{e^{i m \phi}}{\sqrt{2\pi}}$. The configurations are $\xi_k = f_i(1) f_j(2) + f_j(1) f_i(2)$.

The first few basis functions for the $C^1\Pi_u$ state at $R = 1.0a_0$						The first few configurations for the $C^1\Pi_u$ state at $R = 1.0a_0$		
i	n_i	j_i	m_i	α_i	β_i	k	i	j
1	0	0	0	.8	0	1	1	7
2	1	0	0	.8	0	2	1	8
3	0	2	0	.8	0	3	1	9
4	2	0	0	.8	0	4	1	10
5	3	0	0	.8	0	5	1	11
6	1	2	0	.8	0	6	1	12
7	0	0	1	.25	0	7	2	7
8	1	0	1	.25	0	8	2	8
9	2	0	1	.25	0	9	2	9
10	0	2	1	.25	0	10	2	10
11	3	0	1	.25	0	11	2	11
12	1	2	1	.25	0	12	2	12

These wave functions, in the form (1), give quite accurate energies, and are thought to be very accurate wave functions, but they are somewhat awkward to use for the calculation of interaction potential matrix elements or Born scattering amplitudes. However, we can obtain a considerable simplification in form and at the same time retain sufficient accuracy by making use of the "natural orbital expansion"⁹ of (1). The wave functions in the above form consist of sums of products of one electron functions. They can therefore be put in the form

$$\Psi(1,2) = \sum_{i,j} \bar{f}_i(1) C_{ij} \bar{f}_j(2) \quad , \quad (4)$$

where, for singlet states, $C_{ij} = C_{ji}$.

The matrix C is a real, symmetric matrix, and it can therefore be diagonalized. In order for this diagonalization to be carried out in the usual way, however, we must first express (4) in terms of a set of orthonormal basis functions. This is accomplished by the following transformation:

$$\xi_1 = f_1 / [(f_1, f_1)]^{1/2} \quad ,$$

$$\xi_2 = [f_2 - (f_2, \xi_1)\xi_1] / [(f_2, f_2) - (f_2, \xi_1)^2]^{1/2} \quad ,$$

$$\xi_3 = [f_3 - (f_3, \xi_1)\xi_1 - (f_3, \xi_2)\xi_2] / [(f_3, f_3) - (f_3, \xi_2)^2 - (f_3, \xi_1)^2]^{1/2} \quad ,$$

etc.

$$\xi_i = \sum_j G_{ij} f_j \quad ,$$

$$(g_\ell, g_m) = \delta_{\ell,m} \quad . \quad (5)$$

This gives

$$\Psi(1,2) = \sum_{\ell,m} g_\ell(1) D_{\ell m} g_m(2) \quad ,$$

$$\text{where } D = G^{-1} C \tilde{G}^{-1} \quad . \quad (6)$$

The matrix D is then diagonalized in the usual way, i.e., a matrix S is found such that

$$(S^{-1} D S)_{ij} = a_i \delta_{ij} \quad .$$

$$\text{The functions } y_m = \sum_j S_{jm} g_j = \sum_{i,j} G_{ij} S_{jm} f_i \quad ,$$

are then the so-called "natural orbitals", which give the most rapidly convergent expansion of Ψ ,

$$\Psi(1,2) = \sum_i a_i y_i(1) y_i(2) \quad ,$$

$$\sum_i a_i^2 = 1 \quad .$$

The product $y_i(1) y_i(2)$ is called a "natural configuration", and the coefficient a_i is its "weight".

For the ground state ($X^{-1} \Sigma_g^+$), it is sufficient to keep only the first natural configuration, since its weight exceeds .99 for all values of R considered. If the first natural orbital is called u_0 , then the wave function can be written

$$\psi_x(1,2) \approx u_0(1) u_0(2) .$$

u_0 is a $1s\sigma_g$ type orbital, having the form $f_0(\xi, \eta) \cdot \frac{1}{\sqrt{2\pi}}$,

where $f_0(\xi, -\eta) = f_0(\xi, \eta)$.

For the $C \ ^1\Pi_u$ state, there are two natural configurations which occur with non-negligible weights, so that

$$\psi_c(1,2) \approx a_1 y_1(1) y_1(2) + a_2 y_2(1) y_2(2) .$$

In every case (i.e., each value of R), there is a u_c and a v_c such that

$$y_1 = (u_c + v_c) / \sqrt{2} , \text{ and}$$

$$y_2 = (u_c - v_c) / \sqrt{2} .$$

Also, in every case, $a_2 = -a_1$. Thus,

$$\begin{aligned} \psi_c(1,2) &\approx a_1 \left\{ \frac{1}{2} \left[u_c(1) + v_c(1) \right] \left[u_c(2) + v_c(2) \right] \right. \\ &\quad \left. - \frac{1}{2} \left[u_c(1) - v_c(1) \right] \left[u_c(2) - v_c(2) \right] \right\} \\ &= a_1 \left\{ u_c(1)v_c(2) + v_c(1)u_c(2) \right\} , \\ a_1^2 &\approx 1/2 . \end{aligned}$$

u_c is a $1s\sigma_g$ type orbital, very similar to the u_0 described above. v_c is a $2p\pi_u$ type orbital, having the form

$$v_c = f_c(\xi, \eta) \frac{e^{i\phi}}{\sqrt{2\pi}}, \quad f_c(\xi, -\eta) = f_c(\xi, \eta) \quad .$$

Clearly $(v_c, u_c) = 0$, and

$$(v_c, u_0) = 0 \quad .$$

For the B ${}^1\Sigma_u^+$ and E ${}^1\Sigma_g^+$ states, the functions which were furnished to us by Prof. Davidson were not tabulated over the range of R values desired. However, Prof. Davidson, in his Ph.D. dissertation^a, develops all the necessary equations for the calculation of the matrix elements of the Hamiltonian, so that it was possible to do the variational calculation and obtain the wave functions for the above states without too much difficulty.

The electronic Hamiltonian is, in atomic units,

$$H = -\frac{1}{2} \nabla_1^2 - \left(\frac{1}{r_A} + \frac{1}{r_B}\right)_1 - \frac{1}{2} \nabla_2^2 - \left(\frac{1}{r_A} + \frac{1}{r_B}\right)_2 + \frac{1}{r_{12}} \quad .$$

Expressed in elliptic coordinates,

$$\nabla^2 = \frac{4}{R^2(\xi^2 - \eta^2)} \left[\frac{\partial}{\partial \xi} (\xi^2 - 1) \frac{\partial}{\partial \xi} + \frac{\partial}{\partial \eta} (1 - \eta^2) \frac{\partial}{\partial \eta} \right] \\ + \frac{1}{R^2(\xi^2 - 1)(1 - \eta^2)} \frac{\partial^2}{\partial \phi^2} \quad ,$$

$$\frac{1}{r_A} + \frac{1}{r_B} = \frac{4\xi}{R(\xi^2 - \eta^2)} \quad , \text{ and}$$

$$\frac{1}{r_{12}} = \frac{4}{R} \sum_{\ell=0}^{\infty} \sum_{m=-\ell}^{\ell} (-1)^m \frac{(\ell-|m|)!}{(\ell+|m|)!} P_{\ell}^{|m|}(\xi_{<}) Q_{\ell}^{|m|}(\xi_{>})$$

$$P_{\ell}^{|m|}(\eta_1) P_{\ell}^{|m|}(\eta_2) e^{im(\varphi_1 - \varphi_2)} .$$

where $P_{\ell}^{|m|}$ is a Legendre function of the first kind, $Q_{\ell}^{|m|}$ is a Legendre function of the second kind, and $P_{\ell}^{|m|}$ is a Legendre function of the first kind, normalized on the interval $(-1,1)$.

Since the interest here is for Σ states only, we will use σ - type basis functions, defined by

$$(nj\alpha) \equiv \left(\frac{2}{R}\right)^{3/2} \xi^{-n} \eta^j e^{-\alpha\xi} \frac{1}{\sqrt{2\pi}} .$$

The quantities needed for the construction of the energy matrix are the overlap integrals,

$$(n'j'\alpha' | nj\alpha) = \left[\frac{2}{j'+j+1} G_{n'+n+2}(\alpha'+\alpha) - \frac{2}{j'+j+3} G_{n'+n}(\alpha'+\alpha) \right] \delta(j'+j, \text{even}) ,$$

where

$$G_n(\alpha) \equiv \int_1^{\infty} \xi^n e^{-\alpha\xi} d\xi , \text{ and}$$

$$\delta(j'+j, \text{even}) = \begin{cases} 0 & \text{if } j'+j \text{ is odd,} \\ 1 & \text{if } j'+j \text{ is even} \end{cases} ,$$

the kinetic energy integrals,

$$\begin{aligned}
& (n'j'\alpha' | -\frac{1}{2} \nabla^2 | n j \alpha) \\
&= -\frac{2}{R^2} \left\{ \frac{2}{j+j'+1} \left[\alpha^2 G_{n'+n+2}(\alpha'+\alpha) - (2n+2)\alpha G_{n'+n+1}(\alpha'+\alpha) \right. \right. \\
&\quad + \left. \left. \left\{ n(n+1) - j(j+1) - \alpha^2 \right\} G_{n'+n}(\alpha'+\alpha) + 2n\alpha G_{n'+n-1}(\alpha'+\alpha) \right. \right. \\
&\quad \left. \left. - n(n-1)G_{n'+n+2}(\alpha'+\alpha) \right] \right. \\
&\quad \left. + \frac{2}{j'+j-1} j(j-1)G_{n'+n}(\alpha'+\alpha) \right\} \delta(j'+j, \text{even}) \quad ,
\end{aligned}$$

the nuclear attraction integrals,

$$\begin{aligned}
& (n'j'\alpha' | -\frac{1}{r_A} - \frac{1}{r_B} | n j \alpha) \\
&= -\frac{4}{R} G_{n'+n+1}(\alpha'+\alpha) \frac{2}{j+j'+1} \delta(j'+j, \text{even}) \quad ,
\end{aligned}$$

and the electron repulsion integrals, which take the form

$$\begin{aligned}
(NJ\alpha; \bar{N}\bar{J}\bar{\alpha}) &\equiv \int_1^\infty d\xi_1 \int_{-1}^1 d\eta_1 (\xi_1^2 - \eta_1^2) \xi_1^{\bar{N}} \eta_1^{\bar{J}} e^{-\alpha\xi_1} \\
&\quad \int_1^\infty d\xi_2 \int_{-1}^1 d\eta_2 (\xi_2^2 - \eta_2^2) \xi_2^{\bar{N}} \eta_2^{\bar{J}} e^{-\alpha\xi_2} \\
&\quad \frac{1}{2\pi} \int_0^{2\pi} d\varphi_1 \frac{1}{2\pi} \int_0^{2\pi} d\varphi_2 \left(\frac{1}{r_{12}} \right) \quad , \\
(NJ\alpha; \bar{N}\bar{J}\bar{\alpha}) &= \frac{4}{R} \sum_{l=0}^{\infty} I_l(NJ\alpha, \bar{N}\bar{J}\bar{\alpha}) \quad ,
\end{aligned}$$

$$I_{\ell}(\overline{NJ\alpha}, \overline{N\bar{J}\bar{\alpha}}) = \varepsilon_{\ell, J} \varepsilon_{\ell, \bar{J}} f_{\ell, N+2, \bar{N}+2, \alpha, \bar{\alpha}}^{-\varepsilon_{\ell, J+2} \varepsilon_{\ell, \bar{J}}} f_{\ell, N, \bar{N}+2, \alpha, \bar{\alpha}}$$

$$-\varepsilon_{\ell, J} \varepsilon_{\ell, \bar{J}+2} f_{\ell, N+2, \bar{N}, \alpha, \bar{\alpha}} + \varepsilon_{\ell, J+2} \varepsilon_{\ell, \bar{J}} f_{\ell, N, \bar{N}, \alpha, \bar{\alpha}} \quad ,$$

$$\varepsilon_{\ell, J} = \int_{-1}^1 d\eta \left\{ \eta^J P_{\ell}(\eta) \right\} \quad ,$$

$$f_{\ell, n, n', \alpha, \alpha'} = \int_0^1 \frac{du}{(1-u^2) [P_{\ell}(\frac{1}{u})]^2} h_{n, \alpha}^{\ell}(\frac{1}{u}) h_{n', \alpha'}^{\ell}(\frac{1}{u}) \quad ,$$

and

$$h_{n, \alpha}^{\ell}(\xi) = \int_1^{\xi} dz \left\{ z^n e^{-\alpha z} P_{\ell}(z) \right\} \quad .$$

The infinite sum indicated above reduces to a finite sum, since

$\varepsilon_{\ell, J} = 0$ for $\ell > J$. All of the above integrals can be done analytically, except for the integral

$$f_{\ell, n, n', \alpha, \alpha'} = \int_0^1 \frac{du}{(1-u^2) [P_{\ell}(\frac{1}{u})]^2} h_{n, \alpha}^{\ell}(\frac{1}{u}) h_{n', \alpha'}^{\ell}(\frac{1}{u}) \quad ,$$

which must be done numerically. Thus, all the quantities involved in the construction of the energy matrix are easily calculated on the computer.

Since the aim here is to get the variational wave function in the form

$$\psi(1,2) = \sum_{i,j} f_i(1) C_{ij} f_j(2) \quad ,$$

this form was chosen as the starting point, with the C_{ij} 's as the variational parameters.

Since the interest here is in excited states with one electron in a $1s\sigma_g$ orbital and the other in an excited orbital, the set of basis functions was divided into two subsets, the first subset consisting of basis functions appropriate for a $1s\sigma_g$ orbital, the second consisting of functions appropriate for the excited orbital. The variational parameters C_{ij} were allowed to be non-zero only if the indices i and j belong to different subsets. The condition $C_{ij} = C_{ji}$ further reduces the number of independent parameters, so that, for example, for the B state, where eight basis functions were used (C was therefore an 8×8 matrix), there were only 16 independent parameters.

The basis functions used at $R = 2.0 a_0$ are given in Table 2. These same basis functions were also used for other values of R , with the values of α scaled by the factor $R/2$.

Results for the B State

This variational calculation was carried out for the B state at six values of R from $R = 1.0$ to $R = 2.0$. Since this state is the lowest in energy of the symmetry ${}^1\Sigma_u^+$, the desired wave function is the one corresponding to the first root of the secular equation. In Figure 1, the energies obtained by this procedure are compared to the results obtained by Kolos and Wolniewicz¹⁰, which are the best theoretical energies presently available for this state.

As stated above, the solution of the secular equation yields directly the elements of the matrix C. From this matrix, the natural orbitals are found in exactly the same manner as for the ground state and the C state. Just as in the case of the C state, there are two natural configurations with non-negligible weights, and the same

Table 2. Basis functions for the $B^1\Sigma_u^+$ state and the $E^1\Sigma_g^+$ state. The basis function $(n_j\alpha)$ is defined as $(2/R)^{3/2}\xi^n\eta^j e^{-\alpha R}$.

B State				E State			
i	n_i	j_i	α_i	i	n_i	j_i	α_i
1	0	0	1	1	0	0	1.1
2	1	0	1	2	1	0	1.1
3	2	0	1	3	2	0	1.1
4	0	2	1	4	0	2	1.1
5	0	1	.5	5	0	0	.4
6	1	1	.5	6	1	0	.4
7	2	1	.5	7	2	0	.4
8	0	3	.5	8	0	2	.4

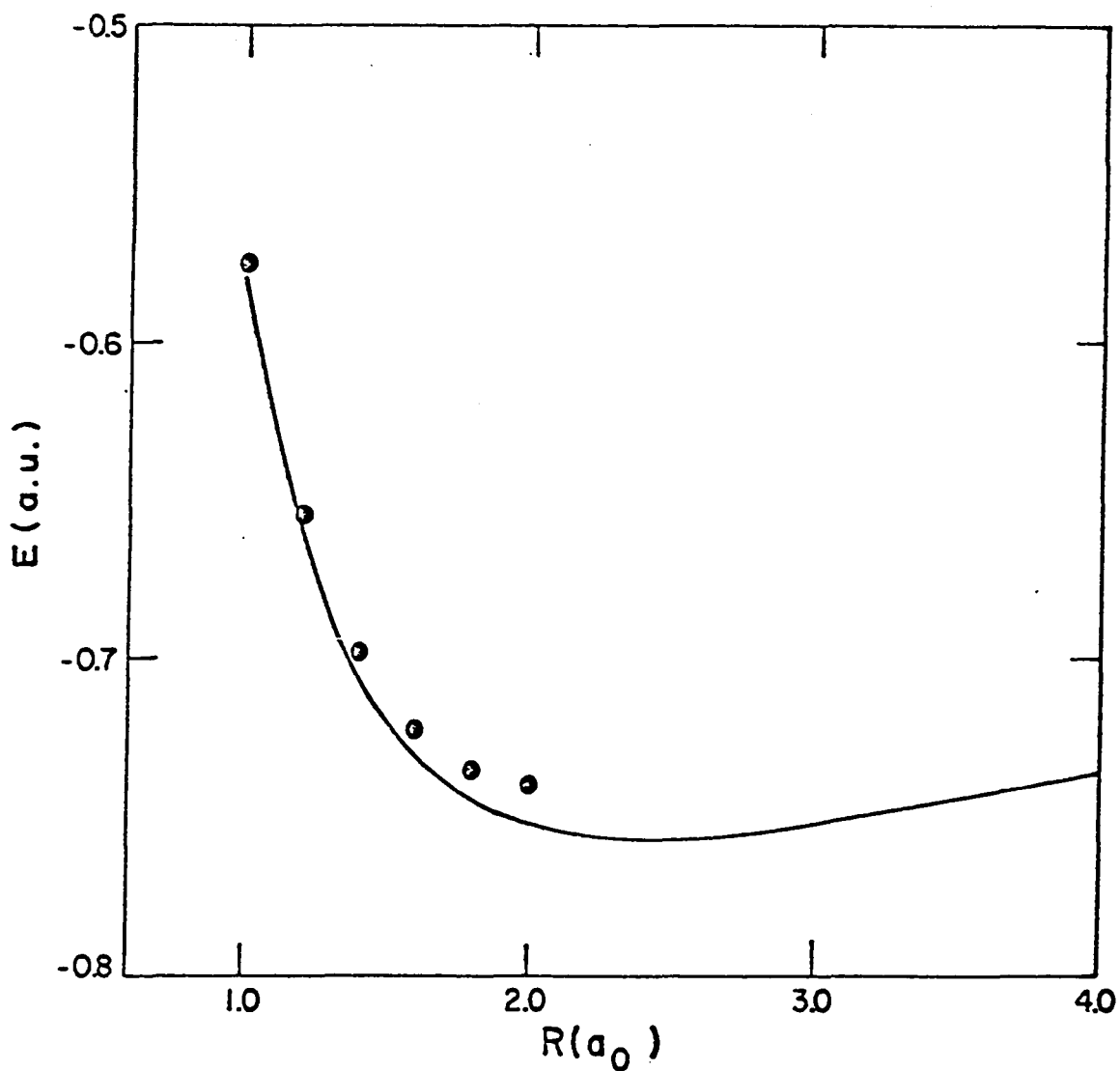


Figure 1. Electronic energies for the B state. The solid curve is the potential obtained by Kolos and Wolniewicz. The points represent the present results.

discussion applies, so that

$$\psi_B(1,2) \approx a_1 y_1(1) y_1(2) + a_2 y_2(1) y_2(2) \quad ,$$

$$y_1 = (u_B + v_B) / \sqrt{2} \quad ,$$

$$y_2 = (u_B - v_B) / \sqrt{2} \quad ,$$

$$\psi_B(1,2) \approx \frac{1}{\sqrt{2}} [u_B(1)v_B(2) + v_B(1)u_B(2)] \quad .$$

where u_B is a $1s\sigma_g$ type orbital and v_B is a $2p\sigma_u$ type orbital. In terms of the elliptic coordinates, we can write

$$v_B = f_B(\xi, \eta) \frac{1}{\sqrt{2\pi}} \quad ,$$

$$f_B(\xi, -\eta) = -f_B(\xi, \eta) \quad .$$

Results for the E State

This calculation was done for the same six values of R as in the case of the B state. Since this state is the second lowest in energy of its symmetry (the lowest being the ground state), the desired wave function is the one corresponding to the second root of the secular equation. In Figure 2 are shown the results of this calculation, along with those of Davidson^a. In doing the natural orbital analysis, we again find two natural configurations with substantial weights, so that

$$\psi_E(1,2) \approx a_1 y_1(1) y_1(2) + a_2 y_2(1) y_2(2) \quad .$$

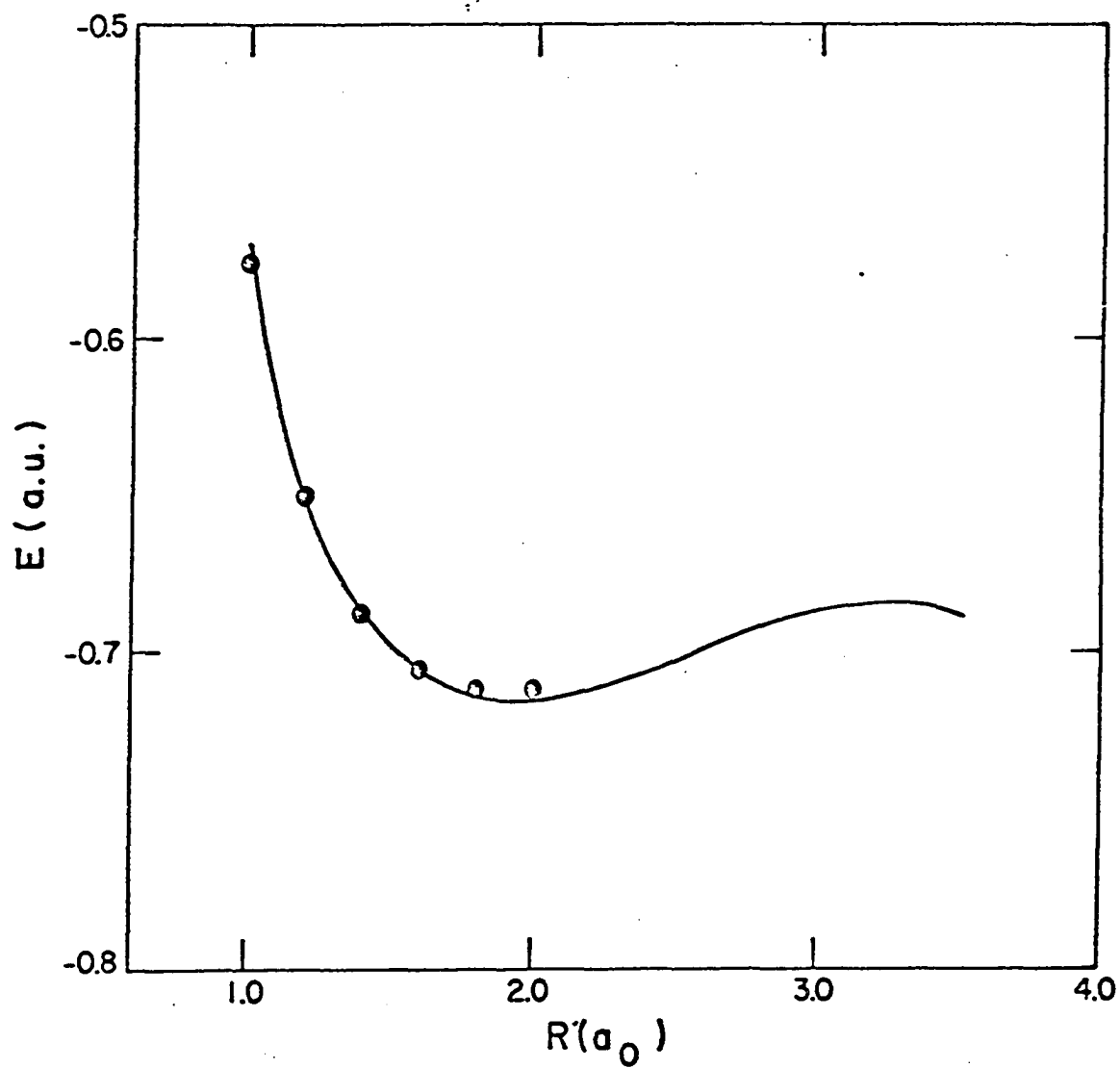


Figure 2. Electronic energies for the E state. The solid curve is the potential obtained by Davidson. The points represent the present results.

This case differs from preceding ones, however, in that $a_2 \neq -a_1$. The transformation to the u, v form is accomplished as follows

$$u_E = (b_1^{1/2} y_1 + b_2^{1/2} y_2) / (b_1 + b_2)^{1/2} ,$$

$$v_E = (b_1^{1/2} y_1 - b_2^{1/2} y_2) / (b_1 + b_2)^{1/2} ,$$

where $b_1 = |a_1| / (a_1^2 + a_2^2)^{1/2}$, and

$$b_2 = |a_2| / (a_1^2 + a_2^2)^{1/2} .$$

u_E is a $1s\sigma_g$ type orbital, and v_E a $2s\sigma_g$ orbital. u_E and v_E are normalized, but not quite orthogonal. Furthermore, v_E is not necessarily orthogonal to the ground state $1s\sigma_g$ orbital, although the overlap is small ($\sim .02$). Since it is necessary to have orthogonality between the electronic wave functions in the development of the scattering theory, we explicitly orthogonalize v_E to the ground state orbital u_0 :

$$v_E' = [v_E - (v_E, u_0)u_0] / [1 - (v_E, u_0)^2]^{1/2} .$$

The wave function for the E state is then approximated by

$$v_E(1,2) \approx \frac{1}{\sqrt{2}} [u_E(1)v_E'(2) + v_E'(1)u_E(2)] .$$

Vibrational Wave Functions

The vibrational wave functions used for this work were obtained from an approximate numerical solution of the wave equation. For the ground state, the B state and the C state, the theoretical potential curves obtained by Kolos and Wolniewicz¹⁰ were used. For the E state,

Davidson's theoretical potential curve was used.

The wave equation for the vibrational motion is

$$\left\{ -\frac{1}{2\mu} \frac{d^2}{dR^2} + \frac{1}{2\mu R^2} [J(J+1) - \Lambda^2] + V_n(R) \right\} \chi_{nv}(R) \\ = E_{nv} \chi_{nv}(R) \quad ,$$

where $\chi_{nv}(R) = R\varphi_n(v|R)$,

and where n labels the electronic state, v the vibrational state, and J the rotational state. Λ is the component of electronic angular momentum along the internuclear axis, μ is the reduced nuclear mass, and R is the internuclear separation.

Neglecting the rotational energy contribution, which is known to be quite small compared to the spacing between vibrational levels, we have the following differential equation which must be satisfied by the $\chi_{nv}(R)$.

$$\chi_{nv}'' - 2\mu [V_n(R) - E_{nv}] \chi_{nv} = 0 \quad .$$

The potential function $V_n(R)$ has the shape indicated schematically by the solid curve in Figure 4. For the integration of the above differential equation, $V_n(R)$ is replaced by the function $U_n(R)$, defined as follows:

$$U_n(R) = \begin{cases} V_n(R_1) & R < R_1 \quad , \\ V_n(R) & R_1 \leq R \leq R_2 \quad , \\ V_n(R_2) & R_2 < R \quad . \end{cases}$$

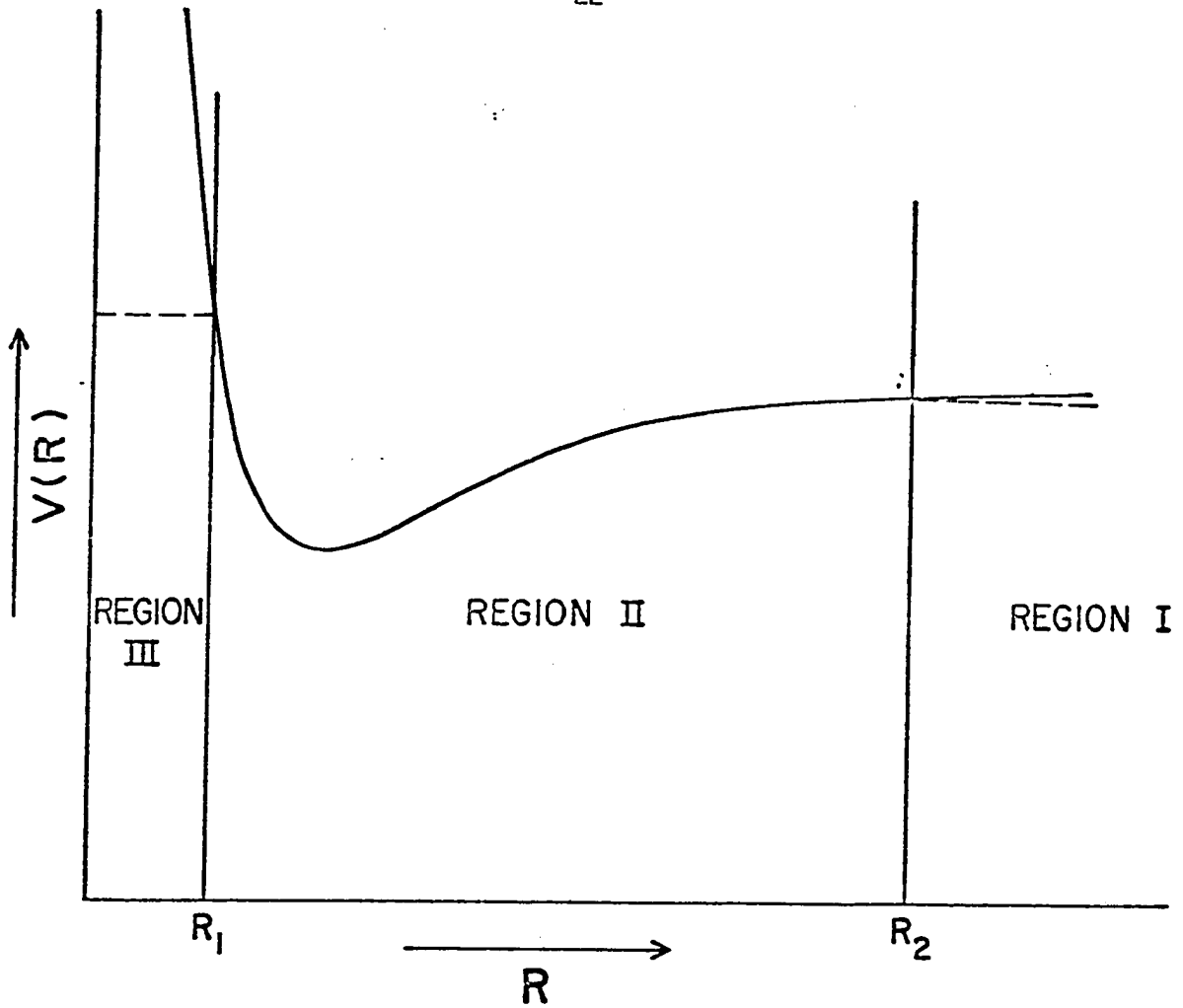


Figure 3. A typical potential curve. The solid curve illustrates the usual shape of $V(R)$. $U(R)$ is given by the dashed lines, where it differs from $V(R)$.

The shape of $U_n(R)$, where it differs from $V_n(R)$, is indicated by the broken lines in Figure 3. The difference between $U_n(R)$ and $V_n(R)$ is significant only in region III, but here, the wave functions will be vanishingly small anyway, especially for the first few vibrational levels. To a good approximation, then, the solutions to

$$\chi'' - 2\mu [U(R) - E] \chi = 0 \quad ,$$

are the required vibrational functions.

In region I (i.e., $R > R_2$), and in region III ($R < R_1$), the differential equation takes the form

$$\chi'' - \alpha^2 \chi = 0 \quad ,$$

and has solutions

$$\chi = Ae^{-\alpha R} + Be^{\alpha R} \quad ,$$

where $\alpha_I = [2\mu(V_n(R_2) - E)]^{1/2} \quad ,$

and $\alpha_{III} = [2\mu(V_n(R_1) - E)]^{1/2} \quad .$

The numerical integration is begun in region I, where we know $\chi = \exp(-\alpha_I R)$. Using the Numerov^b difference scheme, the integration

^b For an equation of the type $y'' = g(x)y$, the Numerov method gives y_{n+1} in terms of y_n and y_{n-1} by the equation

$$y_{n+1} = \frac{[2 + \frac{5}{6}(\delta x)^2 g(x_n)]y_n - [1 - \frac{1}{12}(\delta x)^2 g(x_{n-1})]y_{n-1}}{1 - \frac{1}{12}(\delta x)^2 g(x_{n+1})} \quad ,$$

where $y = y(x_n)$ and the $\{x_n\}$ are a set of equally spaced values of x .

$$\delta x = x_{n+1} - x_n \quad .$$

is carried to the left, through region II and into region III. In region III, the form of the solution is known to be

$$\chi_{\text{III}} = A e^{-\alpha_{\text{III}} R} + B e^{\alpha_{\text{III}} R},$$

and A and B can be determined by matching to the numerical solution at two points. An acceptable solution must have $A = 0$, so that $\chi \rightarrow 0$ as $R \rightarrow -\infty$. Thus we have the condition

$$A(E) = 0.$$

The values of E which cause A to be zero are the required eigenvalues, and the corresponding solutions, after being properly normalized, are the functions χ_{IV} . The roots of A(E) are approximately located by integrating for a large range of values of E, noting where A changes sign. They are then found more precisely by a simple iterative procedure.

In Table 3 the computed energy differences $\Delta E(v + 1/2) = E_{v+1} - E_v$ for the first few vibrational levels of the ground electronic state are compared with the experimental values. The agreement is seen to be satisfactory.

Table 4 gives the computed energies for the first few vibrational levels of each of the electronic states considered. The energies are in a.u. (1 a.u. = 27.21 eV), and the energy -1.0 is that corresponding to two separated H atoms in the ground state.

To a good approximation, the function $\varphi_0(o|R)$ may be expanded in terms of the wave functions of the bound vibrational states of the excited electronic state n. That is,

Table 3. Experimental values vs. computed values of $\Delta E (v + \frac{1}{2})$ for the ground electronic state.

v	Experimental	Computed
0	4161 cm^{-1}	4163
1	3926	3926
2	3695	3698
3	3468	3470
4	3241	3242
5	3014	3016

Table 4. Computed energies (a.u) for the first few vibrational levels of each electronic state.

v	ground state	C state	B state	E state
0	-1.16454	-.71283	-.75354	-.71051
1	-1.14557	-.70230	-.74752	-.69960
2	-1.12767	-.69239	-.74167	-.69800
3	-1.11083	-.68307	-.73597	-.69296
4	-1.09502	-.67435	-.73043	-.68954
5	-1.08025	-.66621	-.72504	-.68809
6	-1.06651	-.65866	-.71980	-.68390

$$\varphi_0(o|R) \approx \sum_{v=0}^N A_v \varphi_n(v|R) \quad ,$$

where

$$A_v = \int R^2 dR \varphi_0(o|R) \varphi_n^*(v|R) \quad ,$$

and $N + 1$ is the number of bound vibrational levels. For example, if we take n as the C state, we find

$$\sum_{v=0}^N A_v^2 = .98 \quad ,$$

while if we take n as the B state, the result is even closer to 1.0. This being the case, it is also possible to express the overlap integral $(oo|nv)$ as

$$\begin{aligned} (oo|nv) &= \int R^2 dR \varphi_0(o|R) \varphi_n^*(v|R) \\ &= \sum_{v'=0}^{N'} (oo|n'v') (n'v'|nv) \quad . \end{aligned}$$

For example, the values of the overlap integrals of $\varphi_0(o|R)$ with the $v=0$ and $v=5$ vibrational functions of the C state are .350 and -.275, respectively, as found by direct numerical integration. The values for these quantities obtained by expanding in terms of the B state vibrational functions are .350 and -.274.

CHAPTER III

FORMULATION OF THE BORN APPROXIMATION

In an inelastic collision of an electron with a diatomic molecule, there may be a transfer of translational energy of the colliding electron to electronic excitation, vibrational excitation, or rotational excitation of the molecule, or any combination of these. Following Craggs and Massey,¹² one may characterize the initial state of the molecule by the set of quantum numbers $n v J M$, where n labels the electronic state, v the vibrational state, and $J M$ the rotational state. The wave function for this state may be written to a good approximation

$$\Psi_{nvJM} = \psi(n|\vec{r}, R) \varphi_n(v|R) \chi(JM|\Theta, \bar{\varphi}) \quad , \quad (7)$$

where \vec{r} represents the electronic coordinates relative to the nuclei, R the internuclear distance and $\Theta, \bar{\varphi}$ are the polar angles describing the orientation of the internuclear axis.

According to the Born approximation, the differential cross section for exciting the molecule from the ground electronic and vibrational state, which we shall label $0 0 J M$ to the state $n v J' M'$ is:¹²

$$\frac{I_{nvJ'M'}}{I_{00JM}} d\omega = \epsilon_n \left| \int \varphi_0(0|R) \varphi_n^*(v|R) \chi(JM|R) \chi^*(J'M'|R) \right. \quad (8)$$

$$\left. M_{on}(q, R, \hat{R}) R^2 dR d\hat{R} \right|^2 d\omega \quad ,$$

where

$$M_{\text{on}}(q, R, \hat{R}) = 2 \left(\frac{k'}{k} \right)^{1/2} \frac{1}{q^2} \epsilon_{\text{on}}(q, R, \hat{R}) ,$$

$$\epsilon_{\text{on}}(q, R, \hat{R}) = \int \psi(o|\vec{r}, R) \sum_{i=1}^2 e^{i\vec{q} \cdot \vec{r}_i} \psi^*(n|\vec{r}, R) d^3r_1 d^3r_2 .$$

Here k is the initial momentum of the colliding electron, k' the final momentum, q the momentum change, \hat{R} the unit vector in the direction Θ , \bar{g} , and g_n the electronic degeneracy of the final state.

In experimental situations, one is normally interested in the cross section summed over the final rotational states. Since the energy differences between the final rotational states are always small compared to the electronic and vibrational energy differences, $M_{\text{on}}(q, R, \hat{R})$ is to a very good approximation independent of $J'M'$. The summed cross section

$$I_{\text{ooJM}}^{\text{nv}} \equiv \sum_{J'M'} I_{\text{ooJM}}^{\text{nv } J'M'} ,$$

then takes the form

$$\begin{aligned} & \sum_{J'M'} \left| \int G(\hat{R}) \chi^*(J'M'|\hat{R}) d\hat{R} \right|^2 \\ &= \sum_{J'M'} \int d\hat{R} \int d\hat{R}' G(\hat{R}) G^*(\hat{R}') \chi^*(J'M'|\hat{R}) \chi(J'M'|\hat{R}') \\ &= \int d\hat{R} \int d\hat{R}' G(\hat{R}) G^*(\hat{R}') \delta(\hat{R}-\hat{R}') = \int d\hat{R} |G(\hat{R})|^2 . \end{aligned}$$

Thus, we have for the summed cross section

$$I_{\infty JM}^{nv} = \xi_n \int d\hat{R} \left| \int R^2 dR \varphi_0(o|R) \varphi_n^*(v|R) M_{on}(q, R, \hat{R}) \chi(JM|\hat{R}) \right|^2 .$$

In the above expression, $\chi(JM|\hat{R})$ is the rotational wave function for the molecule in its ground electronic state, which, in the case of H_2 is a Σ state ($\Lambda = 0$). Thus, $\chi(JM|\hat{R})$ is just the spherical harmonic $Y_{JM}(\hat{R})$. Noting that

$$\sum_M \left| Y_{JM}(\hat{R}) \right|^2 = \frac{2J+1}{4\pi} ,$$

we have the result that the cross section $I_{\infty JM}^{nv}$ averaged over the initial magnetic substates, is

$$\begin{aligned} I_{\infty}^{nv} &= \frac{1}{2J+1} \sum_M I_{\infty JM}^{nv} \\ &= \frac{1}{4\pi} \xi_n \int d\hat{R} \left| \int R^2 dR \varphi_0(o|R) \varphi_n(v|R) M_{on}(q, R, \hat{R}) \right|^2 . \end{aligned} \quad (9)$$

The interpretation of equation (9) is as follows: For the purpose of computing the cross section summed over all final rotational states, we can ignore the rotational states completely, computing the cross section for each orientation of the molecule, and then average over all orientations. Or, equivalently, we can treat the molecule as having a fixed orientation in space and carry out an average over all possible directions of incidence of the colliding electron.

A further simplification can be made if we note that $M_{on}(q, R, \hat{R})$ depends on R only to the extent that the electronic wave functions

depend on R , and this dependence is known to be rather small in most cases. On the other hand, the product $\varphi_0(o|R)\varphi_n^*(v|R)$ has a strong maximum at R_0 , the equilibrium separation in the ground electronic state. It should therefore be a fairly good approximation to replace equation (9) by

$$I_{00}^{nv} = \xi_n \frac{1}{4\pi} \int d\hat{R} \left| M_{on}(q, R_0, \hat{R}) \right|^2 \times \left| \int R^2 dR \varphi_0(o, R) \varphi_n^*(v|R) \right|^2 . \quad (10)$$

Furthermore, if the energy differences of the vibrational states are small compared to the final energy of the colliding electron, so that k' is effectively independent of v , we have the result that the relative probabilities of exciting the different vibrational states within a given electronic state are given by the squares of the appropriate overlap integrals. That is, for a given n ,

$$I_{00}^{nv} \propto \left| \int R^2 dR \varphi_0(o|R) \varphi_n^*(v|R) \right|^2 .$$

The above constitutes the mathematical formulation of the Franck-Condon principle in excitation, and the squares of the overlap integrals are commonly known as the Franck-Condon factors. The validity of the Franck-Condon principle, as expressed above, depends upon $M_{on}(q, R, R)$ being essentially constant over the region where the product $\varphi_0(o|R)\varphi_n^*(v|R)$ has appreciable amplitude.

Within the framework of the Born approximation and the Franck-Condon principle, we obtain the relatively simple expression

$$\begin{aligned}
I_0^n &= \sum_{\mathbf{v}} I_{00}^{nv} \\
&= \sum_{\mathbf{v}} \left| \int R^2 dR \varphi_0(\mathbf{o}|R) \varphi_n^*(\mathbf{v}|R) \right|^2 \cdot \varepsilon_n \frac{1}{4\pi} \int d\hat{R} \left| M_{on}(\mathbf{q}, R_0, \hat{R}) \right|^2 \\
&\approx \varepsilon_n \frac{1}{4\pi} \int d\hat{R} \left| M_{on}(\mathbf{q}, R_0, \hat{R}) \right|^2, \quad (11)
\end{aligned}$$

for the total differential cross section for excitation to the electronic state n . Thus, we find that, for the calculation of the differential cross section summed over all possible states of nuclear motion in the final electronic state, we simply treat the nuclei as fixed in space, but then average the cross section over all possible directions of incidence of the colliding electron.

From equations (8) and (11), we have

$$I_0^n(\mathbf{q}) = \varepsilon_n \frac{1}{4\pi} \cdot 4 \frac{k'}{k} \cdot \frac{1}{q^4} \int d\hat{R} \left| \varepsilon_{on}(\mathbf{q}, R_0, \hat{R}) \right|^2, \quad (12)$$

where

$$\varepsilon_{on}(\mathbf{q}, R_0, \hat{R}) = \int \psi(\mathbf{o}|\vec{r}, R) \sum_{i=1}^2 e^{i\vec{q} \cdot \vec{r}_i} \psi(\mathbf{n}|\vec{r}, R) d^3r_1 d^3r_2.$$

In Chapter II, where the electronic wave functions are discussed, it is shown that these wave functions can be written to a good approximation

$$\psi(\mathbf{o}|\vec{r}, R) \approx u_0(\vec{r}_1) u_0(\vec{r}_2), \quad \text{and}$$

$$\psi(\mathbf{n}|\vec{r}, R) \approx \frac{1}{\sqrt{2}} \left[u_n(\vec{r}_1) v_n(\vec{r}_2) + v_n(\vec{r}_1) u_n(\vec{r}_2) \right].$$

This gives

$$\epsilon_{\text{on}}(a, R, \hat{R}) = \sqrt{2} \int d^3r u_0(\vec{r}) e^{i\vec{q} \cdot \vec{r}} v_n^*(\vec{r}) .$$

Using elliptic coordinates, we have

$$d^3r = \left(\frac{R}{2}\right)^3 (\xi^2 - \eta^2) d\xi d\eta d\varphi ,$$

$$\vec{q} \cdot \vec{r} = q_{\parallel} \left(-\frac{R}{2} \xi \eta\right) + q_{\perp} \frac{R}{2} \left[(\xi^2 - 1)(1 - \eta^2) \right]^{1/2} \sin \varphi ,$$

$$u_0(\vec{r}) = f_0(\xi, \eta) \cdot 1/\sqrt{2\pi} ,$$

$$v_n(\vec{r}) = f_n(\xi, \eta) e^{im\varphi} / \sqrt{2\pi}, \quad m=0 \text{ for } \Sigma \text{ state, } m=1 \text{ for } \pi \text{ state,}$$

etc., and

$$\begin{aligned} \epsilon_{\text{on}}(a, R, \hat{R}) &= \sqrt{2} \left(\frac{R}{2}\right)^3 \int_{-1}^1 d\eta \int_1^{\infty} d\xi (\xi^2 - \eta^2) f_0(\xi, \eta) f_n(\xi, \eta) \\ &\quad e^{-iq_{\parallel} \frac{R}{2} \xi \eta} \int_0^{2\pi} d\varphi e^{im\varphi + iq_{\perp} \left[(\xi^2 - 1)(1 - \eta^2) \right]^{1/2} \sin \varphi} . \end{aligned}$$

The integral over φ is the Bessel function of the first kind¹³

$$\frac{1}{2\pi} \int_0^{2\pi} d\varphi e^{i(m\varphi + x \sin \varphi)} = J_m(x) .$$

Hence,

$$\begin{aligned} \epsilon_{\text{on}}(a, R, \hat{R}) &= \sqrt{2} \left(\frac{R}{2}\right)^3 \int_{-1}^1 d\eta \int_1^{\infty} d\xi (\xi^2 - \eta^2) f_0(\xi, \eta) \\ &\quad f_n(\xi, \eta) e^{-iq_{\parallel} \frac{R}{2} \xi \eta} J_m \left\{ q_{\perp} \frac{R}{2} \left[(\xi^2 - 1)(1 - \eta^2) \right]^{1/2} \right\} . \end{aligned}$$

This integral is performed numerically (see the Appendix on numerical procedures.)

Let us now introduce a quantity $G_n(q)$ related to the differential cross section by the expression

$$I_0^n(q) = \xi_n \frac{k'}{k} \cdot 4qG_n(q) \quad ,$$

$$G_n(q) = \frac{1}{q^3} \frac{1}{4\pi} \int d\hat{R} |\epsilon_{on}(q, R, \hat{R})|^2 \quad .$$

The total cross section, Q_n , is

$$Q_n = \xi_n \frac{8\pi}{k^2} \int_{q_{\min}}^{q_{\max}} dq G_n(q) \quad .$$

The quantity $G_n(q)$ is shown in Figure 4 for the B $1\Sigma_u^+$, C $1\Pi_u$, and E $1\Sigma_g^+$ states.

It may be seen that $G_n(q)$ is proportional to q^{-1} for small q in the case of the B and C states. This is characteristic of resonance transitions, and leads to the familiar $\ln(E)/E$ energy dependence of the cross section at high energies. For the E state, however, $G_n(q)$ has a totally different shape, and the integral

$$\int_{q_{\min}}^{q_{\max}} dq G_n(q)$$

approaches a constant value at large energies, giving the cross section a $1/E$ energy dependence. These excitation functions, shown in Figures 5 and 6, have characteristics very similar to their united atom counter-

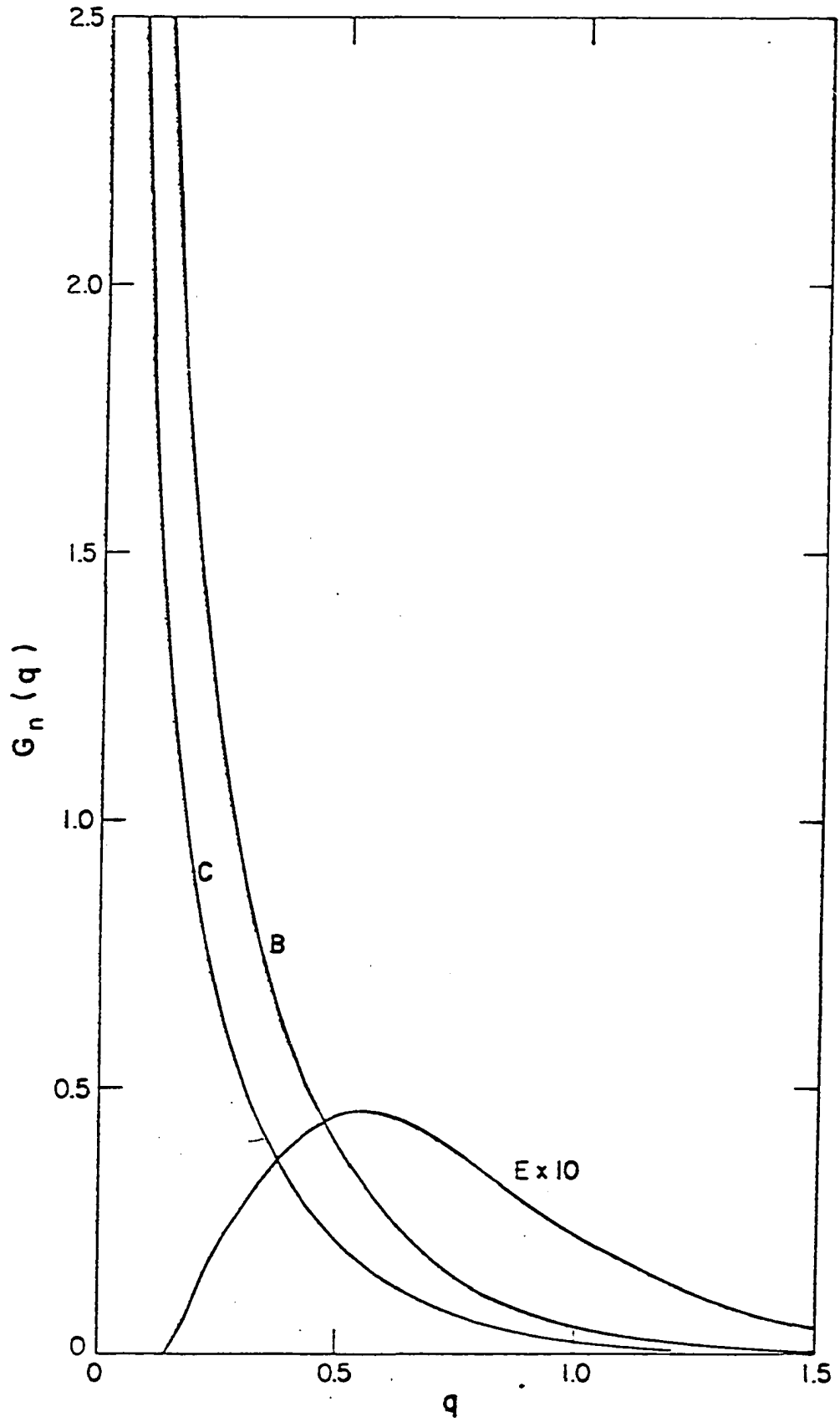


Figure 4. $G_n(q)$ vs q for the C, B, and E states.

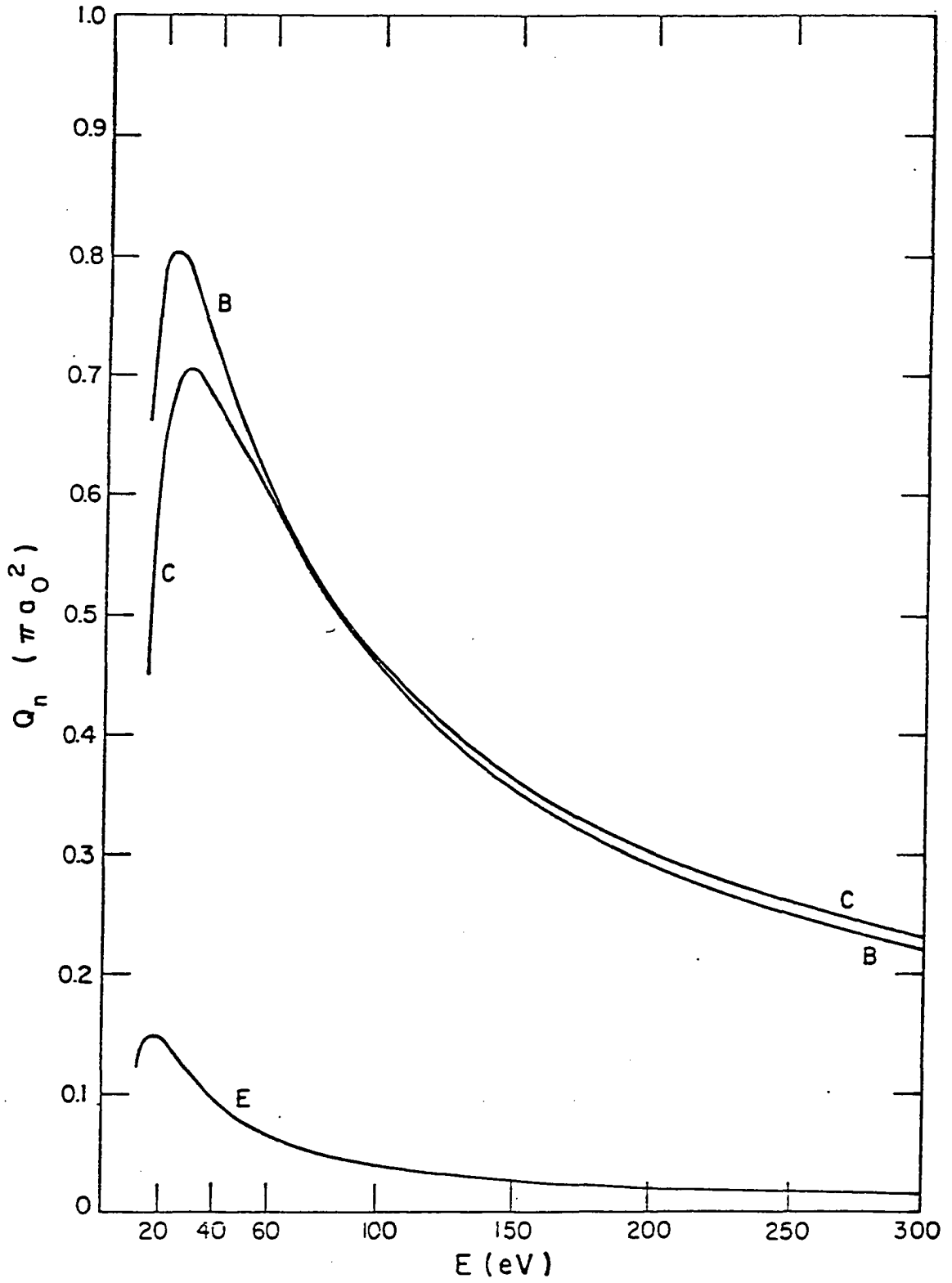


Figure 5. Born cross sections for the C, B, and E states.

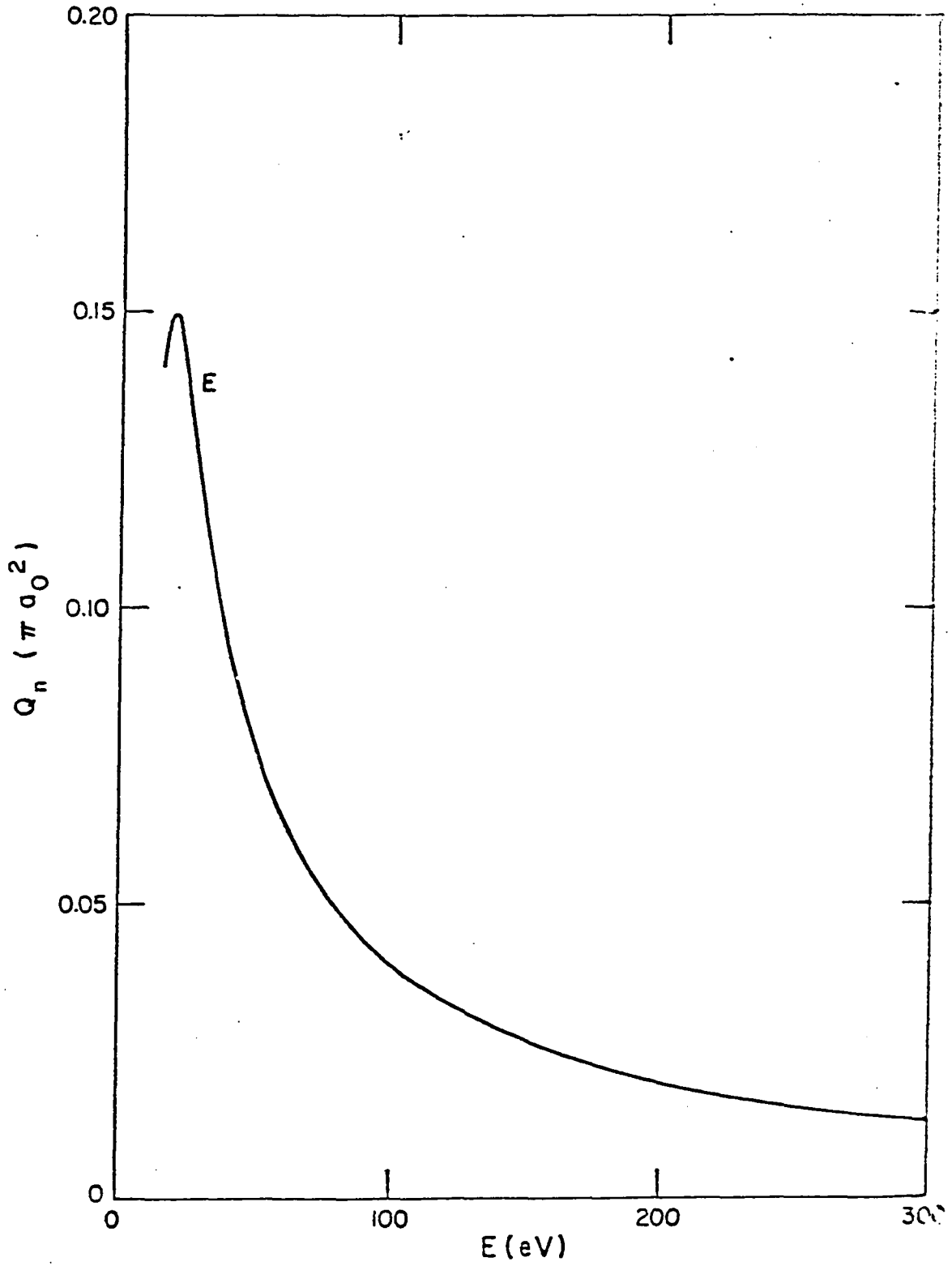


Figure 6. Born cross sections for the E state.

parts, the E state corresponding to the He 1s2s state, while the B and C states correspond to the 1s2p state.

According to the Franck-Condon principle, the cross sections for exciting the various vibrational levels within each electronic state are given by multiplying the Q_n by the square of the appropriate overlap integral. Let us call the cross sections obtained by this method $Q_{nv}^{(FC)}$

$$Q_{nv}^{(FC)} = \left| \int R^2 dR \varphi_0(o|R) \varphi_n^*(v|R) \right|^2 \cdot Q_n .$$

A more accurate determination of the Born cross sections for the individual vibrational levels may be made by using equation (9) for the differential cross section I_{∞}^{nv} . The total cross section is then found by integrating this quantity over all angles,

$$Q_{nv} = \int d\omega I_{\infty}^{nv} .$$

The quantities $Q_{nv}^{(FC)}$ and Q_{nv} are given in Table 5 for electron energies of 40 and 200 eV, for the first ten vibrational levels of each of the above electronic states. It is seen that the Franck-Condon principle gives results which are accurate to within 10 or 15% for the C and E states, but for the B state $Q_{nv}^{(FC)}$ differs from Q_{nv} by about a factor of 1.5 for the first few vibrational levels. These results are in accord with the numerical results published by Miller and Krauss¹¹. They make the statement, however, that the use of the Franck-Condon principle produces errors of less than 20 per cent for all cases. We would amend this statement to read, "The use of the Franck-Condon factors to determine the relative probabilities

Table 5. Born cross sections for excitation to the vibrational levels of the C, B, and E states. $Q^{(FC)}$ is the cross section computed by using the Franck-Condon factor.

	V	$Q_{C,v}^{FC}$	$Q_{C,v}$	$Q_{B,v}^{FC}$	$Q_{B,v}$	$Q_{E,v}^{FC}$	$Q_{E,v}$
40eV	0	8.25	9.23	.316	.506	1.31	1.43
	1	12.6	13.6	1.09	1.65	1.83	1.95
	2	12.0	12.5	2.18	3.15	.(4)95	.000101
	3	9.34	9.47	3.33	4.58	.00126	.00133
	4	6.58	6.17	4.29	5.63	1.43	1.49
	5	4.40	4.23	4.94	6.21	.0943	.0977
	6	2.87	2.69	5.26	6.33	.146	.150
	7	1.85	1.70	5.26	6.08	.605	.615
	8	1.19	1.08	5.02	5.58	.398	.402
	9	.771	.684	4.61	4.94	.340	.341
200eV	0	3.68	4.23	.127	.206	.277	.305
	1	5.70	6.26	.442	.677	.390	.417
	2	5.52	5.83	.893	1.30	.(4)203	.(4)216
	3	4.38	4.45	1.37	1.90	.000270	.000285
	4	3.13	3.07	1.78	2.36	.307	.320
	5	2.12	2.02	2.07	2.62	.0202	.0210
	6	1.40	1.29	2.22	2.69	.0315	.0323
	7	.914	.822	2.24	2.60	.130	.133
	8	.595	.523	2.15	2.40	.0859	.0868
	9	.388	.334	1.99	2.13	.0735	.0736

of exciting the different vibrational levels produces errors of less than 20 per cent for all cases except the first five or six levels of the B state".

CHAPTER IV

FORMULATION OF THE CLOSE COUPLING THEORY

It has been shown that, within the framework of the Born approximation and the Franck-Condon principle, one can compute the cross section for electronic excitation according to the following procedure: First, one treats the problem of electronic excitation as though the nuclei were fixed in space, and calculates the cross section for a given relative orientation between the direction of incidence of the incoming electron and the internuclear axis. Then, one performs an average over all possible relative orientations. Physically, this corresponds to the fact that the nuclei, being much heavier than the electrons, move much more slowly, so that they will remain approximately stationary during the excitation process. And, since there is no reason for one relative orientation to be preferred over any other, one should perform the average over all orientations. Although this physical model has been substantiated mathematically only for the Born approximation, it is a very reasonable model, and we shall continue to use it, even in cases where the Born approximation is not assumed to be valid.

Let us then consider the $e\text{-H}_2$ interaction in this "clamped-nuclei" approximation. Since we are considering excitation of singlet states only, and we are interested in cross sections over a large range of energies, rather than just near threshold, where exchange effects

are expected to be important, we will not include exchange between the scattered electron and the molecular electrons.

Let \vec{r} represent the coordinates of the molecular electrons, and \vec{r}_3 the coordinates of the scattered electron. The electronic state of the molecule is specified by the quantum numbers $n\lambda$ ($\lambda = 0$ for Σ state, ± 1 for Π state, etc.), the state of the scattered electron by $k \ell m$. Because of the cylindrical symmetry in which the three electrons move, the component $\Lambda = \lambda + m$ of the total angular momentum along the internuclear axis will be a good quantum number. Hence, we will specify the state of the three electron system by $\mu = n\lambda\ell\Lambda$. The quantum number k of the scattered electron need not be explicitly mentioned, since it is determined by the condition of conservation of total energy in the excitation process,

$$\frac{1}{2} k_0^2 + \epsilon_0 = \frac{1}{2} k_n^2 + \epsilon_n = E \quad . \quad (15)$$

We expand the total wave function Ψ , as follows:

$$\Psi = \sum_{\mu} A_{\mu} \psi_{\mu}(\vec{r}, \vec{r}_3) \quad , \quad (16)$$

$$\begin{aligned} \psi_{\mu}(\vec{r}, \vec{r}_3) &= \frac{1}{r_3} \sum_{\mu'} F_{\mu\mu'}(r_3) \\ &\quad \psi(n'\lambda'|\vec{r}, R) Y_{\ell', \Lambda' - \lambda'}(\hat{r}_3) \quad , \end{aligned} \quad (17)$$

where $\mu' = n'\lambda'\ell'\Lambda'$ ($\mu'' = n''\lambda''\ell''\Lambda''$, etc.) ,

$\psi(n'\lambda'|\vec{r}, R)$ is the molecular electronic wave function,

$Y_{\ell', \ell' - \lambda'}(\hat{r}_3)$ is a spherical harmonic, and

$F_{\mu \mu}(r_3)$ must have the behavior

$$F_{\mu \mu}(0) = 0, \text{ and}$$

$$F_{\mu \mu}(r_3) \underset{r_3 \rightarrow \infty}{\sim} e^{-i(k_n r_3 - \frac{1}{2} \ell' \pi)} \delta_{\mu \mu} - e^{i(k_n r_3 - \frac{1}{2} \ell' \pi)} S_{\mu \mu}. \quad (18)$$

The A_{μ} are to be chosen so that

$$\psi = \psi(0 | \vec{r}, R) e^{i\vec{k}_0 \cdot \vec{r}_3} \underset{r_3 \rightarrow \infty}{\sim} \sum_{n \lambda} \psi(n \lambda | \vec{r}, R)$$

$$= \frac{e^{i k_n r_3}}{r_3} f_{n\lambda}(\vec{R}, \hat{r}_3), \quad (19)$$

that is, ψ is to represent the physical situation of a beam of electrons of momentum \vec{k}_0 incident upon F_2 molecules in the ground state, with the scattered electrons spherically diverging away from the target. The quantity $|f_{n\lambda}(\vec{R}, \hat{r}_3)|^2$ describes the angular distribution of the scattered electrons which have left the molecule in the state $n\lambda$.

With the A_{μ} so chosen, the differential cross section for excitation of the state $n\lambda$ is

$$\frac{I_{n\lambda}}{I_0}(\hat{r}_3) = \frac{k_n}{k_0} \cdot \frac{1}{4\pi} \int d\hat{R} |f_{n\lambda}(\vec{R}, \hat{r}_3)|^2. \quad (20)$$

Now, λ is the component of angular momentum of the molecular electrons along the internuclear axis. Since, in the above expression

for $I_0^{n\lambda}(\hat{r}_3)$, we average over all orientations of the internuclear axis, we expect that $I_0^{n,-\lambda} = I_0^{n,\lambda}$, so that

$$\begin{aligned} I_0^n(\hat{r}_3) &= I_0^{n\lambda}(\hat{r}_3) + I_0^{n,-\lambda}(\hat{r}_3) \\ &= g_n \frac{k_n}{k_0} \frac{1}{4\pi} \int d\hat{R} \left| f_{n\lambda}(\vec{R}, \hat{r}_3) \right|^2, \end{aligned} \quad (21)$$

where g_n is the electronic degeneracy of the state n ($g_n = 1$ for Σ states, $g_n = 2$ for Π, Δ, \dots states.) The total cross section Q_n is given by

$$\begin{aligned} Q_n &= \int d\hat{r}_3 I_0^n(\hat{r}_3) \\ &= g_n \frac{k_n}{k_0} \int d\hat{r}_3 \frac{1}{4\pi} \int d\hat{R} \left| f_{n\lambda}(\vec{R}, \hat{r}_3) \right|^2. \end{aligned} \quad (22)$$

We now evaluate the A_μ by requiring that ψ have the indicated form for $r_3 \rightarrow \infty$. For very large r_3 , the plane wave $\exp(i\vec{k}_0 \cdot \vec{r}_3)$ has the expansion

$$\begin{aligned} e^{i\vec{k}_0 \cdot \vec{r}_3} &\sim 2\pi i (k_0 r_3)^{-1} \sum_{\ell, m} i^\ell Y_{\ell, m}^*(\hat{k}_0) Y_{\ell, m}(\hat{r}_3) \\ &\left[e^{-i(k_0 r_3 - \frac{1}{2} \ell \pi)} \quad e^{i(k_0 r_3 - \frac{1}{2} \ell \pi)} \right], \end{aligned} \quad (23)$$

and we require that

$$F_{\mu\mu}(r_3) \sim e^{-i(k_n r_3 - \frac{1}{2} \ell' \pi)} \delta_{\mu\mu} e^{i(k_n r_3 - \frac{1}{2} \ell' \pi)} S_{\mu\mu}.$$

Thus, we find that

$$\begin{aligned}
 \Psi - \psi(0|\vec{r}, R) e^{i\vec{k}_0 \cdot \vec{r}_3} &\sim \sum_{\mu'} \left\{ \psi(n'\lambda'|\vec{r}, R) Y_{\ell'\lambda' - \lambda'}(\hat{r}_3) \right. \\
 &\times \frac{1}{r_3} \sum_{\mu} \left[A_{\mu} \left\{ e^{-i(k_n r_3 - \frac{1}{2} \ell' \pi)} \delta_{\mu\mu} e^{i(k_{n'} - \frac{1}{2} \ell' \pi)} S_{\mu\mu} \right\} \right. \\
 &- \frac{2\pi i}{k_{n'}} i^{\ell'} Y_{\ell'\lambda' - \lambda'}^*(\hat{k}_0) \left\{ e^{-i(k_n r_3 - \frac{1}{2} \ell' \pi)} \delta_{\mu\mu} \right. \\
 &\left. \left. - e^{i(k_n r_3 - \frac{1}{2} \ell' \pi)} \delta_{\mu\mu} \left[\delta_{n,0} \delta_{\lambda,0} \right] \right\} \right] \left. \right\} .
 \end{aligned}$$

This is the required form, provided that the coefficient of $e^{-i(k_n r_3 - \frac{1}{2} \ell' \pi)}$ vanishes. This gives

$$A_{\mu} = \frac{2\pi i}{k_n} i^{\ell} Y_{\ell, \Lambda - \lambda}^*(\hat{k}_0) \delta_{n,0} \delta_{\lambda,0} .$$

and

$$\begin{aligned}
 f_{n\lambda}(\vec{R}, \hat{r}_3) &= \frac{2\pi i}{k_0} \sum_{\ell, \ell', \Lambda} i^{\ell' - \ell} Y_{\ell', \Lambda}^*(\hat{k}_0) Y_{\ell, \Lambda}(\hat{r}_3) \\
 &\left[\delta_{n\lambda\ell\Lambda, 00\ell'\Lambda} - S_{n\lambda\ell'\Lambda, 00\ell'\Lambda} \right] , \quad (24)
 \end{aligned}$$

where we have used the fact that S is diagonal in Λ .

For the total cross section Q_n , we find

$$Q_n = g_n \frac{k_n}{k_0^3} \pi \sum_{\ell, \ell', \Lambda} \left| T_{n\lambda\ell\Lambda, 00\ell'\Lambda} \right|^2 , \quad (25)$$

where $T \equiv 1 - S$.

Differential Equations

The total wave function Ψ must satisfy

$$(H-E) \Psi = 0 \quad , \quad (26)$$

$$\text{where } H = H_m - \frac{1}{2} \nabla_3^2 + V \quad ,$$

H_m being the electronic Hamiltonian of the molecule,

$$H_m \psi(n\lambda | \vec{r}, R) = \epsilon_n \psi(n\lambda | \vec{r}, R) \quad ,$$

and V being the interaction potential between the colliding electron and the molecule,

$$V = \frac{1}{r_{13}} + \frac{1}{r_{23}} - \frac{1}{r_{3A}} - \frac{1}{r_{3B}} \quad .$$

Multiplying equation (26) by -2 and making use of the expansions (16) and (17), we find that

$$\sum_{\mu'} \left\{ \nabla_3^2 + 2(E - \epsilon_{n'}) - 2V \right\} \frac{1}{r_3} F_{\mu'\mu}(r_3)$$

$$\psi(n'\lambda' | \vec{r}, R) Y_{\ell', \Lambda' - \lambda'}(\hat{r}_3) = 0 \quad ,$$

or

$$\sum_{\mu'} \left\{ \frac{d^2}{dr_3^2} - \frac{\ell'(\ell'+1)}{r_3^2} + k_{n'}^2 - 2V \right\} F_{\mu'\mu}(r_3)$$

$$\psi(n'\lambda' | \vec{r}, R) Y_{\ell', \Lambda' - \lambda'}(\hat{r}_3) = 0 \quad , \quad (27)$$

where we have used the relation $\frac{1}{2} k_n^2 + \epsilon_n = E$. If we multiply (27) by $\psi^*(n''\lambda''|\vec{r},R)Y_{\ell'',\Lambda''-\lambda''}^*(\hat{r}_3)$ and carry out integrations over the coordinates of the molecular electrons and over \hat{r}_3 , we have

$$\left\{ \frac{d^2}{dr_3^2} - \frac{\ell''(\ell''+1)}{r_3^2} + k_n^2 \right\} F_{\mu''\mu''}(r_3) \\ = \sum_{\mu'} U_{\mu''\mu'}(r_3) F_{\mu'\mu'}(r_3) \quad . \quad (28)$$

Or, in matrix notation, we have

$$F'' = G F \quad ,$$

where

$$G_{\mu''\mu'} = \left\{ \frac{\ell'(\ell'+1)}{r_3^2} - k_{n'}^2 \right\} \delta_{\mu''\mu'} + U_{\mu''\mu'} \quad ,$$

with

$$U_{\mu''\mu'} \equiv \int d\vec{r}_3 \int d\vec{r} \psi^*(n'\lambda'|\vec{r},R)Y_{\ell',\Lambda'-\lambda'}^*(\hat{r}_3) 2V \psi(n\lambda|\vec{r},R)Y_{\ell,\Lambda-\lambda}(\hat{r}_3) \quad .(29)$$

Equation (28) represents a set of simultaneous, linear, second order differential equations, the solutions of which are found by a numerical integration. The numerical method is discussed in the Appendix on numerical procedures. The method for finding solutions which have the asymptotic form (18) is discussed by Barnes, Lane, and Lin.⁷ For sufficiently large r_3 , (28) may be replaced by

$$\left[\frac{d^2}{dr_3^2} + k_{n'}^2 \right] F_{\mu''\mu''}(r_3) = 0 \quad . \quad ,$$

which has the solutions of the form

$$F_{\mu\nu} = A_{\mu\nu} \sin(k_n r_3 - \frac{1}{2} \ell' \pi) + B_{\mu\nu} \cos(k_n r_3 - \frac{1}{2} \ell' \pi) .$$

In matrix notation, this has the form

$$F = H_1 A + H_2 B ,$$

where

$$(H_1)_{\mu\nu} = \sin(k_n r_3 - \frac{1}{2} \ell' \pi) \delta_{\mu\nu} , \text{ and}$$

$$(H_2)_{\mu\nu} = \cos(k_n r_3 - \frac{1}{2} \ell' \pi) \delta_{\mu\nu} .$$

Any numerical solution of (28) must assume this form for sufficiently large r_3 , and A and B can be found by matching the numerical solution to F at two values of r_3 .

Now, each column of the matrix F is a solution to (28), and furthermore, any linear combination of columns is also a solution. What we require is that F be a square matrix and that each column be a linearly independent solution. Then, the matrices A and B will be non-singular, and in particular, A^{-1} will exist, so that

$$\begin{aligned} F^{(R)} &= F A^{-1} = H_1 A A^{-1} + H_2 B A^{-1} \\ &= H_1 + H_2 R , \end{aligned}$$

is also a solution of (28). It is then seen that

$$F^{(S)} = (E_2 - i H_1) - (E_2 + i H_1) S$$

is given by

$$F^{(S)} = -2i F^{(R)} (1-iR)^{-1} ,$$

$$\text{with } S = (1+iR) (1-iR)^{-1} ,$$

$$\text{and } R = BA^{-1} .$$

To determine the cross section for excitation to a particular electronic state, then, the following steps are required:

- (a) A numerical solution F is found which has the properties

$$F_{\mu\mu}(0) = 0 , \text{ and}$$

$$\det|F(r_3)| \neq 0 \text{ for } r_3 > 0 .$$

- (b) The matrices A and B are determined as indicated above.

- (c) The matrices $R = BA^{-1}$, $S = (1+iR)(1-iR)^{-1}$, and $T = 1 - S$ are computed.

- (d) Equation (25) is used to find the desired cross section.

The set of coupled differential equations (26), with the interaction potential matrix U defined by (29), yields solutions which are appropriate for the close coupling approximation. By altering the interaction potential matrix in certain ways, the equations (26) can be made to yield solutions which correspond to other approximations. For example, the potential matrix U^{2s} , defined by

$$U_{\mu\mu}^{2s} \equiv \begin{cases} 0 & \text{if } n' \text{ and } n \text{ both refer to excited electronic} \\ & \text{states, and } n' \neq n , \\ U_{\mu\mu} & \text{otherwise} , \end{cases}$$

yields solutions which correspond to the "two-state close coupling" approximation, in which the coupling between the ground state and each excited state is taken into account, but the coupling between different excited states is ignored. The distorted wave approximation is obtained by using the potential matrix U^{DW} , which is defined by

$$U_{\mu\mu'}^{DW} \equiv \begin{cases} 0 & \text{if } n' \text{ refers to the ground state and } n \text{ refers} \\ & \text{to an excited state} \quad , \\ U_{\mu\mu'}^{2s} & \text{otherwise} \quad . \end{cases}$$

This has the effect of not allowing the ground state-excited state coupling to influence the elastically scattered waves.

The Born approximation potential matrix, U^B , is defined by

$$U_{\mu\mu'}^B \equiv \begin{cases} U_{\mu\mu'} & \text{if } n' \text{ refers to an excited electronic} \\ & \text{state, and } n \text{ refers to the ground state,} \\ 0 & \text{, otherwise.} \end{cases}$$

Cross sections have been calculated by all four of these approximations, as will be discussed below.

CHAPTER V

APPLICATION OF CLOSE COUPLING THEORY TO EXCITATION OF H₂

The close coupling theory, as it is formulated here, is appropriate for the calculation of cross sections summed over all possible states of nuclear motion in the final electronic state. We will first apply the theory in this form to the excitation of the H₂ molecule. The extension of the theory to include vibrational effects is straightforward, and will be done later.

Evaluation of the Interaction Potential Matrix

From equation (15) we have

$$U_{\mu',\mu}(\vec{r}_3) = \int d\vec{r}_3 Y_{\ell',\Lambda'-\lambda'}^*(\hat{r}_3) V_{n'\lambda',n\lambda}(\vec{r}_3) Y_{\ell,\Lambda-\lambda}(\hat{r}_3) \quad , \quad (32)$$

where

$$\begin{aligned} V_{n'\lambda',n\lambda}(\vec{r}_3) &= \int d\vec{r} \psi^*(n'\lambda'|\vec{r},R) \left[\left(\frac{2}{r_{13}} + \frac{2}{r_{23}} \right) \right. \\ &\quad \left. + \left(-\frac{2}{r_{3A}} - \frac{2}{r_{3B}} \right) \right] \psi(n\lambda|\vec{r},R) \\ &= V_{n'\lambda',n\lambda}^e(\vec{r}_3) + V_{n'\lambda',n\lambda}^N(\vec{r}_3) \quad . \end{aligned}$$

Let us first consider $V_{n'\lambda',n\lambda}^e(\vec{r}_3)$. The electronic wave functions

can be written

$$\psi(\mathbf{0}|\vec{r}, R) = u_0(\vec{r}_1)u_0(\vec{r}_2) ,$$

$$\psi(\mu\lambda|\vec{r}, R) = \frac{1}{\sqrt{2}} \left[u_\mu(\vec{r}_1)v_\mu(\vec{r}_2) + v_\mu(\vec{r}_1)u_\mu(\vec{r}_2) \right] ,$$

$$(v_\mu, u_0) = 0 , (u_\mu, u_0) \approx 1 , (u_\mu, v_{\mu'}) \approx 1 .$$

Thus, we have

$$\begin{aligned} V_{0,0}^E(\vec{r}_3) &= \int d^3r_1 \int d^3r_2 u_0(\vec{r}_1)u_0(\vec{r}_2) \frac{4}{r_{13}} u_0(\vec{r}_1)u_0(\vec{r}_2) \\ &= \int d^3r_1 u_0(\vec{r}_1) \frac{4}{r_{13}} u_0(\vec{r}_1) , \end{aligned}$$

$$\begin{aligned} V_{0,\mu\lambda}^E(\vec{r}_3) &= \int d^3r_1 \int d^3r_2 u_0(r_1)v_0(\vec{r}_2) \frac{4}{r_{13}} \\ &\quad \frac{1}{\sqrt{2}} \left[u_\mu(\vec{r}_1)v_\mu(\vec{r}_2) + v_\mu(\vec{r}_1)u_\mu(\vec{r}_2) \right] \\ &= \int d^3r_1 u_0(\vec{r}_1) \frac{4}{r_{13}} \frac{1}{\sqrt{2}} v_\mu(\vec{r}_1) , \end{aligned}$$

$$\begin{aligned} V_{\mu\lambda\lambda',\mu\lambda}^E(\vec{r}_3) &= \int d^3r_1 \int d^3r_2 \frac{1}{\sqrt{2}} \left[u_{\mu'}(\vec{r}_1)v_{\mu'}(\vec{r}_2) \right. \\ &\quad \left. + v_{\mu'}(\vec{r}_1)u_{\mu'}(\vec{r}_2) \right] \frac{4}{r_{13}} \frac{1}{\sqrt{2}} \left[u_\mu(\vec{r}_1)v_\mu(\vec{r}_2) + v_\mu(\vec{r}_1)u_\mu(\vec{r}_2) \right] \\ &= \frac{1}{2} \delta_{\mu\lambda\lambda',\mu\lambda} \int d^3r_1 u_{\mu'}(\vec{r}_1) \frac{4}{r_{13}} u_\mu(\vec{r}_1) \\ &\quad + \frac{1}{2} \int d^3r_1 v_{\mu'}(\vec{r}_1) \frac{4}{r_{13}} v_\mu(\vec{r}_1) , \end{aligned}$$

where $u_n \approx u_0 = f_0(\xi, \eta) \cdot \frac{1}{\sqrt{2\pi}}$, $v_n = f_n(\xi, \eta) \frac{e^{i\lambda\varphi}}{\sqrt{2\pi}}$,

expressed in elliptic coordinates. Each of the above integrals is of the form

$$I_{n', \lambda', n\lambda} = \left(\frac{R}{2}\right)^3 \int_1^\infty d\xi \int_{-1}^1 d\eta (\xi^2 - \eta^2) \int_0^{2\pi} d\varphi f_{n'}(\xi, \eta) \frac{e^{-i\lambda'\varphi}}{\sqrt{2\pi}} \frac{1}{r_{13}} f_n(\xi, \eta) \frac{e^{i\lambda\varphi}}{\sqrt{2\pi}} \quad (33)$$

Expanding $\frac{1}{r_{13}}$, we have

$$\frac{1}{r_{13}} = \sum_{K,m} \frac{4\pi}{2K+1} \frac{r_{<}^K}{r_{>}^{K+1}} Y_{K,m}^*(\hat{r}_3) Y_{K,m}(\hat{r}_1),$$

where $r_{<}$ is the smaller of r_3 , r_1 and $r_{>}$ is the larger of the two.

Substituting this expansion into (33), we get

$$I_{n', \lambda', n\lambda} = \sum_{K,m} \frac{4\pi}{2K+1} Y_{K,m}^*(\hat{r}_3) \left(\frac{R}{2}\right)^3 \int_1^\infty d\xi \int_{-1}^1 d\eta (\xi^2 - \eta^2) f_{n'}(\xi, \eta) \frac{r_{<}^K}{r_{>}^{K+1}} P_{K,m}(\cos \theta_1) f_n(\xi, \eta) \int_0^{2\pi} d\varphi \frac{e^{-i\lambda'\varphi}}{\sqrt{2\pi}} \frac{e^{im\varphi}}{\sqrt{2\pi}} \frac{e^{i\lambda\varphi}}{\sqrt{2\pi}}.$$

It is clear that the integral over φ will give zero unless $m = \lambda' - \lambda$.

Hence,

$$I_{n'\lambda', n\lambda} = \sum_K \sqrt{2\pi} \frac{2}{2K+1} Y_{K, \lambda' - \lambda}^* (\hat{r}_3) u_K(R, r_3, n'\lambda', n\lambda) \quad ,$$

where

$$u_K(R, r_3, n'\lambda', n\lambda) = \left(\frac{R}{2}\right)^3 \int_1^\infty d\xi \int_{-1}^1 d\eta (\xi^2 - \eta^2)$$

$$f_n^{\frac{r <}{r >}}(\xi, \eta) \frac{r <}{r >}{K+1} P_{K, \lambda' - \lambda}(\cos \theta) f_n(\xi, \eta) \quad .$$

This integral is evaluated by two-dimensional numerical integration.

See Appendix I for the numerical details.

We then find that

$$V_{n'\lambda', n\lambda}^e(\vec{r}_3) = 4\sqrt{2\pi} \sum_K \sqrt{\frac{2}{2K+1}} Y_{K, \lambda' - \lambda}^* (\hat{r}_3) V_K(R, r_3, n'\lambda', n\lambda) \quad ,$$

where

$$V_K(R, r_3, n'\lambda', n\lambda) = N_{n', n} \left\{ u_K(R, r_3, 0, 0) \delta_{n'\lambda', n\lambda} \right. \\ \left. + u_K(R, r_3, n'\lambda', 0) \delta_{n\lambda, 0} + u_K(R, r_3, 0, n\lambda) \delta_{n'\lambda', 0} \right. \\ \left. + u_K(R, r_3, n'\lambda', n\lambda) \right\} \quad ,$$

and

$$N_n = \begin{cases} 1/2 & \text{for } n=0 \text{ (ground state)} \\ 1/\sqrt{2} & \text{otherwise} \end{cases} \quad .$$

We will now examine the contribution to $V_{n'\lambda',n\lambda}(\vec{r}_3)$ made by the nuclear attraction terms.

$$\begin{aligned} V_{n'\lambda',n\lambda}^N(\vec{r}_3) &= \int d\vec{r} \psi^*(n'\lambda'|\vec{r},R) \left[-\frac{2}{r_{3A}} - \frac{2}{r_{3B}} \right] \psi(n\lambda|\vec{r},R) \\ &= \left(-\frac{2}{r_{3A}} - \frac{2}{r_{3B}} \right) \delta_{n'\lambda',n\lambda} \\ &= -4 \sum_{\text{even } K} \frac{4\pi}{2K+1} \frac{R_{<}^K}{R_{>}^{K+1}} Y_{K,0}^*(\hat{r}_3) Y_{K,0}(0) \quad , \end{aligned}$$

where $R_{<}$ is the smaller of r_3 , $R/2$, and $R_{>}$ is the larger of the two quantities. Using the fact that

$$Y_{K,0}(0) = \sqrt{\frac{2K+1}{2}} \cdot \frac{1}{\sqrt{2\pi}} \quad ,$$

we have

$$\begin{aligned} V_{n'\lambda',n\lambda}^N(\vec{r}_3) &= -4\sqrt{2\pi} \sum_K \sqrt{\frac{2}{2K+1}} Y_{K,0}^*(\hat{r}_3) \\ &\quad \frac{R_{<}^K}{R_{>}^{K+1}} \delta_{n'\lambda',n\lambda} \delta_{K,\text{even}} \quad , \end{aligned}$$

and

$$\begin{aligned} V_{n'\lambda',n\lambda}(\vec{r}_3) &= 4\sqrt{2\pi} \sum_K \sqrt{\frac{2}{2K+1}} Y_{K,\lambda'-\lambda}^*(\hat{r}_3) \\ &\quad \left\{ V_K(R,r_3,n'\lambda',n\lambda) - \frac{R_{<}^K}{R_{>}^{K+1}} \delta_{n'\lambda',n\lambda} \delta_{K,\text{even}} \right\} . \end{aligned}$$

Now, according to equation (32),

$$U_{\mu\mu'}(r_3) = \int d\vec{r}_3 Y_{\ell',\Lambda'-\lambda'}^*(\vec{r}_3) V_{n',\lambda',n\lambda}(\vec{r}_3) Y_{\ell,\Lambda-\lambda}(\vec{r}_3) .$$

But^a

$$\begin{aligned} & \int d\vec{r}_3 Y_{\ell',\Lambda'-\lambda'}^* Y_{K,\lambda'-\lambda} Y_{\ell,\Lambda-\lambda} \\ &= \frac{1}{\sqrt{2\pi}} \sqrt{\frac{2K+1}{2}} C^K(\ell,\Lambda'-\lambda';\ell',\Lambda'-\lambda') \delta_{\Lambda',\Lambda} . \end{aligned}$$

which demonstrates the diagonality of $U_{\mu\mu'}$ with respect to Λ . We therefore have

$$U_{\mu\mu'}(r_3) = 4 \sum_K C^K(\ell,\Lambda'-\lambda';\ell',\Lambda'-\lambda') \delta_{\Lambda',\Lambda} \left\{ V_K(R,r_3,n'\lambda',n\lambda) - \frac{R_{<}^K}{R_{>}^{K+1}} \delta_{n'\lambda',n\lambda} \delta_{K,\text{even}} \right\} . \quad (34)$$

The sum over K in this expression goes from $K = |l-l'|$ to $K = l+l'$. Now, each integral in the expression for $V_K(R,r_3,n'\lambda',n\lambda)$ has in the integrand the factor $r_{<}^K / r_{>}^{K+1}$. Thus we see the V_K will decrease rapidly with increasing K , and that for large r_3 , $V_K \propto 1/r_3^{K+1}$. This means that the elements of the potential matrix U between widely different l values will be very small, or that the "coupling" between widely different l values will be small.

^a For the definition of the quantity $C^K(\ell,n;\ell'm')$, see E. U. Condon and G. H. Shortley, The Theory of Atomic Spectra, page 175.

Calculation of Cross Sections

In the application of the close coupling theory to the calculation of cross sections, the first problem we face is that the system of coupled differential equations is not a finite system. The index $\mu = n\lambda \ell \Lambda$ has a two fold infinite range, since n runs over all the bound (singlet) states, as well as the continuum, while ℓ runs from 0 to ∞ . Since we can only solve finite systems, we must limit the range of both n and ℓ .

Since we are primarily interested in the $n = 2$ manifold (see the electronic energy level diagram in Figure 7), we choose to include only the states of this manifold along with the ground state in the close coupling scheme. This is a reasonable choice, since these states are fairly well separated in energy from all the other singlet states, and we expect the strongest coupling to occur between states which are close together in energy.

Having limited the number of electronic states, however, we still have to contend with the infinite range of ℓ values. Equation (25) gives for the total cross section for excitation to the electronic state n ,

$$Q_n = \epsilon_n \frac{k_n}{k_0^3} \pi \sum_{\ell, \ell', \Lambda} |T_{n\lambda\ell\Lambda, 00\ell'\Lambda}|^2 ,$$

which we may write

$$Q_n = \sum_{\ell, \ell', \Lambda} Q_{n, \ell, \ell', \Lambda} ,$$

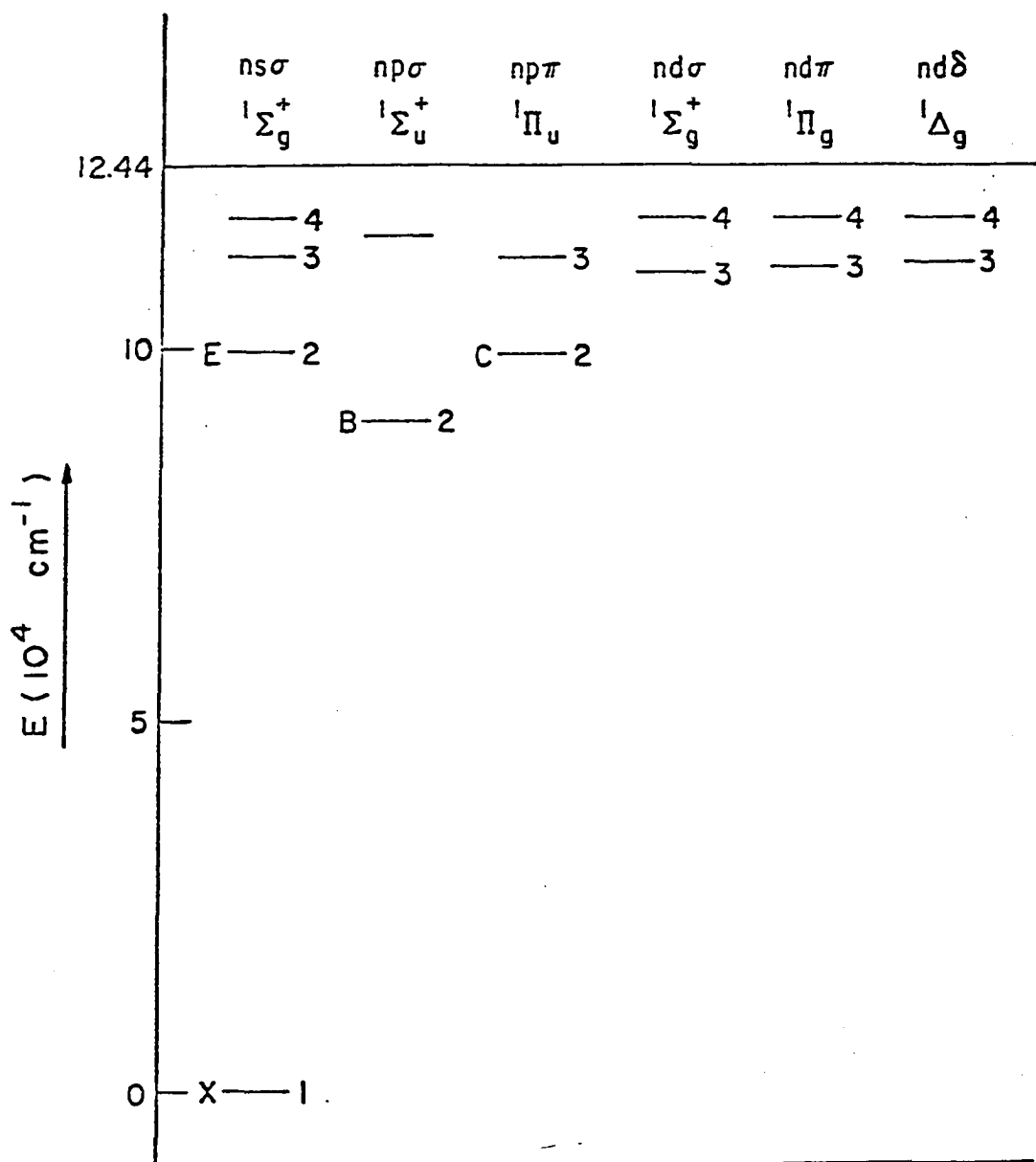


Figure 7. Electronic energy level diagram, showing the approximate position of the $v = 0$ vibrational level of some of the singlet electronic states.

with
$$Q_{n,l,l',\Lambda} = \xi_n \frac{k_n}{k_0^3} \pi |T_{n\lambda l\Lambda, 00l'\Lambda}|^2 .$$

If, for sufficiently large l and l' , the Born approximation gives accurate partial cross sections, then, for some value of L ,

$$Q_{n,l,l',\Lambda} = Q_{n,l,l',\Lambda}^{\text{Born}} \text{ for } l, l' > L ,$$

and the infinite sum for the total cross section may be replaced by the expression

$$Q_n = Q_n^{\text{Born}} + \sum_{l=0}^L \sum_{l'=0}^L \sum_{\Lambda=-L}^L Q_{n,l,l',\Lambda} - Q_{n,l,l',\Lambda}^{\text{Born}} , \quad (35)$$

which contains only a finite number of partial cross sections. Furthermore, the validity of the Born partial cross sections implies that the coupling between different l values is unimportant for $l, l' > L$.

In view of these arguments, it is reasonable to adopt the following procedure. The system of coupled differential equations is set up, including in the system the electronic states X , $C_+(\lambda=+1)$, $C_-(\lambda=-1)$, B , and E , and l values 0 through L . This results in a system of $5L+5$ equations^b

^bSince the interaction potential does not have matrix elements connecting states of different parity, this set of $5L+5$ equations can be further reduced to two sets, one set for states of even parity, and one for states of odd parity. The even parity states are the molecular state X , with even l for the scattered electron; E , with even l ; B , odd l ; C_- , odd l ; and C_+ , odd l . The odd parity states are X , odd l ; E , odd l ; B , even l ; C_- , even l ; and C_+ , even l . The effects of this "diagonality with respect to parity" can be seen in Tables 6, 7, and 8, where alternate partial cross sections vanish.

for each value of Λ , the solutions to which yield the desired partial cross sections. This procedure has been used to obtain partial cross sections at incident electron energies of 15, 25, and 50 eV, and for $L = 3$ and $L = 5$.

The partial cross sections for $\Lambda = 0$ and for 25 eV are given in Table 6 (close coupling with $L = 5$), Table 7 (close coupling with $L = 3$), and Table 8 (Born partial cross sections). For the B and C states, it is seen that the partial cross sections for $l, l' > 3$ which contribute significantly to the total cross section, are given with sufficient accuracy by the Born approximation. That this is so may be seen by the comparison given in Table 9 of some of the larger partial cross sections, as computed by the close coupling and Born approximations. These same conclusions are reached when the corresponding comparisons are made for other values of Λ , so that the total cross section may be obtained by equation (35), using $L \geq 3$. However, these same conclusions are not valid in the case of the E state. Here, the partial cross section for $l = 3, l' = 3$ for the $L = 3$ case differs from that of the $L = 5$ case by about a factor of 3. Also, the Born partial cross sections do not approach the close coupling results for the larger l values.

As was discussed above, by altering the interaction potential matrix in the appropriate manner, solutions can be obtained corresponding to the two-state close coupling approximation (2s), the distorted wave approximation (DW), or the Born approximation (B). Calculations have been done for each of these approximations, as well as for the "full" close coupling method (CC) described above. Table 10 gives the total cross sections for the B state for each of the four approxi-

Table 6. Partial cross sections found by the close coupling approximation with $L = 5$. These cross sections are for $\Lambda=0$, and for 25 eV incident electron energy. The units are $10^{-4} \pi a_0^2$.

	$l' = 0$	1	2	3	4	5	
B state	$l=0$	1160		16.9		.021	
	1	31.1		362		2.98	
	2		88.3		647	1.01	
	3	3.85		15.7		282	
	4		.087		12.0		132
	5	.001		.004		2.87	
	$l' = 0$	1	2	3	4	5	
C state	$l=0$						
	1	388		115		.56	
	2		43.0		171		.17
	3	4.78		7.88		90.2	
	4		.02		11.2		43.2
	5	0.		0.		3.48	
	$l' = 0$	1	2	3	4	5	
E state	$l=0$	178		61.8		.129	
	1		213		7.8		.038
	2	27.9		33.0		3.35	
	3		.174		22.0		2.11
	4	.031		.006		19.7	
	5		0.		.132		13.2

Table 7. Partial cross sections found by the close coupling approximation with $L = 3$. These cross sections are for $\Lambda = 0$ and for 25 eV incident electron energy. The units are $10^{-4} \pi a_0^2$.

		$l' = 0$	1	2	3
B state	$l=0$		1160		12.3
	1	32.8		350	
	2		85.5		631
	3	4.01		13.4	
		$l' = 0$	1	2	3
C state	$l=0$				
	1	406		110	
	2		42.6		204
	3	4.84		8.20	
		$l' = 0$	1	2	3
E state	$l=0$	183		57.6	
	1		210		6.65
	2	27.3		29.2	
	3		.20		61.9

Table 8. Born partial cross sections for $\Lambda=0$ and for 25 eV incident electron energy. The units are $10^{-4} \pi a_0^2$.

	$l' = 0$	1	2	3	4	5	
B state	$l=0$	1240		.009		.0	
	1	29.5		875		.07	
	2		.484		481		.058
	3	.001		2.98		238	
	4		.001		2.14		120
	5	.0		.0		.86	
		$l' = 0$	1	2	3	4	5
C state	$l=0$						
	1	54.6		174		.02	
	2		.30		130		.03
	3	.01		.84		75.0	
	4		.0		.79		36.6
	5	.0		.0		.47	
		$l' = 0$	1	2	3	4	5
E state	$l=0$	657		.282		.0	
	1		191		.043		.0
	2	.006		31.9		.0	
	3		.006		4.05		.0
	4	.0		.0		.44	
	5		.0		.0		.034

Table 9. Some of the larger partial cross sections for the B and C states, showing the agreement between CC and Born for large l . These cross sections are for $\Lambda=0$ and for 25 eV incident electron energy. The units are $10^{-4} \pi a_0^2$.

B State			C State		
(l, l')	CC	Born	(l, l')	CC	Born
(0,1)	1180	1280	(1,2)	117	172
(1,2)	365	881	(2,3)	173	137
(2,3)	649	496	(3,4)	90.1	76.0
(3,4)	289	245	(4,5)	39.8	37.0
(4,5)	127	119	(5,6)	17.4	17.1
(5,6)	55.3	56.6	(6,7)	7.6	7.7
(6,7)	25.9	27.5	(7,8)	3.3	3.5
(7,8)	12.5	13.6	(8,9)	1.5	1.5
(8,9)	6.3	6.8	(9,10)	.70	.74
(9,10)	3.3	3.6	(10,11)	.30	.31
(10,11)	1.9	2.0			

Table 10. Total cross sections for excitation to the B state. Cross sections are in units of πa_0^2 .

Electron energy	CC	2s	DW	Born
15 eV	.97	.90	.97	.67
25 eV	.88	.88	.91	.80
50 eV	.65	.65	.65	.66

mations. The agreement is fairly good between the DW, 2s, and CC results at all of the electron energies given. At 15 eV, we have the unexpected situation that the DW result agrees very well with the CC cross section, while the 2s result is somewhat lower. However, this discrepancy is less than 10 per cent. The Born cross section agrees with the others at 50 eV, but is about 10 per cent lower at 25 eV and 30% lower at 15 eV. It is apparent from these results that, for the B state, the main error in the Born approximation is its neglect of distortion and that the coupling with the other excited states does not affect this cross section very much.

It will be demonstrated later that the coupling between the B state and the other two excited states (C and E) is much weaker than the coupling between the C state and the E state. This being the case, it is reasonable to remove the B state from consideration in the close coupling scheme. Since the situation with regard to the E state was not made very clear by the calculations presented above with $L = 3$ and $L = 5$, more extensive calculations have been done, including in the close coupling scheme the states X, C₋, C₊, and E, and with $L = 7$. These calculations were carried out in the CC, 2s, and Born approximations.

Some of the larger partial cross sections for the E state are shown in Table 11. It is seen that for large l , the Born and 2s partial cross sections agree pretty well.^c For the 75 eV electron

^cThe very small partial cross sections ($\sim .01 \times 10^{-4} \pi a_0^2$) are subject to relatively more numerical error than the larger ones. The values given for these very small cross sections should therefore not be taken too seriously.

Table 11. Some partial cross sections $Q_{l,l',\Lambda}$ ($\Lambda=0$) for excitation to the E state. Units are $10^{-4} \pi a_0^2$.

Electron energy	(l, l')	CC	2s	Born	Electron energy	(l, l')	CC	2s	Born
15 eV	(0,0)	841	880	1190	50 eV	(0,0)	66.8	108	176
	(1,1)	971	1360	83.5		(1,1)	94.4	105	100
	(2,2)	84.3	22.6	3.36		(2,2)	67.3	74.4	40.7
	(3,3)	5.69	.18	.09		(3,3)	15.3	17.8	12.1
	(4,4)	.188	.034	.036		(4,4)	3.44	4.45	3.22
	(5,5)	.041	.006	.006		(5,5)	1.18	.78	.66
	(6,6)	.022	.018	.018		(6,6)	.72	.093	.086
	(7,7)	.035	.024	.023		(7,7)	.72	.0005	.002
25 eV	(0,0)	173	358	655	75 eV	(0,0)	39.5	52.7	73.2
	(1,1)	413	481	190		(1,1)	44.3	49.5	59.0
	(2,2)	69.8	97.1	32.4		(2,2)	39.4	42.9	29.0
	(3,3)	6.22	8.30	3.98		(3,3)	16.5	16.9	13.4
	(4,4)	4.78	.61	.45		(4,4)	5.78	6.51	4.97
	(5,5)	1.88	.030	.034		(5,5)	1.79	2.01	1.76
	(6,6)	.69	.004	.007		(6,6)	.65	.59	.52
	(7,7)	.24	.0004	.001		(7,7)	.22	.14	.14

energy, the CC results for large l are in fair agreement with the 2s and Born results, but for the lower energies this is not the case. For the lower energies, the Born and 2s partial cross sections fall off very rapidly with increasing l . This is due to the fact that the elements of the potential matrix between the ground state and the E state are proportional to $1/r^3$ for large r . The transitions X-C and C-E, however, are optically allowed, so that the corresponding potential matrix elements are proportional to r^{-2} . One would therefore expect a substantial "indirect" contribution to the large l partial cross sections for the E state. This explains the discrepancy between the CC results and the 2s and Born results in the cases where the latter partial cross sections are very small.

From the results given in Table 11, it is clear that, even for the CC approximation, the partial cross sections decrease rapidly with increasing l , so that the total cross section can be found by the expression

$$Q = \sum_{l=0}^L \sum_{l'=0}^L \sum_{\Lambda=-L}^L Q_{l,l',\Lambda}$$

For electron energies of 75 eV and lower, $L = 11$ was found to be adequate.^d The total cross sections for several electron energies are given in Table 13. It is seen that the total cross sections found by the CC and 2s approximations actually agree fairly well (within about 10%) for all electron energies given, even though some of the

^dInclusion of all l values up to $l = 15$ was found to give less than 2% change in the cross section for an electron energy of 75 eV.

partial cross sections were seen to differ by as much as a factor of two. The Born total cross section agrees with the CC and 2s results at the 50 eV and 75 eV energies, but is seen to underestimate the cross section for lower energies.

Some of the larger partial cross sections for the C state are given in Table 12. Here we see that the CC, 2s, and Born results for large l are in adequate agreement, especially for the higher electron energies, where the large l partial cross sections are important. This confirms the conclusions reached above, namely that the total cross section for the C state may be computed by the use of equation (35), with $L \geq 3$. The total cross sections for the C state, computed by equation (35) with $L = 7$, are given in Table 13. The CC and 2s results are in very good agreement over the whole energy range. The Born cross section is within 10 per cent of the CC and 2s results for incident electron energies of 25 eV and higher.

The total cross sections for the B state, computed by the 2s and Born approximations, are also given in Table 13. As in the case of the C state, the Born result is within 10 per cent of the 2s cross section for electron energies of 25 eV and higher.

It has thus been demonstrated that, in the computation of the total excitation cross sections to the electronic states E, B, and C, the coupling between excited states has very little effect. The CC and 2s approximations agree to within 10 per cent for all electron energies above 15 eV, and the Born approximation results fall within this 10% range for electron energies above 50 eV (25 eV for the B and C states). Figures 8, 9, and 10 show the computed cross sections

Table 12. Some partial cross sections $Q_{l,l'}, \Lambda$ ($\Lambda=0$) for excitation to the C state. Units are $10^{-4} \pi a_0^2$.

Electron energy	(l, l')	CC	2s	Born	Electron energy	(l, l')	CC	2s	Born
15 eV	(1,0)	219	260	12.5	50 eV	(1,0)	45.3	25.4	11.7
	(1,2)	9.90	284	63.5		(1,2)	25.4	21.8	24.2
	(2,3)	9.49	44.2	16.2		(2,3)	29.0	25.8	33.5
	(3,4)	1.47	4.27	2.81		(3,4)	29.7	29.5	29.4
	(4,5)	.38	.53	.40		(4,5)	24.6	25.4	24.7
	(5,6)	.084	.099	.086		(5,6)	16.9	19.5	17.6
	(6,7)	.008	.004	.003		(6,7)	12.9	14.3	12.8
25 eV	(1,0)	190	117	27.4	75 eV	(1,0)	14.7	8.36	5.60
	(1,2)	90.2	101	88.5		(1,2)	9.93	8.89	9.67
	(2,3)	86.0	102	64.7		(2,3)	12.5	10.0	15.0
	(3,4)	39.5	55.9	37.5		(3,4)	12.7	11.9	15.7
	(4,5)	14.7	23.6	18.3		(4,5)	15.2	14.4	15.2
	(5,6)	6.22	10.1	8.31		(5,6)	11.4	11.9	12.5
	(6,7)	2.91	4.61	3.91		(6,7)	11.6	11.7	10.6

Table 13. Total cross sections for excitation to the $n = 2$ electronic states, in units of πa_0^2 .

Electron energy	C state			E state			B state	
	CC	2S	B	CC	2s	B	2s	B
15 eV	.688	.699	.448	.389	.346	.142	.897	.666
20 eV	.730	.715	.639	.238	.240	.149	.902	.790
25 eV	.732	.730	.694	.176	.185	.133	.874	.802
30 eV	.706	.708	.703	.143	.150	.118	.819	.782
50 eV	.604	.600	.631	.093	.0862	.0764	.653	.657
75 eV	.511	.502	.532	.059	.0560	.0521	.524	.537

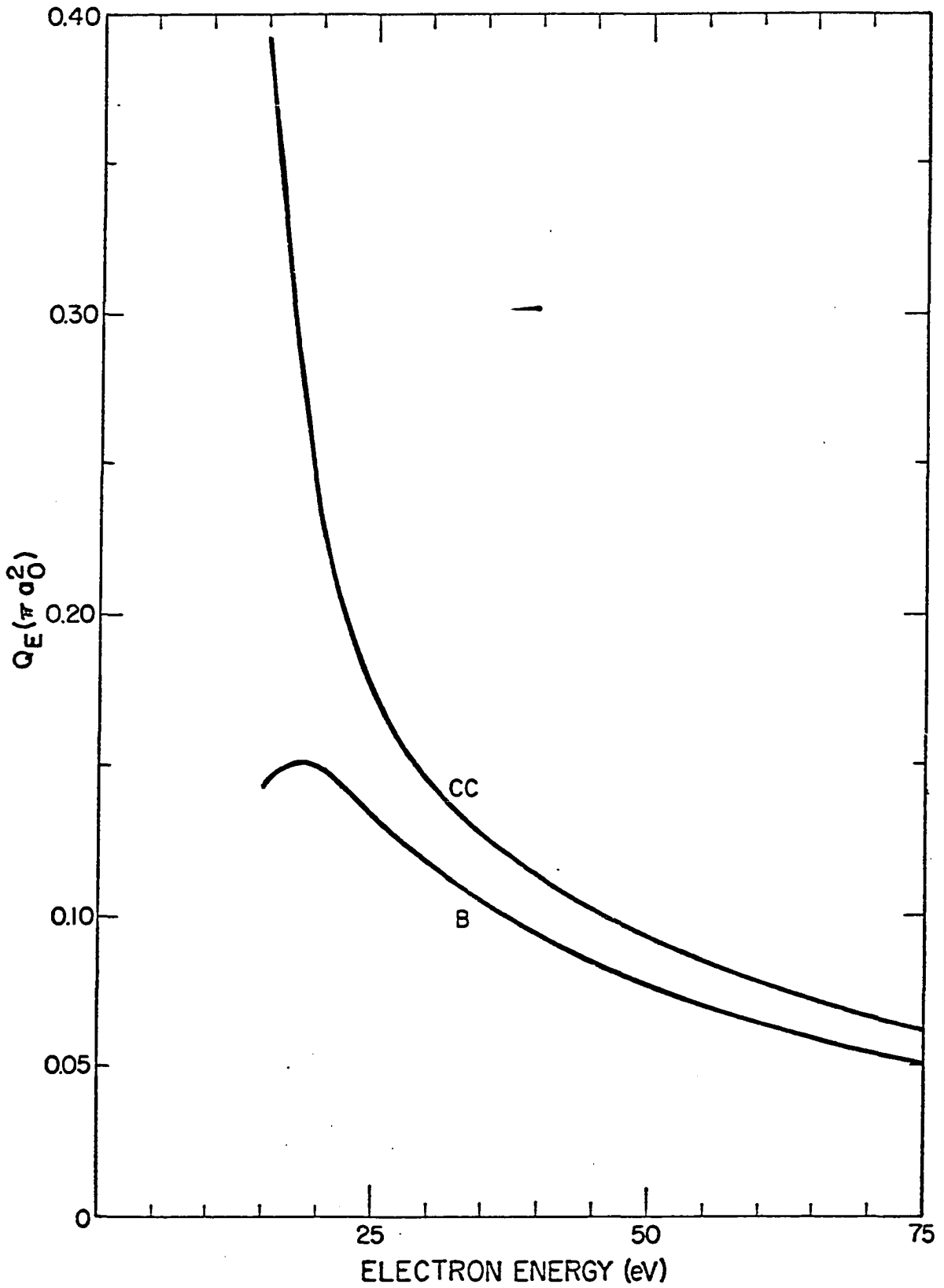


Figure 8. Total cross sections for the E state, as given by the close coupling and Born approximations.

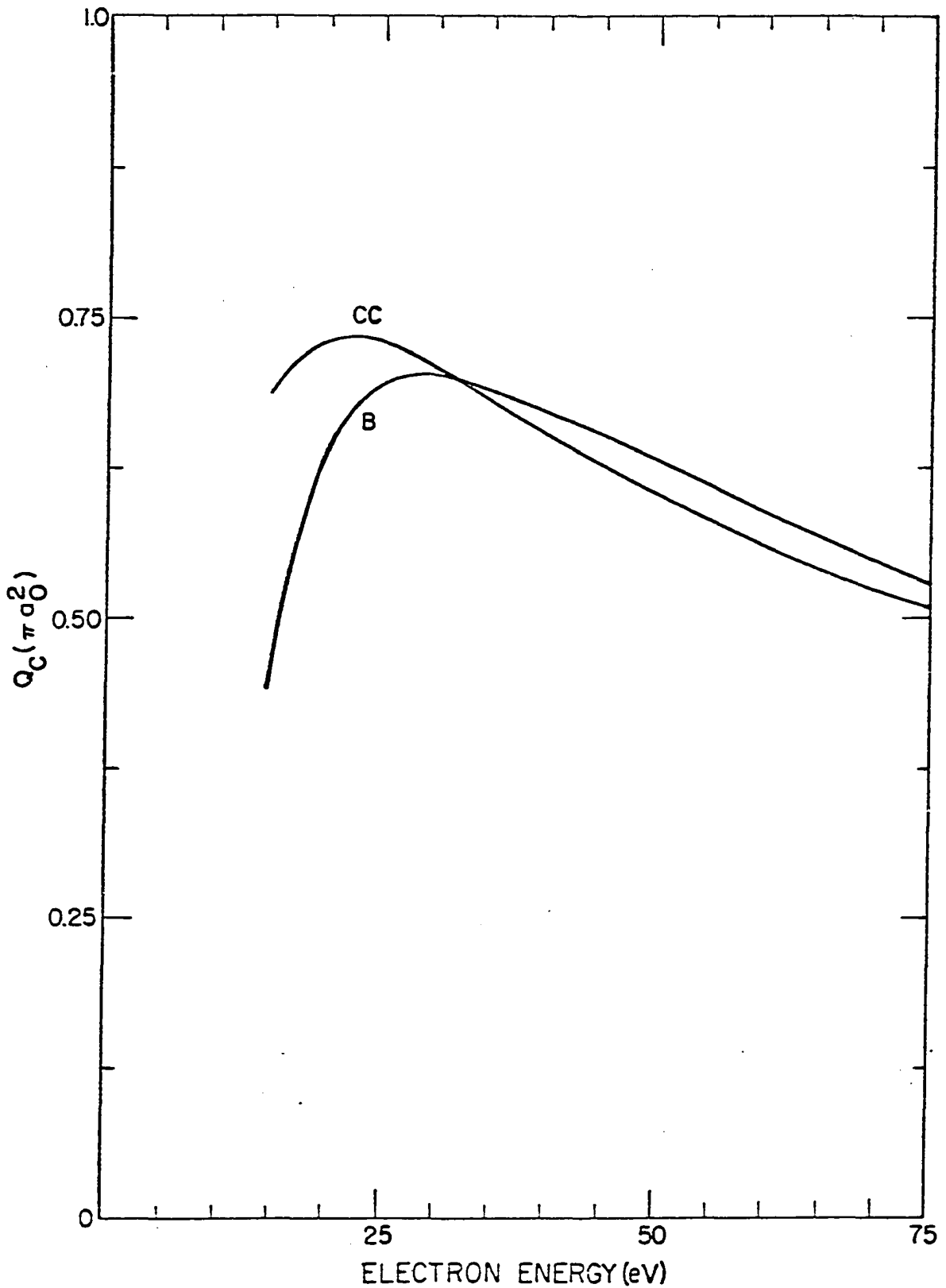


Figure 9. Total cross sections for the C state, as given by the close coupling and Born approximations.

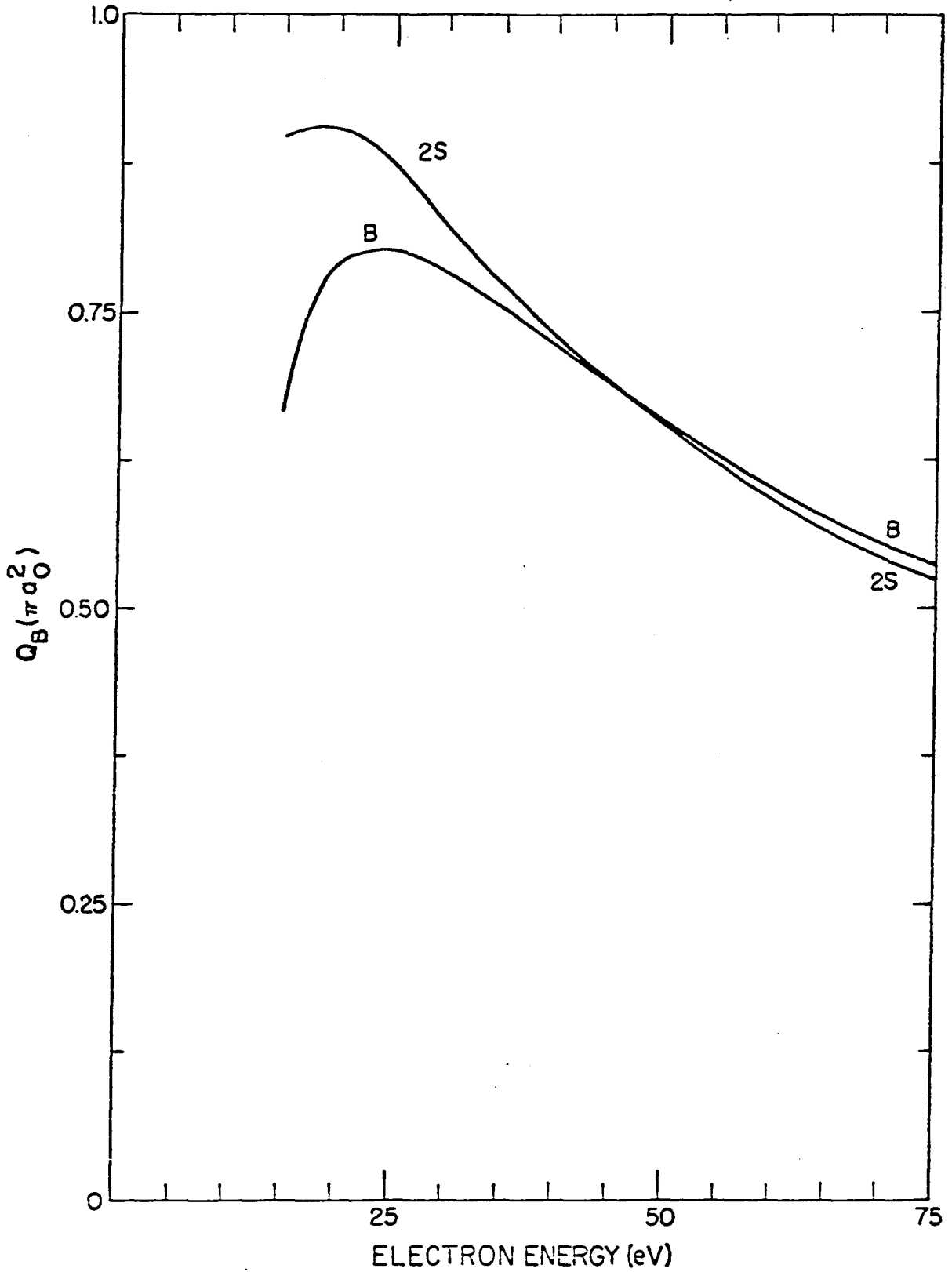


Figure 10. Total cross sections for the B state, as given by the two state close coupling and Born approximations.

for electron energies between 15 eV and 75 eV. For the E and C states, the CC and Born results are plotted vs electron energy, while the 2s and Born results are given for the B state.

In order to see under what conditions the coupling between excited states will have some effect, a "numerical experiment" has been done, in which the various direct matrix elements (i.e., the matrix elements connecting the ground state with excited states) of the interaction potential have been artificially reduced. This has the effect of reducing the "direct" excitation to a particular electronic state relative to the "indirect", so that the coupling effects can be observed. Tables 14, 15, and 16 give the results of these calculations. Column one of each table indicates which direct matrix element has been reduced, and the factor by which it is reduced. For example, "B/10" indicates that the matrix elements connecting the B state with the ground state were reduced by a factor of ten. The results given are not total cross sections, but rather the quantity

$$Q'_n = \sum_{l=0}^3 \sum_{l'=0}^3 \sum_{\Lambda=-3}^3 Q_{n,l,l',\Lambda} .$$

From these numerical results, the following conclusions are evident:

1. In all cases, the 2s approximation gives cross sections which are proportional to the square of the direct matrix elements. Thus, the ground state-excited state coupling may be classified as "weak". This is consistent with the good agreement between the DW and 2s results given in Table 10.
2. The coupling between the C and E states is relatively more

Table 14. Results of the "numerical experiment" for an incident electron energy of 15 eV. The first column indicates which direct matrix elements were reduced, and the factor by which they were reduced.

	Full close coupling			Two-state close coupling		
	C	B	E	C	B	E
C/1	.622	.949	.317	.644	.835	.334
C/3	.245	.942	.156	.077	.842	.339
C/10	.194	.936	.134	.0069	.846	.337
C/30	.188	.940	.131	.00078	.846	.338
	C	B	E	C	B	E
B/1	.622	.949	.317	.644	.835	.334
B/3	.613	.257	.293	.663	.101	.350
B/10	.621	.147	.298	.665	.00903	.353
B/30	.623	.131	.300	.665	.00101	.351
	C	B	E	C	B	E
E/1	.622	.949	.317	.644	.835	.334
E/3	.465	.808	.239	.656	.852	.0383
E/10	.444	.767	.234	.656	.844	.00351
E/30	.440	.751	.234	.656	.848	.000387

Table 15. Results of the numerical experiment for an electron energy of 25 eV. The first column indicates which direct matrix elements were reduced, and the factor by which they were reduced.

	Full close coupling			Two-state close coupling		
	C	B	E	C	B	E
C/1	.454	.547	.139	.418	.505	.178
C/3	.0799	.540	.119	.0477	.514	.181
C/10	.0559	.542	.122	.0043	.512	.181
C/30	.0501	.538	.125	.00048	.511	.181
	C	B	E	C	B	E
B/1	.454	.547	.139	.418	.505	.178
B/3	.465	.102	.128	.425	.0590	.181
B/10	.472	.0378	.133	.427	.0053	.183
B/30	.470	.0286	.134	.425	.000595	.182
	C	B	E	C	B	E
E/1	.454	.547	.139	.418	.505	.178
E/3	.374	.493	.0865	.418	.511	.0199
E/10	.356	.478	.0912	.419	.512	.00180
E/30	.352	.474	.0956	.418	.512	.000201

Table 16. Results of the numerical experiment for an electron energy of 50 eV. The first column indicates which direct matrix elements were reduced, and the factor by which they were reduced.

	Full close coupling			Two-state close coupling		
	C	B	E	C	B	E
c/1	.123	.138	.0514	.101	.123	.0778
c/3	.0251	.139	.0580	.0113	.124	.0787
c/10	.0105	.138	.0608	.00102	.123	.0785
c/30	.00826	.137	.0616	.000113	.123	.0785
	C	B	E	C	B	E
B/1	.123	.138	.0514	.101	.123	.0778
B/3	.125	.0230	.0557	.102	.0139	.0787
B/10	.125	.0069	.0575	.102	.00127	.0791
B/30	.125	.0047	.0581	.102	.000141	.0785
	C	B	E	C	B	E
E/1	.123	.138	.0514	.101	.123	.0778
E/3	.103	.126	.00840	.101	.123	.00868
E/10	.0969	.121	.00727	.101	.123	.000786
E/30	.0948	.121	.00834	.101	.124	.0000871

important than their coupling with the B state.

3. The coupling effects decrease in importance with increasing incident electron energies.

It is of interest to see whether or not the coupling between excited states can also be classified as weak. To this end, a close coupling calculation was done including the ground state, the C state, and the E state, in which the matrix elements connecting the ground state and the E state were effectively reduced to zero, and the matrix elements connecting the E and C states were varied. This calculation was done for an electron energy of 25 eV. It was found that reducing the C-E matrix elements by a factor of two reduced the cross section to the E state for "indirect excitation" from .0540 to .0145, which is approximately a factor of four. It is therefore concluded that the coupling between the excited states is also weak.

Thus it is seen that, at least for incident electron energies of 25 eV and higher, the coupling between each pair of electronic states is in the weak coupling regime, and although the effects of the coupling between the different excited states can be observed in certain aspects of the calculation, they do not have much effect on the total cross sections.

CHAPTER VI

CLOSE COUPLING WITH VIBRATION INCLUDED

To obtain the cross sections for excitation to the individual vibrational levels of each electronic state, the vibrational motion of the nuclei must be taken into account in the close coupling theory. This may be done by a straightforward generalization of the equations (25), (28), and (29). The equations become

$$Q_{nv} = \xi_n \frac{k_{nv}}{k_0^3} \pi \sum_{l, l', \Lambda} \left| T_{n\lambda v l \Lambda; 000 l' \Lambda} \right|^2, \quad (25')$$

$$\left\{ \frac{d^2}{dr_3^2} - \frac{l''(l''+1)}{r_3^2} + k_{n''v''}^2 \right\} F_{\mu''\mu''}(r_3) \\ = \sum_{\mu'} U_{\mu''\mu'}(r_3) F_{\mu'\mu'}(r_3), \quad (28')$$

where the index μ now stands for the set of quantum numbers $n\lambda v l \Lambda$, v being the vibrational quantum number, and

$$U_{\mu''\mu'}(r_3) = \int R^2 dR \int d\hat{r}_3 \int d\vec{r} \left\{ \varphi_{n''}^*(v''|R) \right. \\ \left. \psi^*(n'\lambda'|\vec{r}, R) Y_{l', \Lambda' - \lambda'}^*(\hat{r}_3) 2V \varphi_n(v|R) \right. \\ \left. - \psi(n\lambda|\vec{r}, R) Y_{l, \Lambda - \lambda}(\hat{r}_3) \right\}, \quad (29')$$

which becomes

$$U_{\mu\mu'}(r_3) = 4 \sum_K C^K(\ell, \Lambda' - \lambda; \ell', \Lambda' - \lambda') \delta_{\Lambda'; \Lambda}$$

$$\int_{R^2 dR} \left\{ \varphi_n^*(v'|R) \left[V_K(R, r_3, n'\lambda', n\lambda) - \frac{R^K}{R^{K+1}} \delta_{n'\lambda', n\lambda} \delta_{K, \text{even}} \right] \varphi_n(v|R) \right\} .$$

It has been previously concluded, for the case where vibrational effects were ignored, that the coupling between the different electronic states has little effect on the computed cross sections. This coupling was shown to become important, however, if the direct matrix elements were artificially reduced. Since the inclusion of the vibrational portion of the wave functions will appreciably reduce all of the non-diagonal elements of $U_{\mu\mu'}$, the importance of the coupling between electronic states must be re-examined.

In the "numerical experiment" that was described in the previous chapter, it was seen that the cross section for direct excitation is proportional to the square of the matrix element of the potential between the ground state and the excited state in question. But since the cross section is given by the square of the appropriate elements of the T matrix, we have the result that for direct excitation,

$$T_{n\lambda v \ell \Lambda; 000 \ell' \Lambda}^{(\text{direct})} = U_{n\lambda v \ell \Lambda; 000 \ell' \Lambda} .$$

Similarly, at least for electron energies of 25 eV and higher, where the coupling between excited states was also shown to be in the weak

regime, it is expected that the contribution due to indirect excitation via the state $n'\lambda'v'$ will be proportional to the product of the two matrix elements involved,

$$T_{n\lambda v\ell\Lambda;000\ell''\Lambda}^{(\text{indirect, via } n'\lambda'v')} \approx U_{n\lambda v\ell\Lambda;n'\lambda'v'\ell'\Lambda} U_{n'\lambda'v'\ell'\Lambda;000\ell''\Lambda} .$$

But this has the form

$$\int R^2 dR \varphi_n^*(v|R) f(R) \varphi_{n'}(v'|R) \int R^2 dR \varphi_{n'}^*(v'|R) g(R) \varphi_0(o|R) ,$$

which, upon summing over v' , becomes

$$\begin{aligned} & \sum_{v'} \int R^2 dR \varphi_n^*(v|R) f(R) \varphi_{n'}(v'|R) \int R^2 dR \varphi_{n'}^*(v'|R) g(R) \varphi_0(o|R) \\ &= \int R^2 dR \varphi_n^*(v|R) f(R) g(R) \varphi_0(o|R) \\ &\approx f(R_0) g(R_0) \int R^2 dR \varphi_n^*(v|R) \varphi_0(o|R) . \end{aligned}$$

Since the direct contribution is also approximately proportional to this same overlap integral

$$\int R^2 dR \varphi_n^*(v|R) \varphi_0(o|R) ,$$

the result is obtained that the indirect contribution, summed over all the vibrational levels of the intermediate electronic state, is reduced by the same factor as the direct contribution. It is therefore to be expected that, for the higher electron energies, the coupling between the different excited electronic states will not be any more important for the case with vibration included than it was for the problem without vibration.

Within an electronic state, however, there may be coupling between the various vibrational levels, since the interaction potential will have matrix elements which connect them. Consider the expression

$$\int R^2 dR \varphi_n^*(v'|R) \varphi_n(v|R) \left\{ V_K(R, r_3, n\lambda, n\lambda) - \frac{R^K}{R^{K+1}} \delta_{K, \text{even}} \right\} .$$

V_K will be non-zero only for even values of K . The $K = 0$ term will vanish for large r_3 , owing to the orthogonality of the vibrational wave functions. Thus, the $K = 2$ term will be the first non-vanishing term, and it is seen that the matrix elements connecting the different vibrational levels are proportional to $1/r_3^3$ for large r_3 . This indicates that this type of coupling should be small, at least for high electron energies.

To see whether or not this is so, calculations were done for the B and E states, taking into account the coupling between the vibrational levels. The higher vibrational levels of the ground electronic state are not included here. The effects of the inclusion of these levels will be shown below. Table 17 shows the results for the B state. The column labelled CC gives the cross sections calculated by the close coupling method, in which the ground vibrational level of the ground state, and the first four vibrational levels of the B state were included. The column labelled 2s gives the corresponding two-state close coupling cross sections (coupling between the vibrational levels of the B state is not included), while the Born results are given in the next column. It is seen, by comparison of the CC and 2s results, that the coupling between the B state vibrational levels has very little effect on the cross sections. In fact, for all but the

Table 17. Cross sections for excitation of the first four vibrational levels of the B state. The cross sections are in units of πa_0^2 .

Electron energy		CC	2s	Born	2s*
15 eV	v = 0	.0061	.0066	.0046	.0059
	1	.020	.023	.0146	.019
	2	.043	.048	.027	.035
	3	.063	.074	.0382	.049
25 eV	v = 0	.0053	.0057	.0056	.0055
	1	.017	.019	.018	.018
	2	.035	.037	.035	.034
	3	.050	.055	.050	.050
50 eV	v = 0	.0043	.0044	.0046	.0043
	1	.014	.014	.015	.014
	2	.027	.028	.029	.027
	3	.040	.041	.042	.040

lowest electron energy, the CC, 2s, and Born results are practically identical.

Table 18 gives the results for the E state. The E state is a particularly interesting case, because of the fact that the $v = 2$ and $v = 3$ levels have "direct" excitation cross sections which are several orders of magnitude less than those for the neighboring vibrational levels. This is because of the unusual double minimum in the E state potential curve, and the fact that the $v = 2$ and $v = 3$ levels lie almost entirely in the outer minimum. Even in this very extreme situation, however, the coupling between vibrational levels doesn't appear to be very important, especially for the higher electron energies.

Thus, it can be concluded that, for incident electron energies of 25 eV and higher, the coupling between the vibrational levels of the excited electronic states can be neglected. Furthermore, because of the absence of coupling effects, one might suspect that the Born approximation (with the R variation of the scattering amplitude taken into account) should give about the right relative cross sections for the vibrational levels of a given electronic state. In Tables 17 and 18, the columns labelled 2s* give cross sections calculated by the expression

$$Q_{nv}^{2s*} = Q_n^{2s} \left(Q_{nv}^{\text{Born}} / Q_n^{\text{Born}} \right) ,$$

where Q_n^{2s} is the total cross section for excitation to the electronic state n, calculated by the 2s approximation, Q_n^{Born} is the corresponding Born result, and Q_{nv}^{Born} is the Born cross section for excitation to the

Table 18. Cross sections for excitation of the first four vibrational levels of the \bar{E} state. The cross sections are in units of πa_0^2 .

Electron energy		CC	2s	Born	2s*
15 eV	v = 0	.061	.057	.021	.048
	1	.080	.075	.028	.061
	2	.(5)46	.(5)25	.(5)14	.(5)32
	3	.(4)41	.(4)33	.(4)18	.(4)40
25 eV	v = 0	.030	.029	.021	.028
	1	.041	.040	.028	.037
	2	.(5)22	.(5)16	.(5)14	.(5)19
	3	.(4)24	.(4)22	.(4)19	.(4)25
50 eV	v = 0	.014	.013	.012	.013
	1	.018	.018	.016	.018
	2	.(6)96	.(6)83	.(6)83	.(6)92
	3	.(4)12	.(4)11	.(4)11	.(4)12

vibrational level v of the electronic state n . The $2s^*$ results differ from the CC results by about 20 per cent at the most, and for electron energies of 25 eV and 50 eV, the two sets of results are in very good agreement.

Having concluded that the coupling between the vibrational levels of a given electronic state can safely be ignored for all but the lowest electron energies, it is of interest to perform calculations to check the earlier conclusion that the coupling between different excited electronic states could also be ignored. To this end, a close coupling calculation was done including the electronic-vibrational states $X, v=0$; $X, v=1$; $X, v=2$; $C_-, v=0$; $C_-, v=1$; $C_+, v=0$; $C_+, v=1$; and $E, v=0$; and with $L = 7$. As we have concluded previously, the E state couples more strongly with the C state than with the B state, and examination of the various overlap integrals reveals that the $E, v=0$ state will couple much more strongly with the first two levels of the C state than with any of the higher levels. Thus, this calculation should reveal any important coupling effects. The two higher levels of the ground electronic state were included in order to see if their presence would affect the cross sections for the higher electronic states.

The results of this calculation are presented in Table 19, and compared with the corresponding $2s$ cross sections. For the $v=0$ and $v=1$ levels of the C state, the CC and $2s$ results agree to within 10 per cent for each electron energy. The same is true of the $E, v=0$ state for the 25 eV and 50 eV electron energies, but for the 15 eV energy the two results differ by about 50 per cent. For incident

Table 19. Results of the close coupling calculation including some vibrational levels of the X, C, and E states.

Electron energy		CC	2s
15 eV	X, v=1	.057	.049
	X, v=2	.0074	.0015
	C, v=0	.11	.11
	C, v=1	.14	.16
	E, v=0	.084	.060
25 eV	X, v=1	.029	.026
	X, v=2	.0027	.0012
	C, v=0	.083	.083
	C, v=1	.12	.13
	E, v=0	.029	.031
50 eV	X, v=1	.013	.012
	X, v=2	.00096	.00082
	C, v=0	.040	.038
	C, v=1	.057	.059
	E, v=0	.0134	.015

electron energies of 25 eV and higher, then, it may be said that the two-state close coupling approximation is adequate, both for calculating the total cross sections (summed over vibrational levels) and for the cross sections to the individual vibrational levels of the excited electronic states. For electron energies below 25 eV, these conclusions are not always valid.

It is interesting to note that the cross sections for vibrational excitation within the ground electronic state are apparently affected quite strongly by the coupling between these vibrational levels and the higher electronic states. The CC result for the X, $v=2$ state differs from the 2s result by a factor of five at 15 eV, while a CC calculation^a of this same cross section which did not include the higher electronic states gave a result which was within 10 per cent of the 2s cross section. This is apparently due to the fact that the coupling between the vibrational levels of any single electronic state is very weak, while the coupling between the X electronic state and the C electronic state, for example, is much stronger.

To further investigate the effects of the inclusion of the levels X, $v=1$; and X, $v=2$ in the close coupling scheme, a CC calculation exactly like the one described above, but with these two levels excluded,

^aThis close coupling calculation included the first few vibrational levels of the ground electronic state, but did not include any of the higher electronic states. The agreement between the results of this CC calculation and the corresponding 2s results further supports the above conclusion that the coupling between the vibrational levels of a given electronic state is very weak.

was performed. The resulting cross sections for the vibrational levels of the C state were within 5% of those reported in Table 19, while the cross sections for the E, $v=0$ state were within 10%. In view of these results, it may be concluded that the excited vibrational levels of the ground electronic state need not be included in the close coupling scheme for the calculation of cross sections for the excitation to the higher electronic states.

To summarize, then, it has been demonstrated that for electron energies greater than 15 eV, the coupling between the different excited electronic states has relatively little effect on the total cross sections. In the case of excitation to the B state, this indirect coupling also has little effect on the partial cross sections. The C state partial cross sections are affected to a greater extent than those for the B state, but for electron energies of 25 eV and higher, the indirect coupling effects are still not too important. Thus, for these two states, the main error in the Born approximation is its neglect of distortion. The partial cross sections for the E state show a stronger dependence than do those for the B and C states on the indirect coupling, but this dependence is also seen to diminish for higher electron energies.

For electron energies of 25 eV and higher, then, the total cross sections for excitation to each electronic state may be computed without including the coupling between excited states. The coupling between the different vibrational levels is also unimportant. Furthermore, the relative cross sections for excitation of the vibrational levels within an excited electronic state are given adequately by the

Born approximation, taking into account the R variation of the scattering amplitude. Thus, the cross sections for excitation to the various vibrational levels of these electronic states may be found by multiplying the total cross section to each electronic state by the factor $(Q_{iv}^{\text{Born}} / Q_n^{\text{Born}})$.

The cross sections for the first few vibrational levels of the B, C, and E states are given in Table 20, for incident electron energies of 25, 50, and 75 eV.

Table 20. Cross sections for excitation to the vibrational levels of the electronic states of the $n = 2$ manifold, in units of πa_0^2 .

	Electron						
	energy	$v = 0$	$v = 1$	$v = 2$	$v = 3$	$v = 4$	$v = 5$
B state	25 eV	.0061	.020	.038	.054	.066	.073
	50 eV	.0046	.0015	.029	.042	.052	.057
	75 eV	.0037	.012	.023	.034	.042	.046
C state	25 eV	.098	.14	.13	.098	.067	.043
	50 eV	.083	.12	.11	.086	.059	.039
	75 eV	.071	.105	.097	.074	.051	.033
E state	25 eV	.027	.036	.(5)18	.(4)25	.028	.0018
	50 eV	.012	.017	.(6)86	.(4)11	.013	.00084
	75 eV	.0077	.011	.(6)55	.(5)72	.0081	.00053

CHAPTER VII

CONCLUSIONS

1. The coupling between each pair of electronic states considered is in the weak coupling regime. The indirect coupling has little effect on the partial cross sections as well as the total cross section for excitation to the B state. The C state partial cross sections are noticeably affected by the indirect coupling only for electron energies below 25 eV, while those for the E state are noticeably affected for all electron energies below 50 eV. The total cross sections for both the C and E states, however, are given with adequate accuracy by the 2s approximation for electron energies of 25 eV and higher.
2. The Born approximation gives accurate results (within about ten per cent of the close coupling results) for incident electron energies of 50 eV and higher. The Born cross sections are smaller than the close coupling results at low energies, owing primarily to the neglect of distortion of the incoming wave.
3. The coupling between the different vibrational levels of a given electronic state is not important for any of the incident electron energies for which calculations were done. For

electron energies of 25 eV and higher, the Born approximation, with the R variation of the scattering amplitude taken into account, gives accurate relative cross sections for excitation of the different vibrational levels.

BIBLIOGRAPHY

1. B. L. Moiseiwitsch, and S. J. Smith, Electron Impact Excitation of Atoms (Review Article), *Rev. Mod. Phys.*, 40, 238 (1968).
2. H. S. W. Massey, and C. B. O. Mohr, *Proc. Roy. Soc. (London)*, A135, 258 (1932).
3. R. Roscoe, *Phil. Mag.*, 31, 349 (1941).
4. J. K. L. MacDonald, *Proc. Roy. Soc. (London)*, A136, 528 (1932).
5. S. P. Khare, *Phys. Rev.*, 149, 33 (1966).
6. S. Huzinaga, *Progr. Theoret. Phys. (Kyoto)*, 17, 162 (1957).
7. L. L. Barnes, N. F. Lane, and C. C. Lin, *Phys. Rev.*, 137, A388 (1965); and S. Chung and C. C. Lin, *Bull. Am. Phys. Soc.*, 13, 214 (1968).
8. E. R. Davidson, *J. Chem. Phys.*, 35, 1189 (1961).
9. S. Rothenberg, and E. R. Davidson, *J. Chem. Phys.*, 45, 2560 (1966).
10. W. Kolos, and L. Wolniewicz, *J. Chem. Phys.*, 43, 2429 (1965); 45, 509 (1966).
11. K. J. Miller, and M. Krauss, *J. Chem. Phys.*, 47, 3754 (1967).
12. J. D. Craggs, and H. S. W. Massey, *Handbuch der Physik (Springer-Verlag, Berlin, 1959)*, Vol. 37, Pt. 1, p. 333.
13. H. and B. S. Jeffries, *Mathematical Physics (Cambridge, University Press, 1962)*.
14. E. U. Condon, and G. H. Shortley, *The Theory of Atomic Spectra (Cambridge, University Press, 1964)*.

15. F. A. Sharpton, et al, Bull. Am. Phys. Soc., 13, 897 (1968).
16. R. D. Cowan, and K. L. Andrew, J. Opt. Soc., 55, 502 (1965).
17. R. D. Cowan, Phys. Rev., 163, 54 (1967).
18. C. E. Moore, Atomic Energy Levels, Vol. I, N. B. S. Circular 467, (1949).

APPENDIX I

NUMERICAL PROCEDURES

Evaluation of the Interaction Potential Matrix Elements

In the expression for the matrix elements of the interaction potential,

$$U_{\mu\mu} = 4 \sum_K C^K(\ell, \Lambda' - \lambda; \ell', \Lambda' - \lambda') \delta_{\Lambda', \Lambda} \int R^2 dR \left\{ \varphi_n(v'|R) \left[V_K(R, r_3, n'\lambda', n\lambda) - \frac{R^K}{R^{K+1}} \delta_{n'\lambda', n\lambda} \delta_{K, \text{even}} \right] \varphi_n(v|R) \right\} ,$$

with

$$V_K(R, r_3, n'\lambda', n\lambda) = N_n N_n \left\{ U_K(R, r_3, \infty, \infty) \delta_{n'\lambda', n\lambda} + U_K(R, r_3, n'\lambda', \infty) \delta_{n\lambda, \infty} + U_K(R, r_3, \infty, n\lambda) \delta_{n'\lambda', \infty} + U_K(R, r_3, n'\lambda', n\lambda) \right\} ,$$

the quantities which must be evaluated by numerical integration are

$$U_K(R, r_3, n'\lambda', n\lambda) = \left(\frac{R}{2}\right)^3 \int_1^\infty d\xi \int_{-1}^1 d\eta (\xi^2 - \eta^2) f_n(\xi, \eta) \frac{R^K}{R^{K+1}} P_{K, \lambda' - \lambda}(\cos\theta) f_n(\xi, \eta) ,$$

and the integrals involving the vibrational wave functions. To evaluate $U_K(R, r_3, n'\lambda', n\lambda)$, the substitutions

$$r = \frac{R}{2} [\xi^2 + \eta^2 - 1]^{1/2}, \text{ and}$$

$$\cos \theta = -\xi\eta / [\xi^2 + \eta^2 - 1]^{1/2},$$

are made, and then the numerical integration is carried out. Twelve point Gauss Legendre quadrature is used for the integration over η , and twelve point Gauss Laguerre quadrature for the integration over ξ .

The quantity $V_K(R, r_3, n'\lambda', n\lambda)$ is evaluated for six values of R from $R = 1.0$ to $R = 2.0$, for 100 values of r_3 , ranging from $r_3 = .01$ to $r_3 = 100$, and for $K = 0$ through $K = 5$. For each value of r_3 and K , the R dependence is approximated by a quadratic least squares fit,

$$V_K(R, r_3, n'\lambda', n\lambda) \approx V_K^0(r_3, n'\lambda', n\lambda) + V_K^1(r_3, n'\lambda', n\lambda)X \\ + V_K^2(r_3, n'\lambda', n\lambda)X^2,$$

with $X = R - R_0$, R_0 being the ground state equilibrium separation.

The quantities

$$(n'v'|nv) = \int R^2 dR \varphi_n(v'|R) \varphi_n(v|R),$$

$$(n'v'|x|nv) = \int R^2 dR \varphi_n(v'|R) (R - R_0) \varphi_n(v|R),$$

$$(n'v'|x^2|nv) = \int R^2 dR \varphi_n(v'|R) (R - R_0)^2 \varphi_n(v|R), \text{ and}$$

$$(n'v'| \frac{R^K}{R^{K+1}} |nv) = \int R^2 dR \varphi_n(v'|R) \frac{R^K}{R^{K+1}} \varphi_n(v|R),$$

are evaluated by a 400 point Simpson's rule integration.

The expression for $U_{\mu\mu}$ is then

$$U_{\mu\mu}(r_3) = 4 \sum_{K=0}^5 C^K(\ell, \Lambda' - \lambda; \ell', \Lambda' - \lambda') \delta_{\Lambda', \Lambda} \left\{ V_K^0(r_3, n'\lambda', n\lambda) (n'v'|nv) + V_K^1(r_3, n'\lambda', n\lambda) (n'v'|x|nv) + V_K^2(r_3, n'\lambda', n\lambda) (n'v'|x^2|nv) - (n'v'| \frac{R^K}{R^{K+1}} |nv) \delta_{n'\lambda', n\lambda} \delta_{K, \text{even}} \right\} ,$$

for the case where the vibrational states are included in the close coupling scheme, and

$$U_{\mu\mu}(r_3) = 4 \sum_{K=0}^5 C^K(\ell, \Lambda' - \lambda; \ell', \Lambda' - \lambda') \delta_{\Lambda', \Lambda} \left\{ V_K^0(r_3, n'\lambda', n\lambda) - (no| \frac{R^K}{R^{K+1}} |no) \delta_{n'\lambda', n\lambda} \delta_{K, \text{even}} \right\} ,$$

for the case where vibrational effects are ignored. It may be noted that for the latter case, the nuclear attraction term is taken to be the average value of this quantity in the ground vibrational level of each electronic state.

$U_{\mu\mu}$ is thus found and tabulated for the 100 values of r_3 . In the course of the numerical solution of the differential equations, the potential matrix is found by linear interpolation in this table.

Solution of the Coupled Differential Equations

In matrix notation, the system (28) of coupled differential equations may be written

$$F''(x) = G(x) F(x)$$

where x is used as the independent variable in place of r_3 . The elements of the matrix G are known at each value of x . It is known that $F(0) = 0$, and the aim is to integrate the differential equation from $x = 0$ out to large values of x so that the matrices A and B can be found from the condition

$$F(x) \underset{\text{large } x}{\sim} H_1(x) A + H_2(x) B .$$

It is known that the "principle of detailed balance" requires that the matrix $R = BA^{-1}$ be symmetric. Thus, any approximate, numerical integration scheme must be such as to yield a symmetric R matrix. It is instructive at this point to see what property of an exact solution of the differential equation guarantees that R is symmetric.

Multiplying the differential equation by \tilde{F} , we have

$$\tilde{F} F'' = \tilde{F} G F .$$

But the G matrix is symmetric, so that

$$\tilde{F} F'' - \tilde{F}'' F = \tilde{F} G F - \tilde{F} \tilde{G} F = 0 ,$$

and, therefore

$$\int_0^x (\tilde{F} F'' - \tilde{F}'' F) dx = 0 .$$

Integrating once by parts, we have

$$(\tilde{F} F' - \tilde{F}' F) \Big|_0^x - \int_0^x (\tilde{F}' F' - \tilde{F} F'') dx = 0 \quad ,$$

and, since $F(0) = 0$, we have the result that

$$\tilde{F} F' - \tilde{F}' F = 0$$

at each value of x . At large x , then, we find

$$(\tilde{A} H_1 + \tilde{B} H_2)(H_1' A + H_2' B) - (\tilde{A} H_1' + \tilde{B} H_2')(H_1 A + H_2 B) = 0 \quad ,$$

or,

$$\begin{aligned} & \tilde{A} H_1 H_2' B + \tilde{B} H_2 H_1' A - \tilde{A} H_1' H_2 B - \tilde{B} H_2' H_1 A \\ & = \tilde{A} (H_1 H_2' - H_1' H_2) B - \tilde{B} (H_1 H_2' - H_1' H_2) A = 0 \quad . \end{aligned}$$

But $H_1 H_2' - H_1' H_2 = -1$, so that $\tilde{A} B = \tilde{B} A$.

Multiplying on the right by A^{-1} , and on the left by \tilde{A}^{-1} , we find

$$B A^{-1} = \tilde{A}^{-1} \tilde{B}, \text{ or } R = \tilde{R} \quad .$$

Thus, we see that an exact solution of the differential equation will have

$$\tilde{F} F' = \tilde{F}' F \quad ,$$

and this guarantees that $R = \tilde{R}$. If the numerical integration scheme is such that $\tilde{F} F'$ is symmetric at each point of the integration, then the R matrix will be symmetric.

We require, then, a scheme with the property that if

$$\tilde{F}_n F'_n = \tilde{F}'_n F_n, \text{ where } F_n = F(x_n),$$

then

$$\tilde{F}_{n+1} F'_{n+1} = \tilde{F}'_{n+1} F_{n+1}.$$

It was found that the following scheme has this property:

$$F'_{n+1} = F'_n + F''_n \Delta x,$$

$$F_{n+1} = F_n + F'_n \Delta x + F''_n \Delta x^2,$$

with $F''_n = G_n F_n,$

or $F'_{n+1} = F'_n + G_n F_n \Delta x,$

$$F_{n+1} = F_n + F'_{n+1} \Delta x.$$

This integration scheme is accurate only to first order in Δx , and therefore requires very small integration steps. However, for the large matrices involved here, this is by far the most efficient method of those that were tried, since it requires only a single matrix product for each integration step, while the Kumerov method, for example, requires a matrix inversion for each step. In trying other integration schemes, which did not automatically preserve the symmetry of the R matrix, it was found that very high accuracy of integration was sometimes required in order to obtain accurate cross sections. In particular, a fourth order Runge-Kutta routine for solving simultaneous differential equations yielded reasonable results only when the integration was

accurate to eight or nine significant figures. In contrast to this, the method described above gives cross sections whose accuracy is comparable to the accuracy of integration.

To start the integration procedure, initial values are needed for F and F' . The requirements are that $F(x_0)$ correspond to a solution that goes to zero at the origin, that

$$\det|F(x_0)| \neq 0 \quad ,$$

and that $\tilde{F}(x_0) F'(x_0)$ be symmetric. These last two requirements are met if we choose $F(x_0)$ to be diagonal. With this choice, the differential equations for the diagonal elements are

$$\left\{ \frac{d^2}{dx^2} - \frac{\ell(\ell+1)}{x^2} + k_n^2 - U_{\mu\mu}(x) \right\} F_{\mu\mu}(x) = 0 \quad .$$

Now, as $x \rightarrow 0$, the diagonal elements of the interaction potential approach constant values, namely

$$U_{\mu\mu}(0) = 2 \left\{ \left(n\lambda \left| \frac{1}{r_1} + \frac{1}{r_2} \right| n\lambda \right) - \frac{4}{R} \right\} \quad ,$$

so that the differential equations are

$$\left\{ \frac{d^2}{dx^2} - \frac{\ell(\ell+1)}{x^2} + b^2 \right\} F_{\mu\mu}(x) = 0 \quad ,$$

where $b^2 = k_n^2 - U_{\mu\mu}(0)$. The solutions of this which go to zero at the origin are the functions

$$f_\ell(x) = b x j_\ell(bx) \quad ,$$

where j_ℓ is a spherical Bessel function. We therefore choose as initial values for F and F' ,

$$F_{\mu\mu}(x_0) = f_\ell(x_0) \delta_{\mu\mu}, \text{ and}$$

$$F'_{\mu\mu}(x_0) = f'_\ell(x_0) \delta_{\mu\mu}.$$

x_0 was normally chosen to be .01 (in units of a_0), and Δx was initially .001. The accuracy of the solution was tested^a at each step of the integration, and the value of Δx adjusted to keep the accuracy within the desired limits. Acceptable upper and lower limits on the error per integration step were found to be .5 per cent and .05 per cent, respectively. Reducing these limits by a factor of ten produced very little change in the calculated cross sections. On the average, the Δx required for the accuracy specified above was about .01 or .02.

Evaluation of the Born Integrals

The basic integral involved in evaluating the Born cross section is

$$\epsilon_{\text{on}}(q, R, \cos \Theta) = \sqrt{2} \left(\frac{R}{2}\right)^3 \int_{-1}^1 d\eta \int_1^\infty d\xi (\xi^2 - \eta^2) f_0(\xi, \eta)$$

$$f_n(\xi, \eta) e^{-iq_{\parallel} \frac{R}{2} \xi \eta} J_m \left\{ q_{\perp} \frac{R}{2} [(\xi^2 - 1)(1 - \eta^2)]^{1/2} \right\},$$

with $q_{\parallel} = q \cos \Theta$, $q_{\perp} = q \sin \Theta$, Θ being the angle between R and the direction of incidence of the incoming electrons. This two

^aThe test for accuracy was made only for the diagonal elements of F and F' .

dimensional integral is evaluated numerically, using twelve point Gauss-Laguerre quadrature for the integral over ξ and twelve point Gauss-Legendre quadrature for the integral over η . It is evaluated for six values of R , ranging from $R = 1.0$ to $R = 2.0$, for twelve values of $\cos \Theta$ (those values appropriate for the Gauss-Legendre quadrature formula), and 35 values of q , ranging from $q = .01$ to $q = 10$. For each value of $\cos \Theta$ and each value of q , the variation of $\varepsilon_{\text{on}}(q, R, \cos \Theta)$ with R is approximated by a quadratic least squares fit, giving

$$\varepsilon_{\text{on}}(q, R, \cos \Theta) = \varepsilon_{\text{on}}^0(q, \cos \Theta) + \varepsilon_{\text{on}}^1(q, \cos \Theta) X + \varepsilon_{\text{on}}^2(q, \cos \Theta) X^2 ,$$

with $X = R - R_0$, R_0 being the ground state equilibrium separation.

If we invoke the Franck-Condon principle, we have

$$G_{\text{nv}}^{(\text{FC})}(q) = \frac{1}{q^3} \frac{1}{4\pi} \int_{-1}^1 2\pi d(\cos \Theta) \left\{ \varepsilon_{\text{on}}^0(q, \cos \Theta) \right\}^2 (\text{oo}|\text{nv})^2 ,$$

which is evaluated by the twelve point Gauss Legendre quadrature formula. The quantity $(\text{oo}|\text{nv})$ is the vibrational overlap integral.

For the "non-Franck-Condon principle" case, we have

$$G_{\text{nv}}(q) = \frac{1}{q^3} \frac{1}{4\pi} \int_{-1}^1 2\pi d(\cos \Theta) \left\{ \varepsilon_{\text{on}}^0(q, \cos \Theta) (\text{oo}|\text{nv}) + \varepsilon_{\text{on}}^1(q, \cos \Theta) (\text{oo}|x|\text{nv}) + \varepsilon_{\text{on}}^2(q, \cos \Theta) (\text{oo}|x^2|\text{nv}) \right\}^2 .$$

The total cross section Q_{nv} is then given by

$$Q_{nv} = \xi_n \frac{e\pi}{k_0^2} \int_{q_{\min}}^{q_{\max}} dq G_{nv}(q) .$$

This integral is done by Simpson's rule, using cubic spline interpolation to find $G_n(q)$ at the desired values of q .

APPENDIX II

SOME TRANSITION PROBABILITIES AND BORN CROSS SECTIONS OF Ne

A program of experimental measurements of the electron impact excitation functions of Ne has been conducted at the University of Oklahoma by F. A. Sharpton and R. M. St. John.¹⁵ To aid in the interpretation of their experimental results, some optical transition probabilities and Born approximation excitation cross sections have been calculated. Ochkur's approximation was used to evaluate cross sections which proceed only by electron exchange.

The ground state of Ne is the configuration $(1s)^2(2s)^2(2p)^6$ 1S_0 . The excited states which we have considered belong to the configurations of the type $(1s)^2(2s)^2(2p)^5 nl$, which we write as simply $(2p)^5 nl$. The coupling problem in configurations of this type may be treated as a two-electron problem, since the $(2p)^5$ core behaves in many respects like a single p electron.

A comprehensive treatment of this two-electron vector coupling problem has been given by Cowan and Andrew.¹⁶ The problem of calculating the level structure and the wave functions for a given configuration is that of finding the eigenvalues and eigenvectors of the electron-interaction Hamiltonian

$$H = \sum_{j>i} \frac{e^2}{r_{ij}} + \sum_i \xi_i(r_i) \vec{l}_i \cdot \vec{s}_i = H_{el} + H_{mag} \quad , \quad (1)$$

where the summations are carried out over all electrons outside of closed shells. The electrostatic portion of (1) is evaluated in the IS representation, where it is diagonal, having diagonal elements

$$(IS|H_{e1}|IS) = \sum_k (f^k F^k + g^k G^k) .$$

Here the F^k and G^k are certain radial integrals (usually known as Slater-Condon parameters) which can be calculated from the radial wave functions, but are commonly treated as adjustable parameters. The magnetic portion of (1) is easily evaluated in the jj representation, where the matrix is diagonal, with diagonal elements

$$(j_1 j_2 | H_{\text{mag}} | j_1 j_2) = \sum_i d_i \zeta_i .$$

The ζ_i are radial integrals related to the strength of the spin-orbit interactions, and are also treated as adjustable parameters. The expressions for the coefficients f^k , g^k , and d_i are given by Cowan and Andrew,¹⁶ and will not be repeated here.

A transformation is carried out to obtain the two portions of the Hamiltonian matrix in the same representation. The Hamiltonian matrix is then diagonalized, subject to the condition that the parameters F^k , G^k , and ζ_i be chosen to give the best fit to the observed energy level structure of the configuration. This is accomplished by an iterative procedure. The resulting intermediate coupling wave functions are then expressed as linear combinations of IS basis functions, to facilitate the calculation of the transition probabilities and the excitation cross sections. That is,

$$\psi_{\gamma\beta J} = \sum_{L,S} (\gamma\beta J | \gamma ISJ) \psi_{\gamma ISJ} ,$$

where γ labels the configuration, βJ labels a level of the configuration, and $\psi_{\gamma ISJ}$ are the IS basis functions. The coefficients $(\gamma\beta J | \gamma ISJ)$ are given in Tables A1, A2, and A3.

The optical transition probability, $A(\gamma\beta J \rightarrow \gamma'\beta'J')$, is given in terms of the line strength, $S(\gamma\beta J, \gamma'\beta'J')$, by the expression

$$A(\gamma\beta J \rightarrow \gamma'\beta'J') = \frac{1}{2J+1} \frac{64\pi^4 e^2 a_0^2}{3h} S(\gamma\beta J, \gamma'\beta'J') \sigma^3 .$$

The expression for the line strength is given by Cowan and Andrew.¹⁶

For a transition of the type

$$(2p)^5 n\ell\beta J \rightarrow (2p)^5 n'\ell'\beta'J', \text{ or}$$

$$\gamma\beta J \rightarrow \gamma'\beta'J',$$

their expression becomes

$$S(\gamma\beta J, \gamma'\beta'J') = |(\gamma\beta J || P^{(1)} || \gamma'\beta'J')|^2 ,$$

$$(\gamma\beta J || P^{(1)} || \gamma'\beta'J') = \sum_{L,S} \sum_{L',S'} (\gamma\beta J | \gamma ISJ)$$

$$(\gamma ISJ || P^{(1)} || \gamma' L' S' J') (\gamma' \beta' J' | \gamma' L' S' J') ,$$

$$(\gamma ISJ || P^{(1)} || \gamma' L' S' J') = \delta_{S,S'} (-1)^{S+J'-L'-1} ([J][J'][L][L'])^{1/2}$$

$$\left\{ \begin{matrix} L & J & S \\ J' & L' & 1 \end{matrix} \right\} \left\{ \begin{matrix} \ell & L & 1 \\ L' & \ell' & 1 \end{matrix} \right\} P ,$$

Table A1. The coefficients $(\gamma\beta J|\gamma LSJ)$ for the configurations $(2p)^5 3s$ and $(2p)^5 4s$. The states are labelled according to the Paschen notation.¹⁸

	$1s_5$	$1s_4$	$1s_2$	$1s_3$
$3p_2$	1.0			
$3p_1$.964	.266	
$1p_1$.266	-.964	
$3p_0$				1.0
	$2s_5$	$2s_4$	$2s_2$	$2s_3$
$3p_2$	1.0			
$3p_1$.749	-.663	
$1p_1$.663	.749	
$3p_0$				1.0

Table A2. The coefficients $(\gamma\beta J|\gamma LSJ)$ for the $(2p)^5 3p$ configuration. The states are labelled according to the Paschen notation.¹⁸

	2p ₀	2p ₈	2p ₆	2p ₄	2p ₁₀	2p ₇	2p ₅	2p ₂	2p ₃	2p ₁
³ D ₃	1.0									
³ D ₂		.910	.320	.263						
¹ D ₂		.400	-.844	-.359						
³ P ₂		-.107	-.431	.896						
³ P ₁					-.083	-.178	.549	.812		
³ D ₁					0.	.951	.308	0.		
¹ P ₁					.059	-.252	.777	-.574		
³ S ₁					.995	0.	0.	.102		
³ P ₀									.990	.141
¹ S ₀									-.141	.990

Table A3. The coefficients $(YBJ|YLSJ)$ for the configuration $(2p)^5 3d$. The states are labelled according to the Paschen notation.^{1a}

	$3d_1'$	$3d_4$	$3d_1'$	$3s_1'''$	$3d_3$	$3d_1''$	$3s_1''''$	$3s_1''$	$3d_3$	$3d_2$	$3s_1'$	$3d_3$
3F_4	1.0											
3F_3		.661	-.404	.633								
1F_3		.750	.366	-.551								
3D_3		-.009	.839	.545								
3D_2					-.466	.529	.339	.623				
3F_2					.001	-.546	.838	.008				
1D_2					.378	.650	.428	-.502				
3P_2					.800	.002	-.006	.600				
3P_1									-.900	-.271	.342	
3D_1									.114	.609	.785	
1P_1									.421	-.745	.517	
3P_0												1.0

$$P = \delta_{l', l \pm 1} (-1)^{l+l' > l_{>}} \int_0^{\infty} (-er) R_{nl}(r) R_{n'l'}(r) r^2 dr ,$$

where $l_{>}$ is the larger of l, l' , $[J] = 2J+1$, the quantities in brackets are 6-J symbols, and $R_{nl}(r)$ is the radial portion of the one electron orbital for the optical electron. These radial wave functions were obtained by the Hartree-Fock-Slater self consistent field method, by R. D. Cowan.¹⁷

Recently, Bennett and Kindlemann obtained measurements of the radiative lifetimes of the levels of the $(2p)^5 3p$ configuration. From these measurements, they obtained the transition moment integral

$$\int_0^{\infty} R_{3s}(r)(er)R_{3p}(r)r^2dr = 4.52 .$$

Our calculated value using the Hartree-Fock-Slater wave functions is 4.75.

The optical transition probabilities have been calculated for all transitions between the configurations $(2p)^5 3s$, $(2p)^5 3p$, $(2p)^5 3d$, $(2p)^5 4s$, and $(2p)^6$. The quantities

$$g A(\gamma\beta J \rightarrow \gamma'\beta'J') = (2J+1) A(\gamma\beta J \rightarrow \gamma'\beta'J') ,$$

are given in Table A4. The quantity $g A$ is symmetric with respect to interchange of initial and final levels.

Assuming that the unpolarized beam of incident electrons can be represented by the plane wave

$$e^{i\vec{k}_0 \cdot \vec{r}} \frac{1}{\sqrt{2}} \left[\chi\left(+\frac{1}{2}\right) + \chi\left(-\frac{1}{2}\right) \right] ,$$

Table A4. The quantities $g A(\gamma\beta J, \gamma'\beta' J')$ which connect the levels of the configuration $(2p)^5 3s$, $(2p)^5 3p$, $(2p)^5 3d$, $(2p)^5 4s$, and $(2p)^6$. The levels are labeled according to the Paschen notation. The units are 10^8 sec^{-1} .

	2p ₁	2p ₂	2p ₃	2p ₄	2p ₅	2p ₆	2p ₇	2p ₈	2p ₉	2p ₁₀	ground state
1s ₂	.748	.730	.0084	.705	.801	1.576	.0041	.0748		.0063	13.3
1s ₃		.494			.556		.603			.0894	
1s ₄	.0157	.182	.669	1.04	.155	.0027	.975	1.84		.337	.980
1s ₅		.452		1.51	.197	.936	.142	.900	4.07	.831	
2s ₂	.029	.149	.029	.250	.085	.264	.0287	.024		.061	2.07
2s ₃		.066			.085		.130			.050	
2s ₄	.0089	.00022	.051	.027	.0754	.120	.140	.358		.100	1.60
2s ₅		.039		.144	.020	.121	.0204	.151	.747	.313	
3d ₁ '				.632		1.71		.0957	1.17		
3d ₁ ''		0.		.093	.629	.0032	.923	.866	.0589	0.	
3d ₂	.171	.0034	.167	.040	.374	.0030	.283	.102		.112	2.20
3d ₃		.0812		.479	.0715	.577	.0499	.0421	.133	1.56	

Table A4. Continued

	2p ₁	2p ₂	2p ₃	2p ₄	2p ₅	2p ₆	2p ₇	2p ₈	2p ₉	2p ₁₀	ground state
3d ₄				.0364		.644		2.91	.200		
3d ₄ '									5.21		
3d ₅	.049	.166	.114	.099	.0002	.112	.0016	.0040		1.21	.721
3d ₆		.0787			.0387		.0376			.501	
3s ₁ '	.192	.355	.514	.0144	.060	.0209	.202	.019		.124	1.08
3s ₁ ''		1.74		.136	.0108	.236	.0447	.0891	.0034	.641	
3s ₁ '''				2.36		.971		.600	.0106		
3s ₁ ''''		0.		.177	1.26	.0916	1.36	.0165	.00052	0.	

the Born-Ochkur scattering amplitude can be written in the uncoupled representation as

$$f(\theta, \varphi, \sigma) = \left\{ \frac{2}{k_0^2 \sqrt{2}} \chi(\sigma_0) - \frac{2}{q^2 \sqrt{2}} \left[\chi\left(+\frac{1}{2}\right) + \chi\left(-\frac{1}{2}\right) \right] \delta_{\sigma_e, \sigma_0} \right\} \\ \int R_{nl}(r) Y_{\ell, m_e}^*(\hat{r}) e^{i\vec{q} \cdot \vec{r}} R_{2p}(r) Y_{1, m_0}(\hat{r}) d\vec{r} \quad ,$$

where χ is an electron spin function, σ is the spin quantum number, m_e and σ_e are quantum numbers of the excited orbital, and m_0, σ_0 are quantum numbers of the vacant orbital in the $(2p)^5$ core. Making use of the expressions

$$\psi(\gamma_S J M) = \sum_{L, S} (\gamma_S J | \gamma_L S J) \psi(\gamma_L S J M) \quad ,$$

$$\psi(\gamma_L S J M) = \sum_{M_S} C(L, S, J; M - M_S, M_S) \psi(\gamma_L M_S M_S) \quad ,$$

$$\psi(\gamma_L M_S M_S) = \sum_{m_0, \sigma_0} (-1)^{-m_0 - \sigma_0 - 3/2} C(\ell, 1, L; M_S + m_0, -m_0) \\ C\left(\frac{1}{2}, \frac{1}{2}, S; -\sigma_0, M_S + \sigma_0\right) \psi\left(\gamma \ell m_e \sigma_e m_0 \sigma_0\right) \quad ,$$

$$e^{i\vec{q} \cdot \vec{r}} = 4\pi \sum_{\ell, m} i^\ell j_\ell(qr) Y_{\ell, m}^*(\hat{r}) Y_{\ell, m}(\hat{r}) \quad ,$$

$$\int Y_{\ell, m_e}^* Y_{\ell', m_0 - m_e}^* Y_{1, m_0} = \left[\frac{(2\ell+1)(2\ell'+1)}{3 \cdot 4\pi} \right]^{1/2} \\ C(\ell, \ell', 1; m_e, m_0 - m_e) C(\ell, \ell', 1; 0, 0) \quad ,$$

$$\sum_{m_0} C(l, l, L; M_L + m_0, -m_0) C(l, l, l'; M_L + m_0, -m_0) = \delta_{l', L} ,$$

and

$$C(L, l, l; 0, 0) = (-1)^{\frac{1}{2}(l > - L)} \left[\frac{3 l >}{(2l+1)(2L+1)} \right]^{\frac{1}{2}} \delta_{L, l \pm 1} ,$$

where $l >$ is the larger of the two quantities l, L ; the expression for the cross section becomes

$$\begin{aligned} Q(\gamma_S J M) &= \frac{8\pi}{k_0^2} \sum_{L, L'} \sum_{S, M_S} (\gamma_S J | \gamma_L S J) (\gamma_S J' | \gamma_{L'} S J) \\ &\left[\frac{3 l >}{2L+1} \right]^{\frac{1}{2}} \delta_{L, l \pm 1} \left[\frac{3 l' >}{2L'+1} \right]^{\frac{1}{2}} \delta_{L', l' \pm 1} C(L, S, J; M-M_S, M_S) \\ &C(L', S, J; M-M_S, M_S) \int_{q_{\min}}^{q_{\max}} q \, dq \left\{ I_{L'}(q) I_L(q) \right. \\ &\left. P_{L, -M+M_S}(\cos \theta_q) P_{L', -M+M_S}(\cos \theta_q) X(S) \right\} , \end{aligned}$$

where $I_L(q) = \int_0^{\infty} R_{2p}(r) j_L(qr) R_{nl}(r) r^2 dr$, and

$$X(S) = \begin{cases} 4/q \delta_{S,0} & \text{for the ordinary Born approximation,} \\ \text{or} \\ \left(\frac{1}{k_0^2} - \frac{2}{q^2} \delta_{S,0} \right)^2 & \text{for the Ochkur-Born approximation} . \end{cases}$$

In the above expressions, $C(L, S, J; M-M_S, M_S)$ is a Clebsch-Gordan

coefficient, $l_{>}$ is the larger of (l, L) , $l'_{>}$ is the larger of (l, L') , q is the momentum change of the scattered electron, θ_q is the angle between \vec{k}_0 and \vec{q} , $P_{L,M}$ is a normalized Legendre function, and j_L is a spherical Bessel function. The cross sections for excitation to each level of the configurations $(2p)^5 \bar{3}s$, $(2p)^5 \bar{3}p$, $(2p)^5 \bar{3}d$, and $(2p)^5 4s$ have been calculated. They are displayed in Figures A1 through A50, as a function of incident electron energy.

The direct coupling between the ground state and the excited states with either even parity and odd J , or odd parity and even J , can be shown to vanish. This results, of course, in the "non-exchange" Born cross sections vanishing. In the approximation used here, then, these excitations proceed by electron exchange only. The cross sections for these states were calculated by the Ochkur approximation. The cross sections for states with even parity and even J , or odd parity and odd J , were calculated by the ordinary Born approximation.

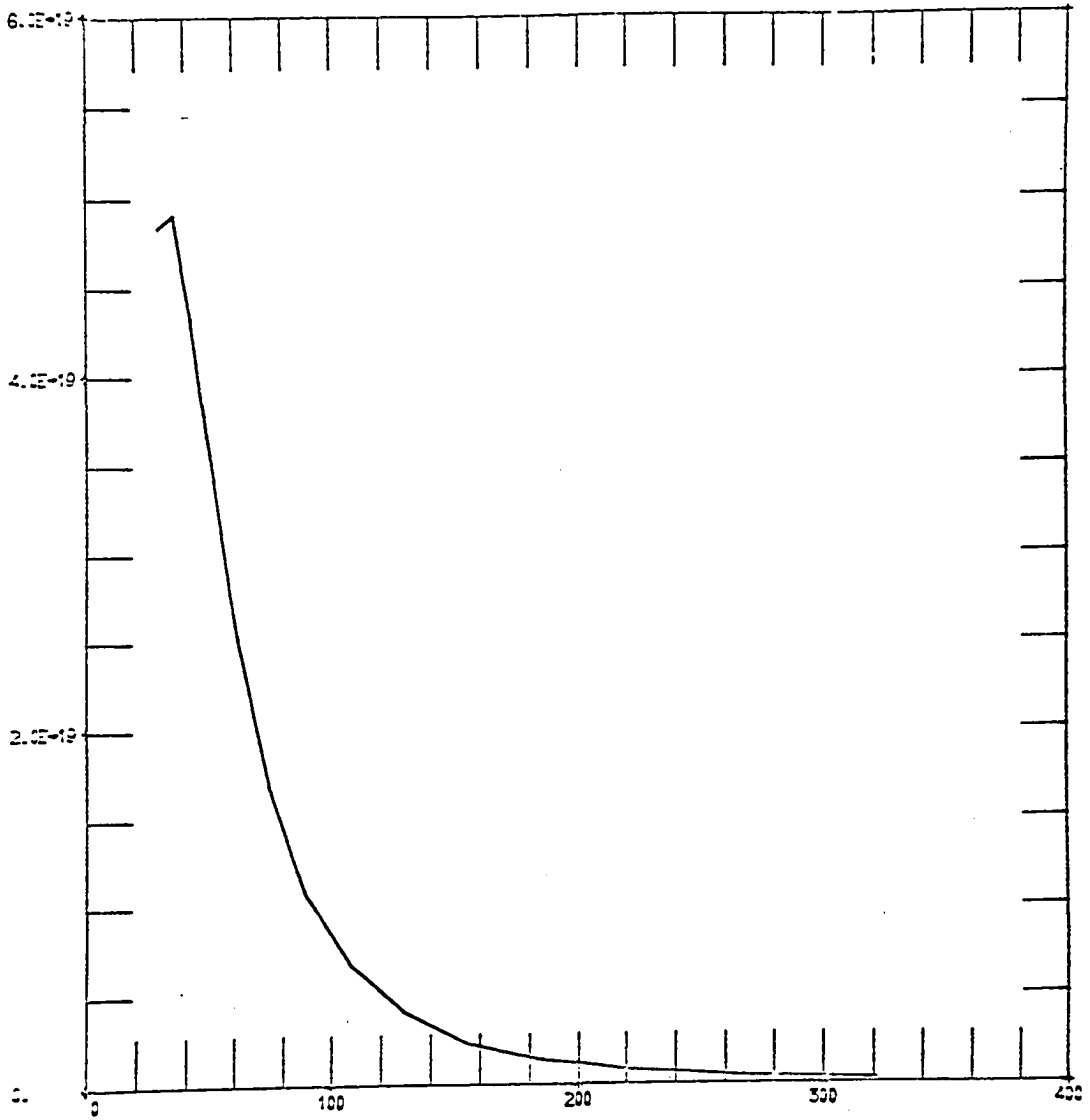


Figure A1. Cross section (cm^2) vs Electron Energy (eV)
for the $1s_5$ state.

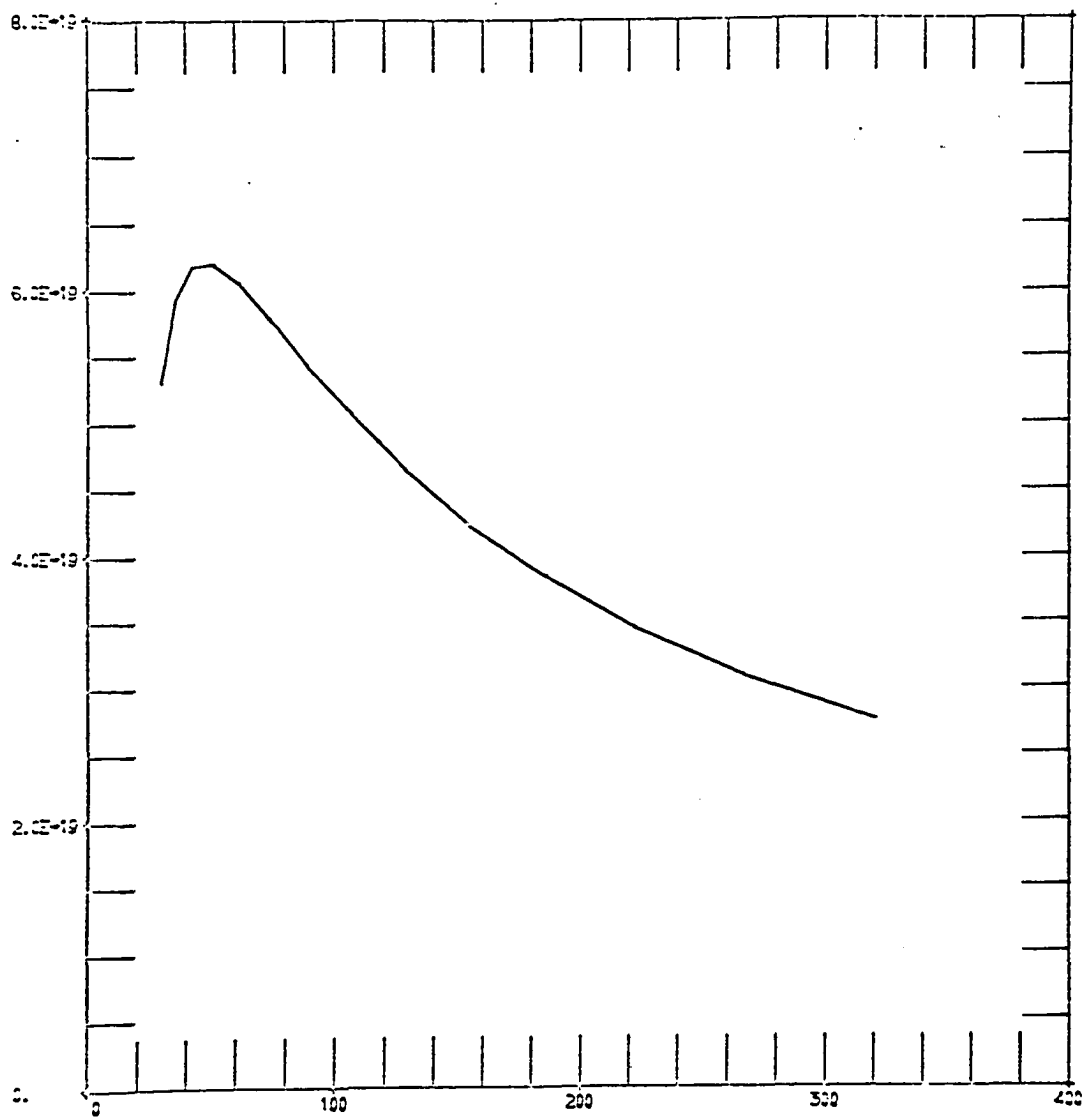


Figure A2. Cross section (cm²) vs Electron Energy (e)
for the 1s₄ state.

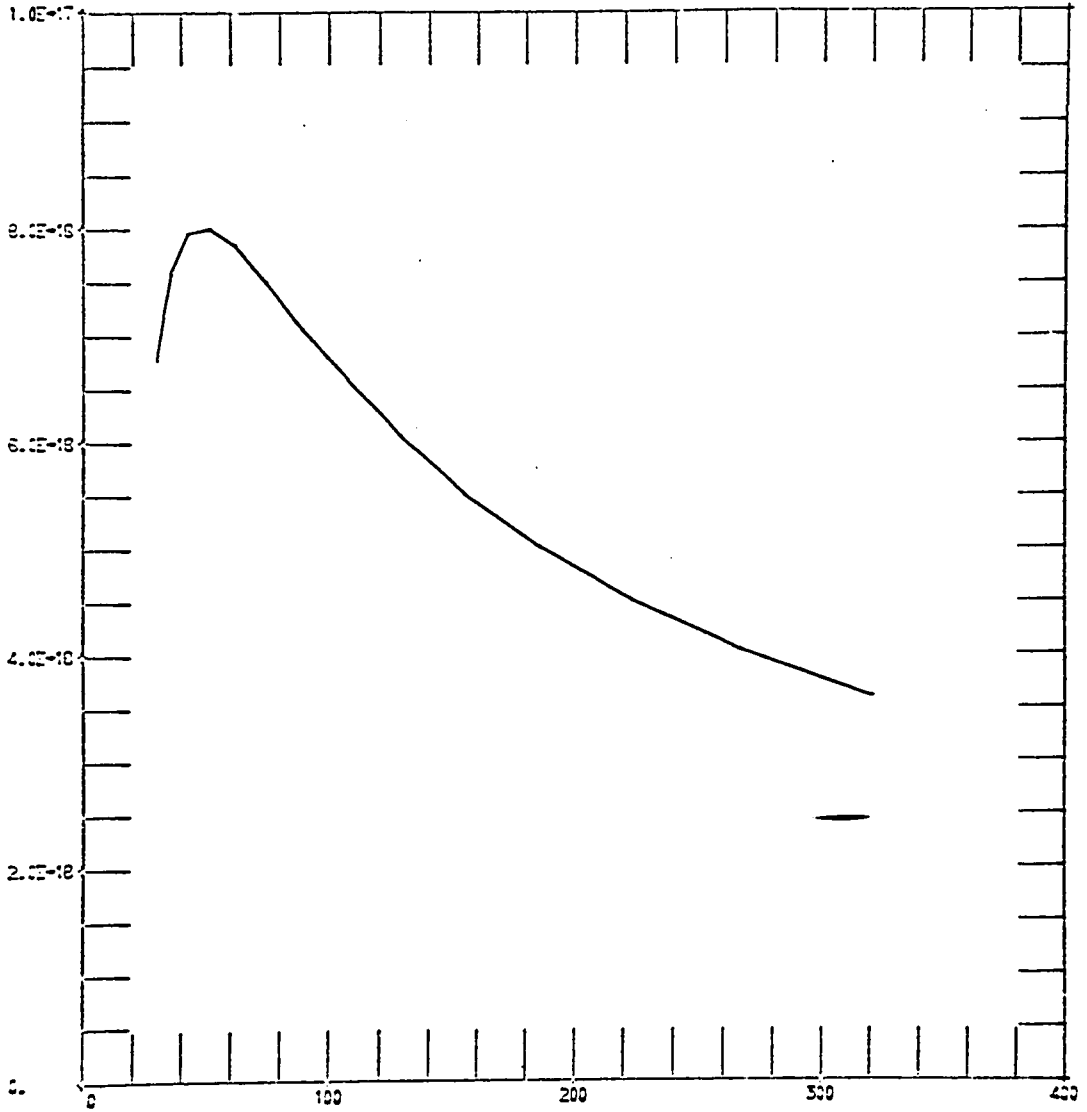


Figure A3. Cross section (cm²) vs Electron Energy (eV)
for the 1s₂ state.

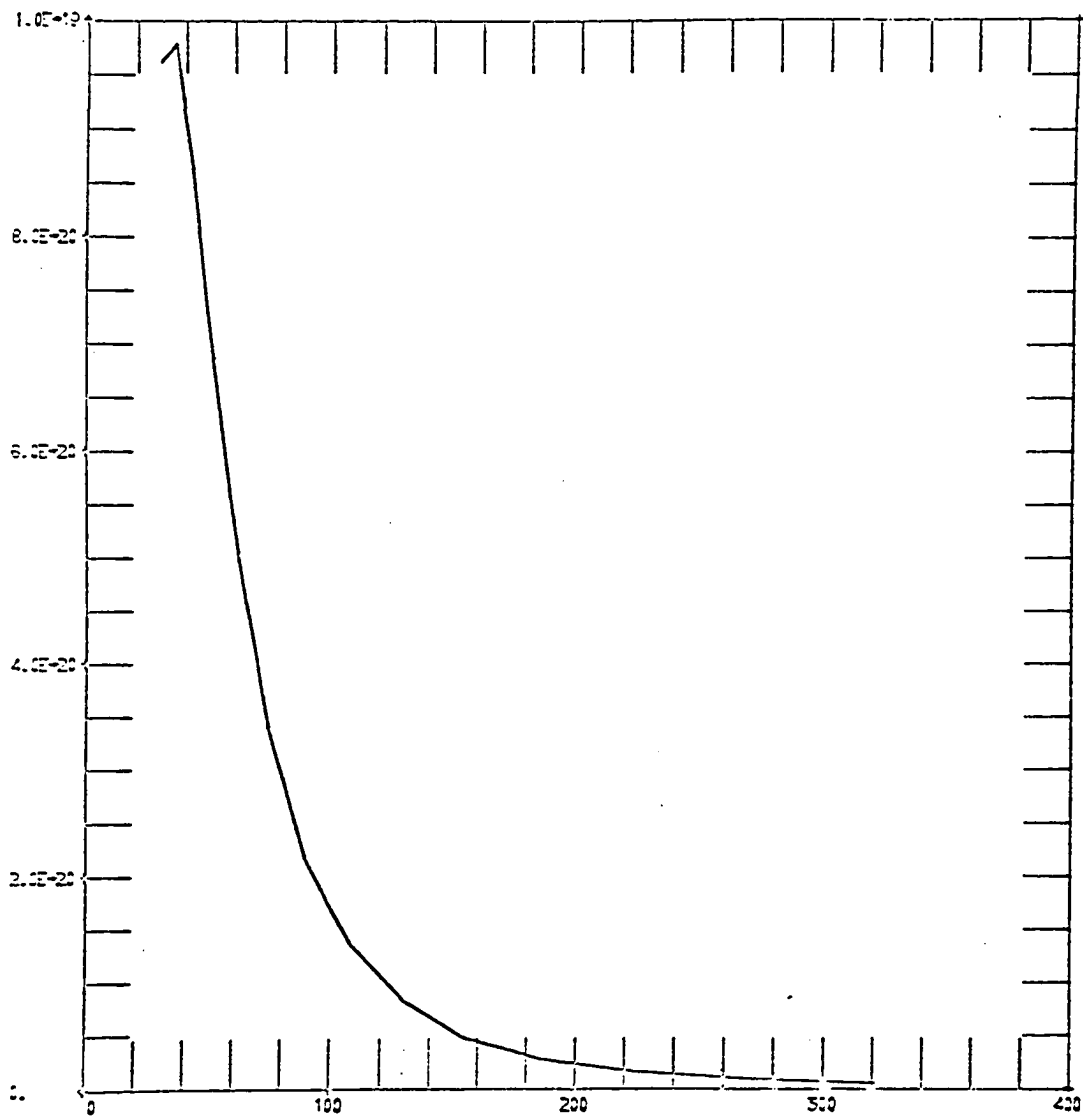


Figure A4. Cross section (cm²) vs Electron Energy (eV)
for the $1s_3$ state.

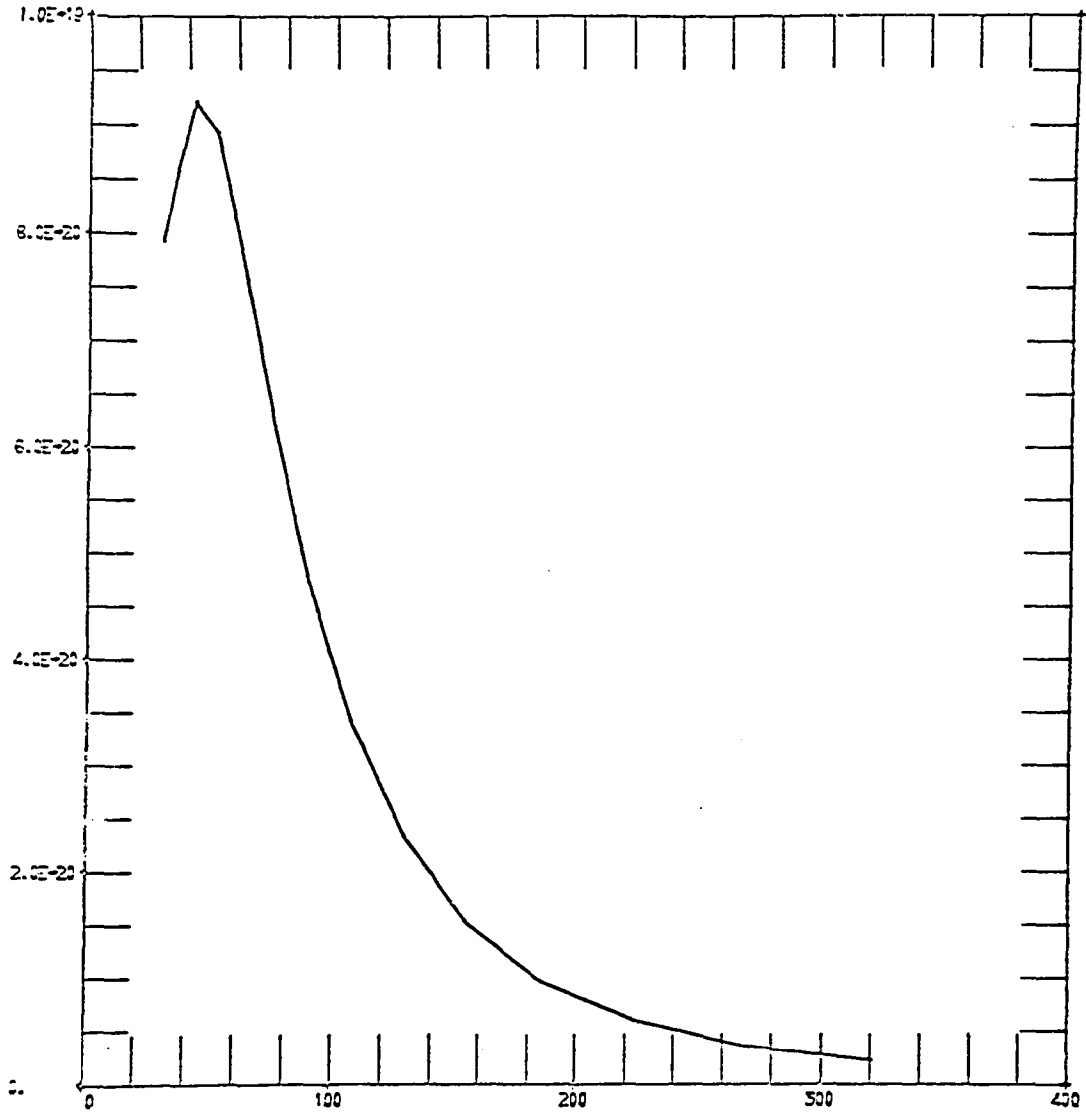


Figure A5. Cross section (cm²) vs Electron Energy (eV)
for the 2p₉ state.

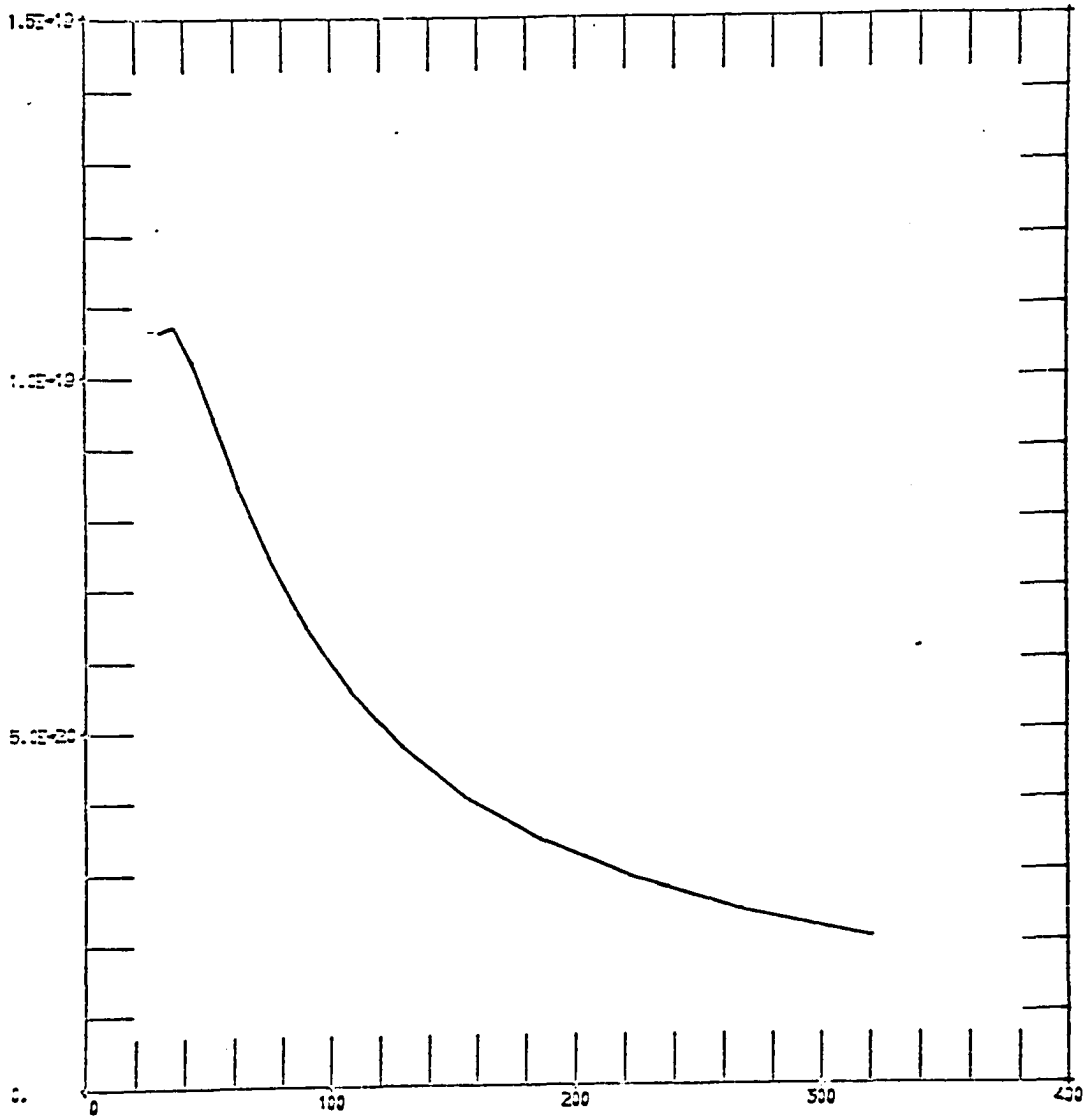


Figure A6. Cross section (cm²) vs Electron Energy (eV)
for the 2p_s state.

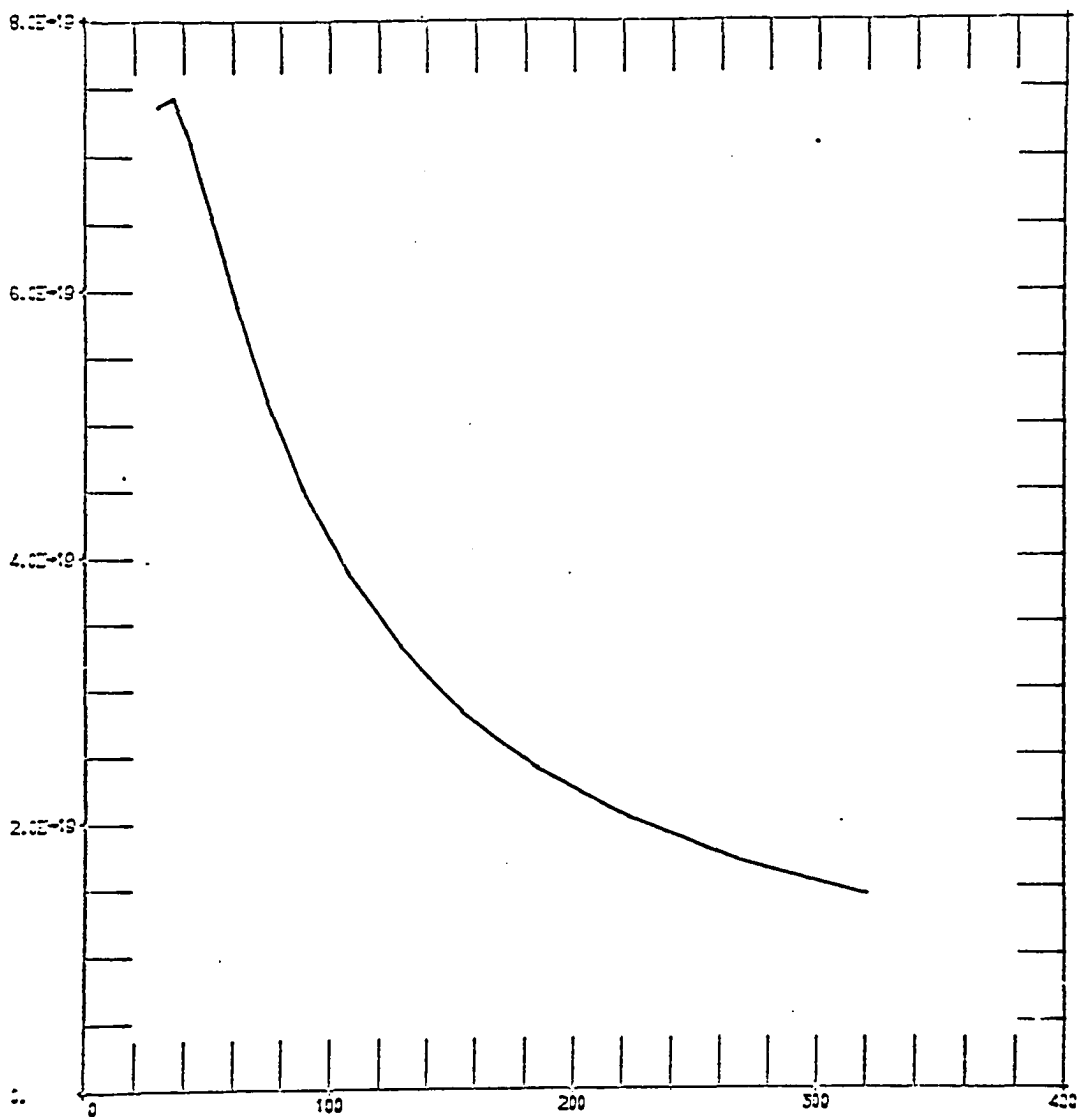


Figure A7. Cross section (cm²) vs Electron Energy (eV)
for the 2p₆ state.

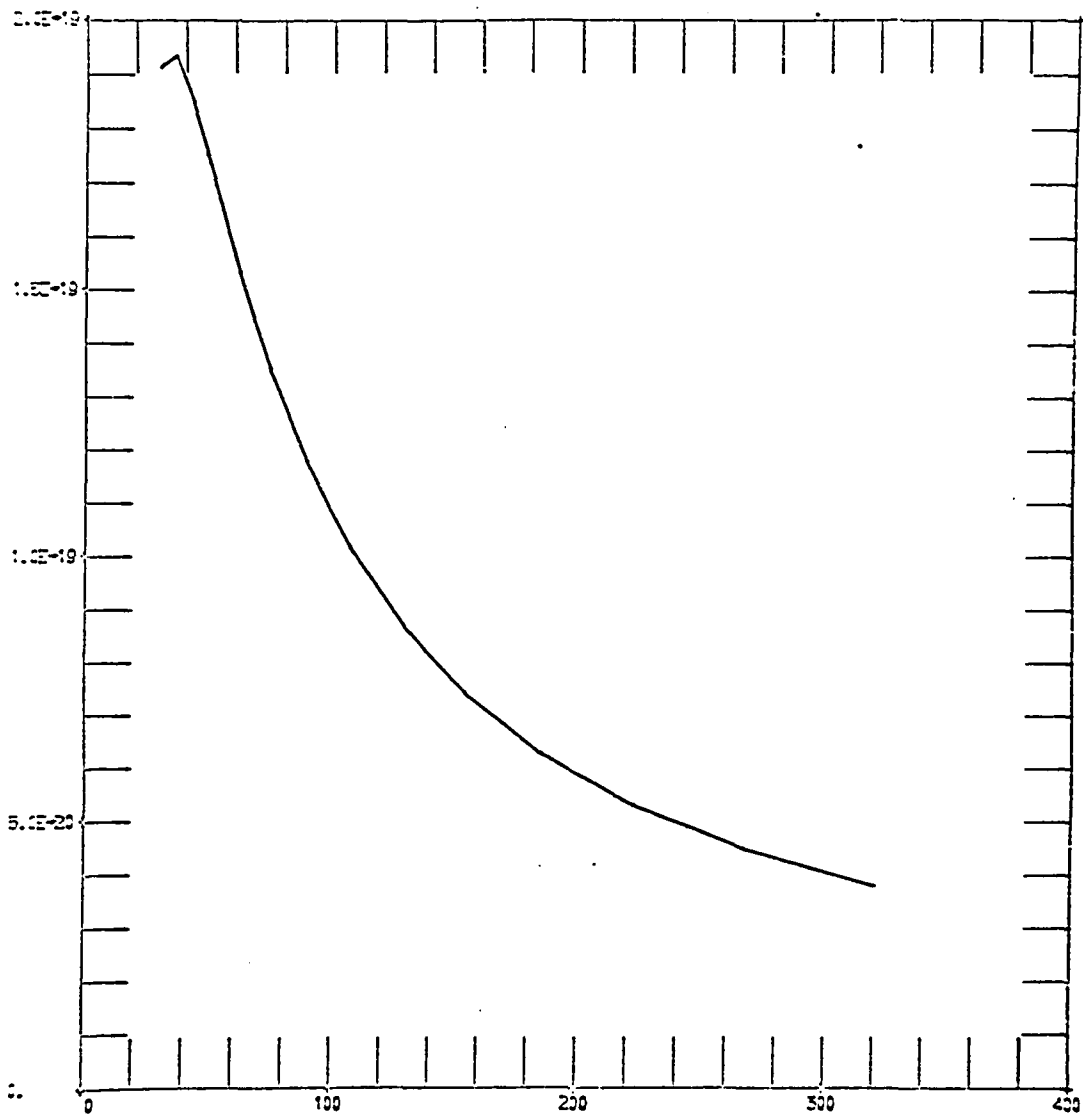


Figure A8. Cross section (cm²) vs Electron Energy (eV)
for the 2p₂ state.

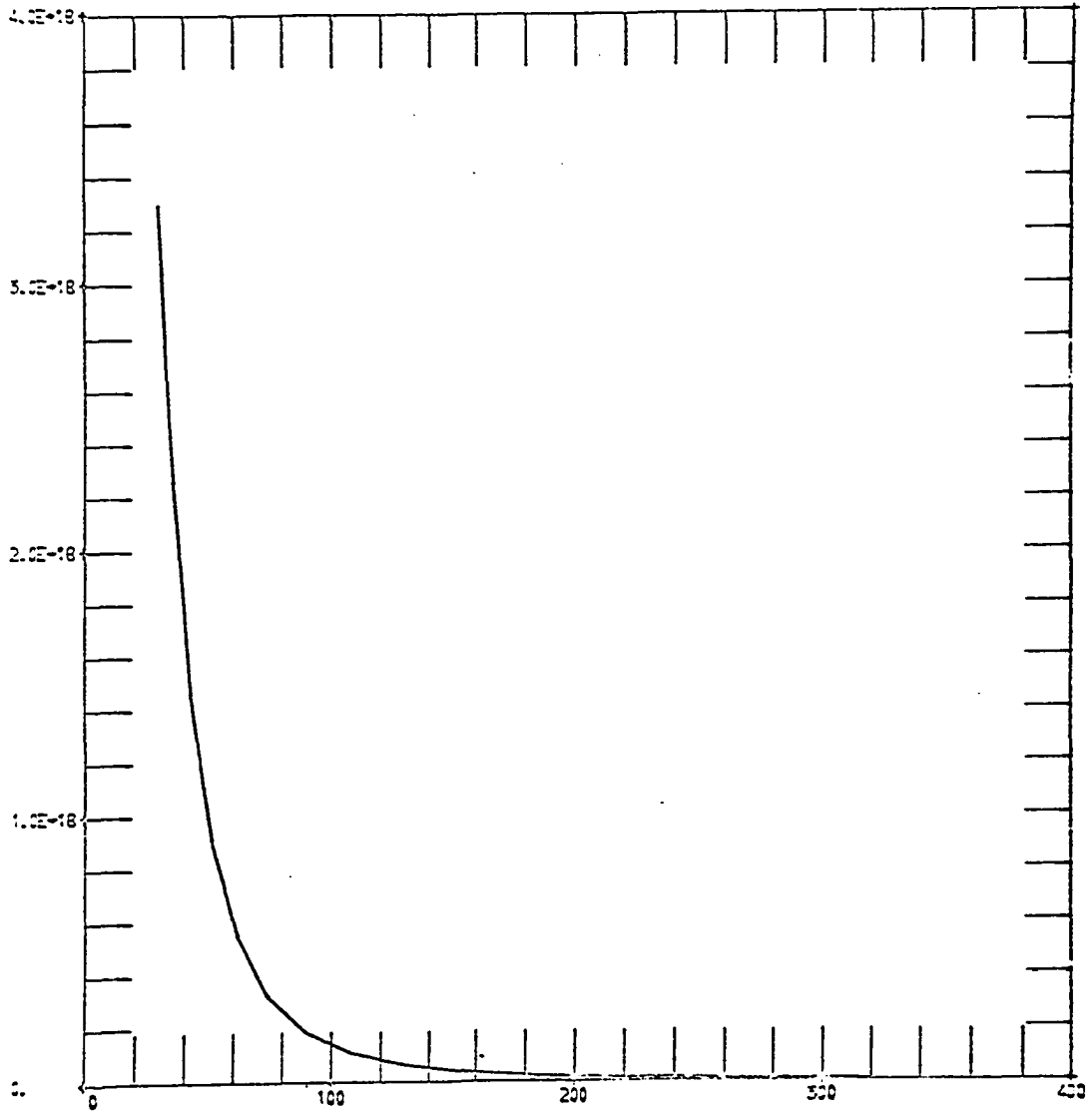


Figure A9. Cross section (cm²) vs Electron Energy (eV)
for the 2p₁₀ state.

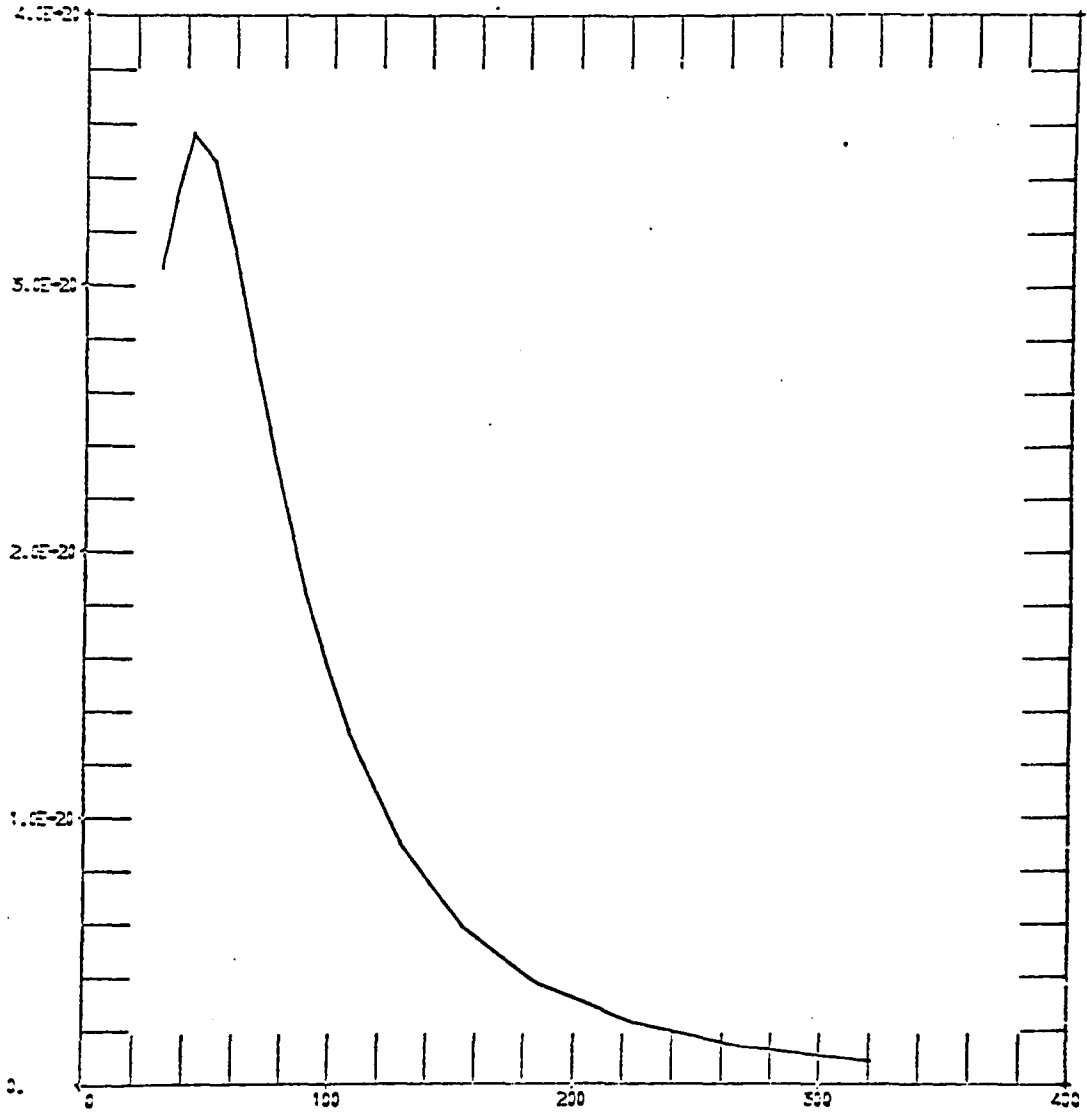


Figure A10. Cross section (cm²) vs Electron Energy (eV)
for the 2p₇ state.

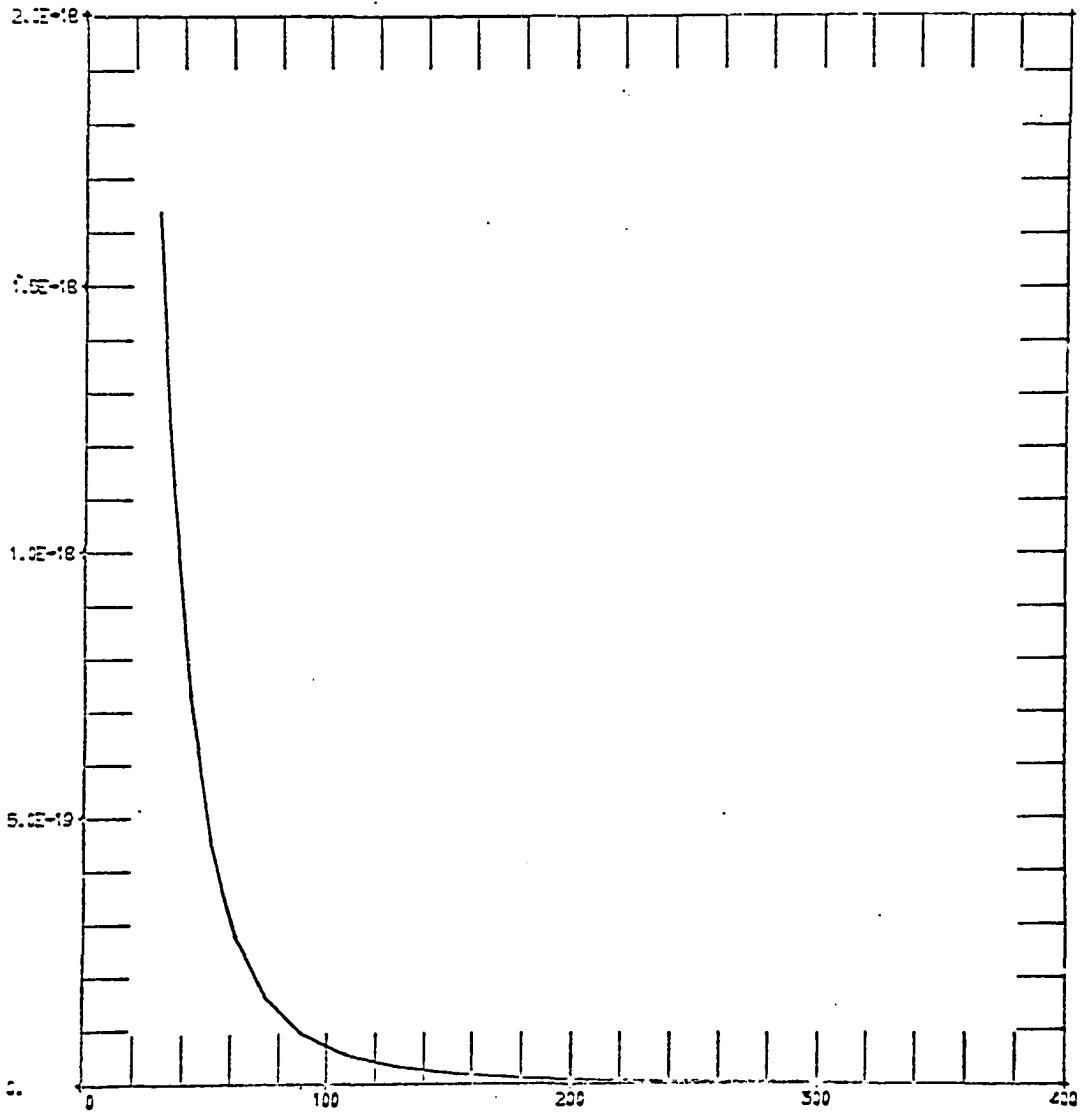


Figure All. Cross section (cm²) vs Electron Energy (eV)
for the 2p₃ state.

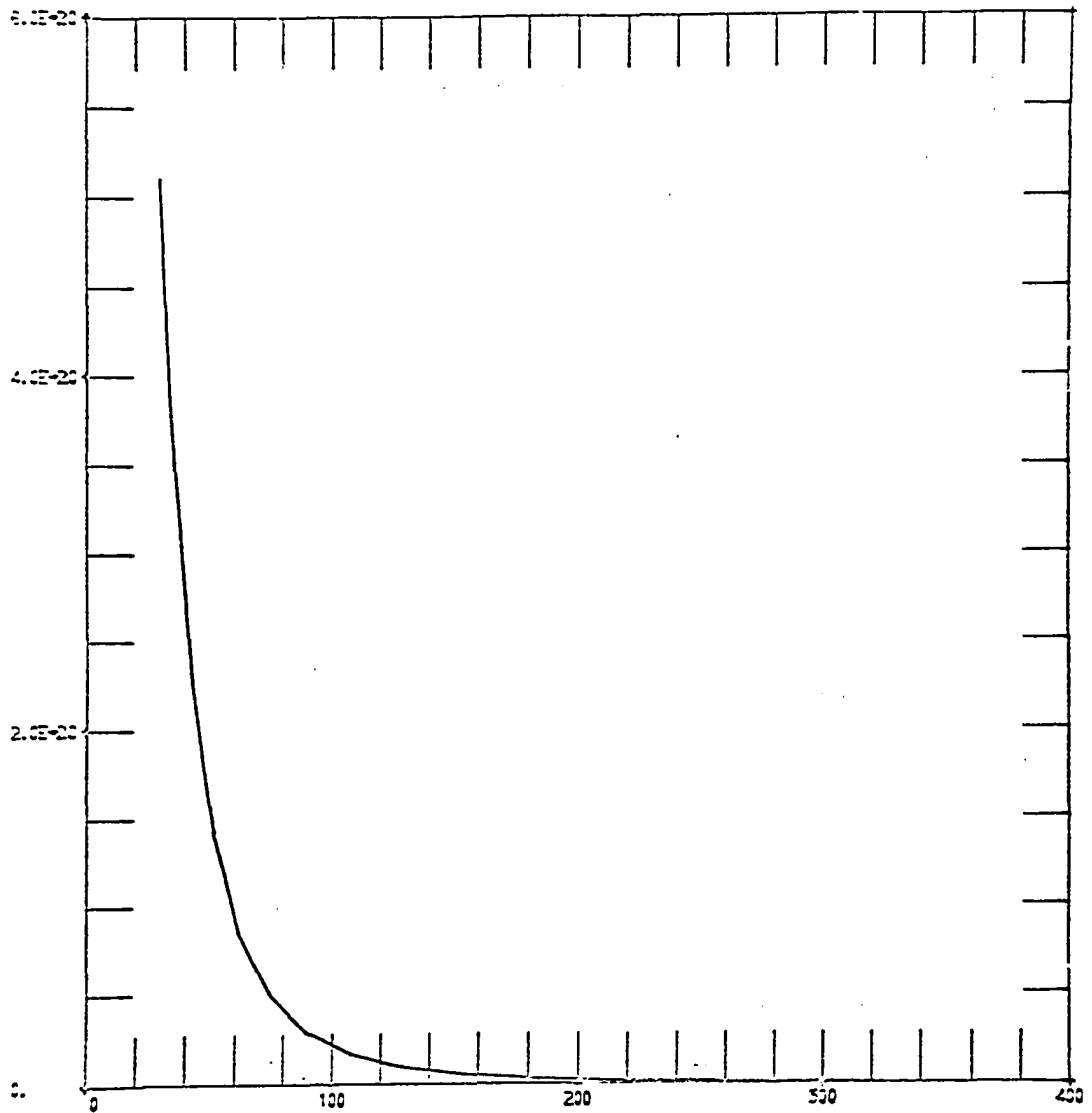


Figure A12. Cross section (cm^2) vs Electron Energy (eV)
for the $2p_2$ state.

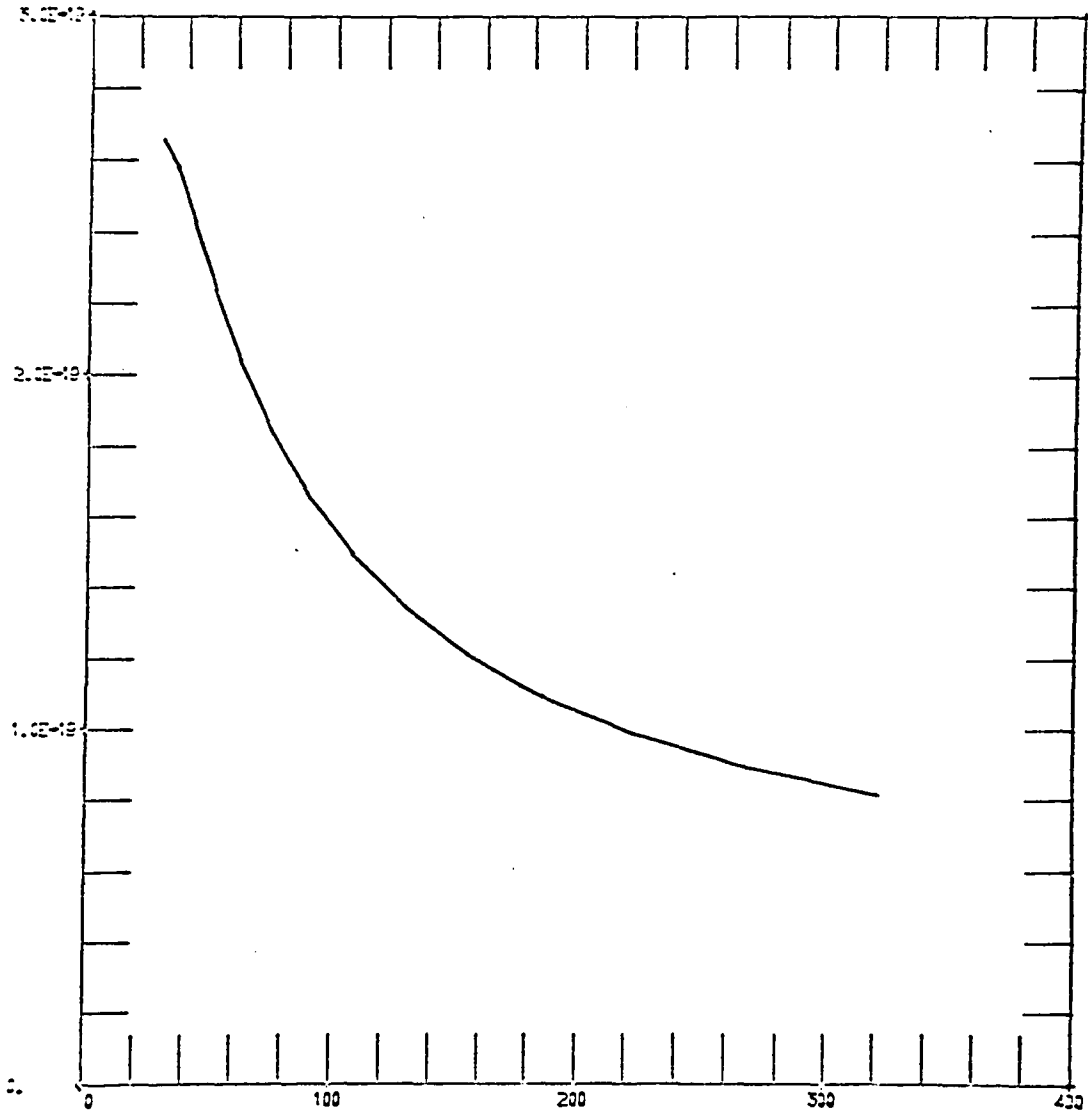


Figure A13. Cross section (cm²) vs Electron Energy (eV)
for the 2p₃ state.

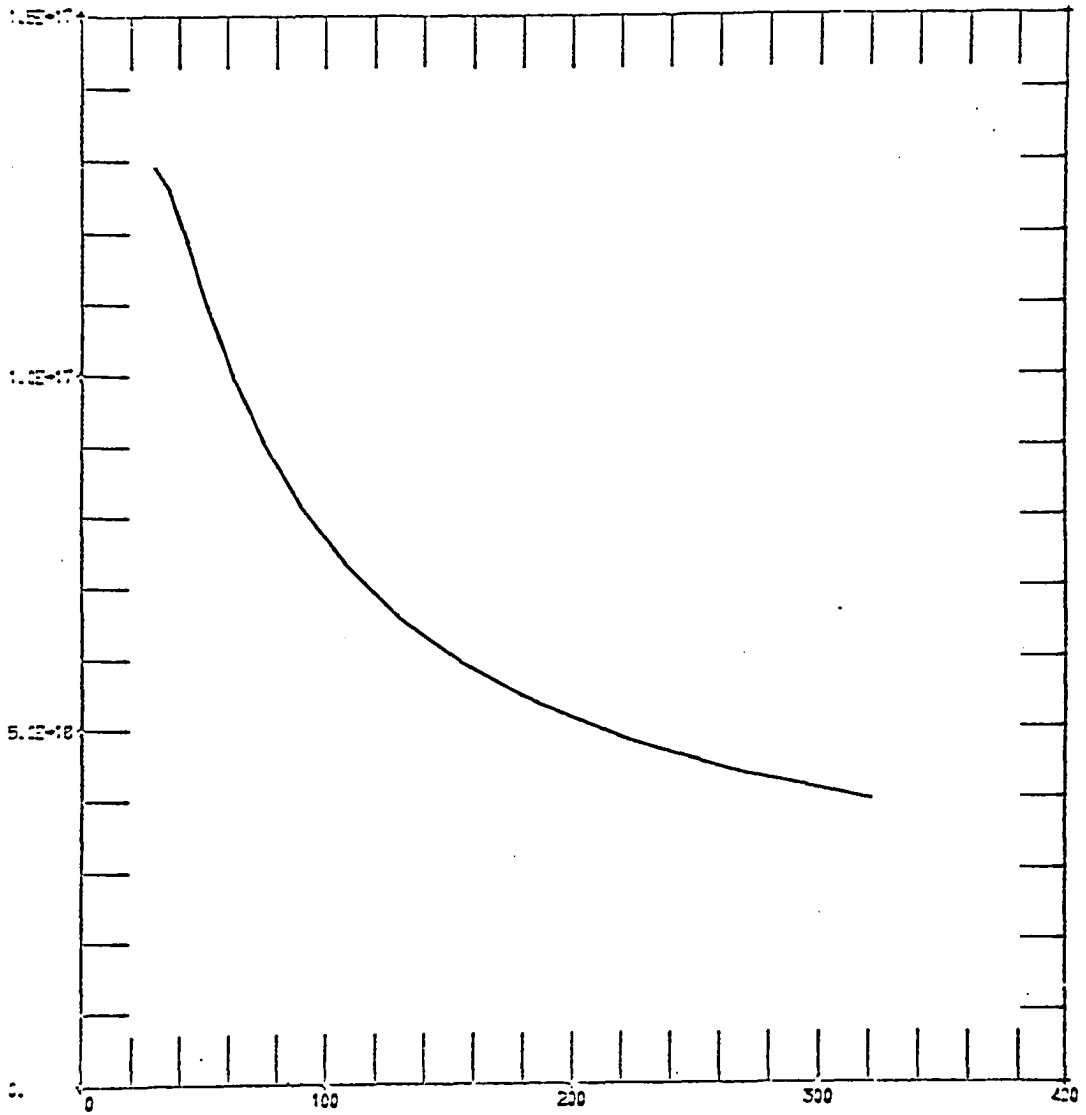


Figure A14. Cross section (cm²) vs Electron Energy (eV)
for the 2p₁ state.

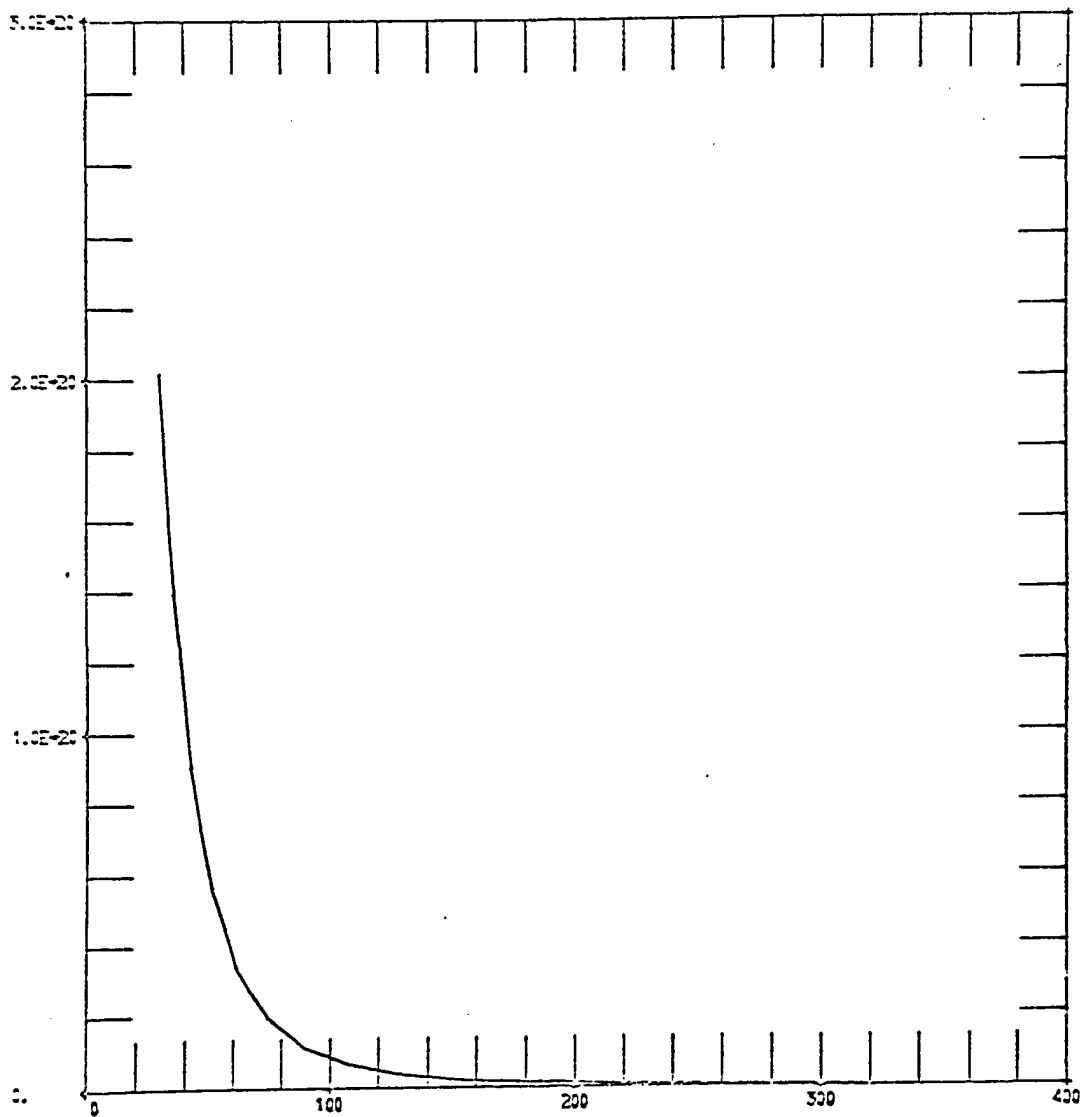


Figure A15. Cross section (cm^2) vs Electron Energy (eV)
for the $3d_4$ state.

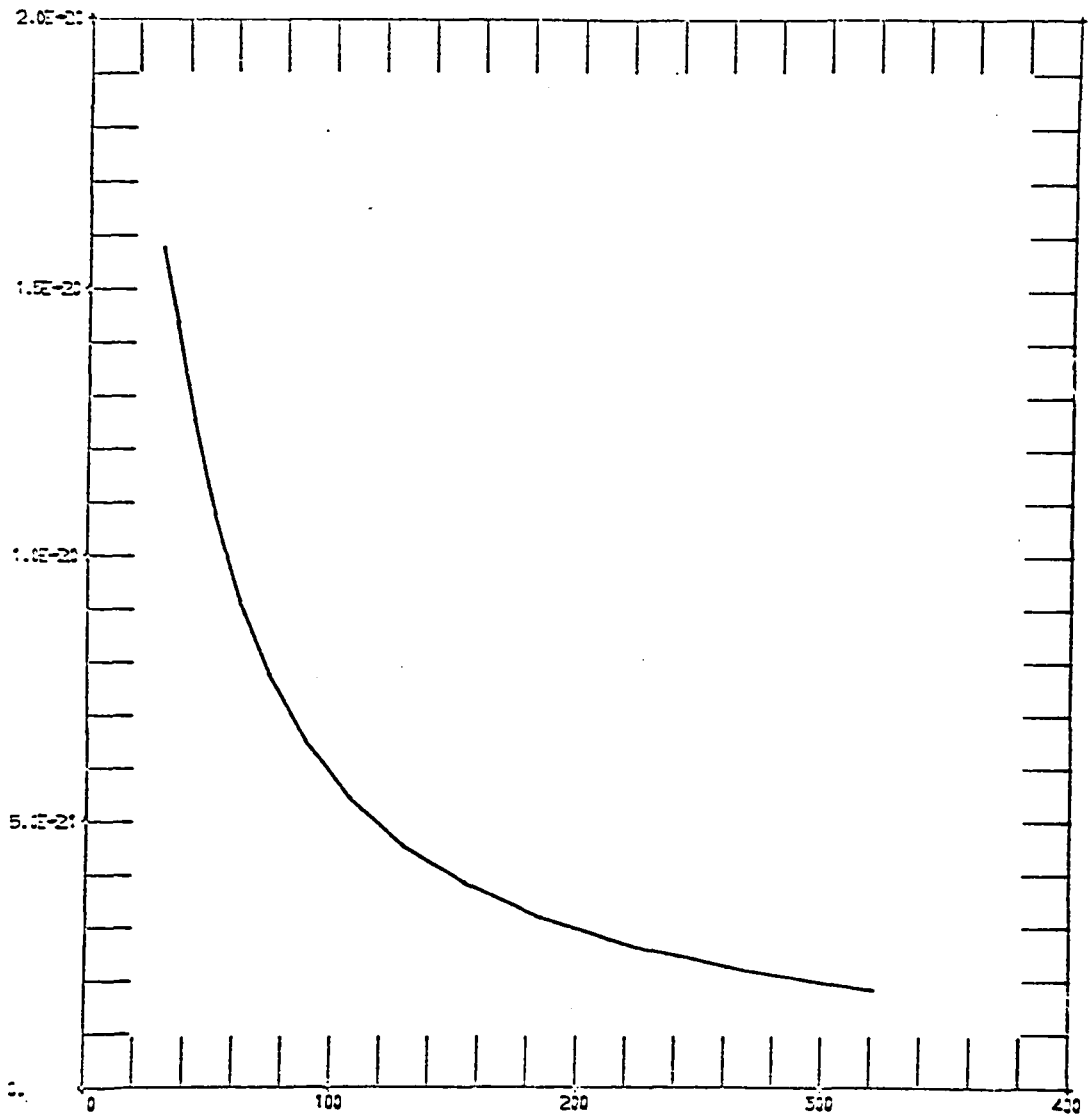


Figure A16. Cross section (cm²) vs Electron Energy (eV)
for the 3d₄ state.

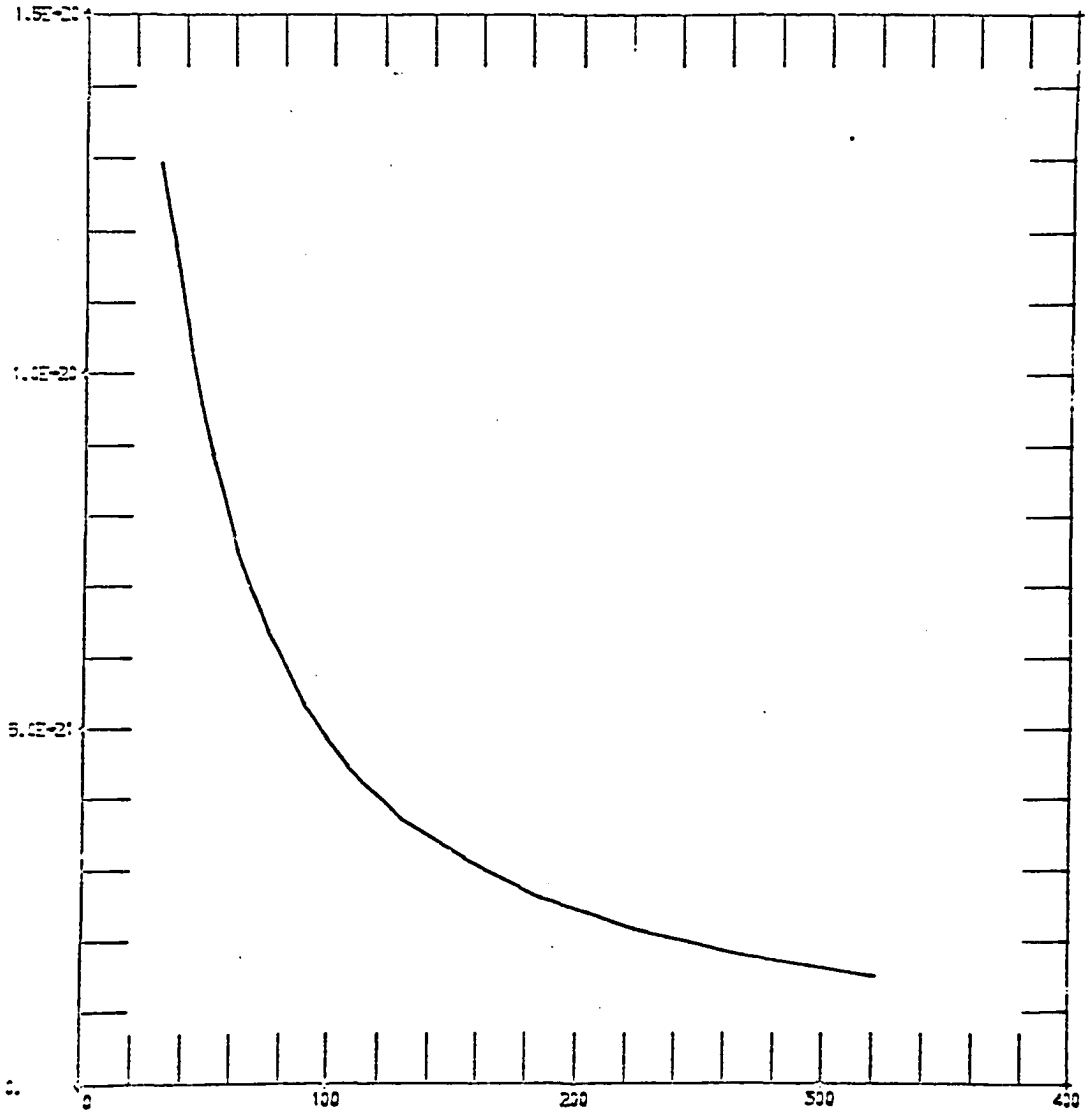


Figure A17. Cross section (cm²) vs Electron Energy (eV)
for the $3d_1$ state.

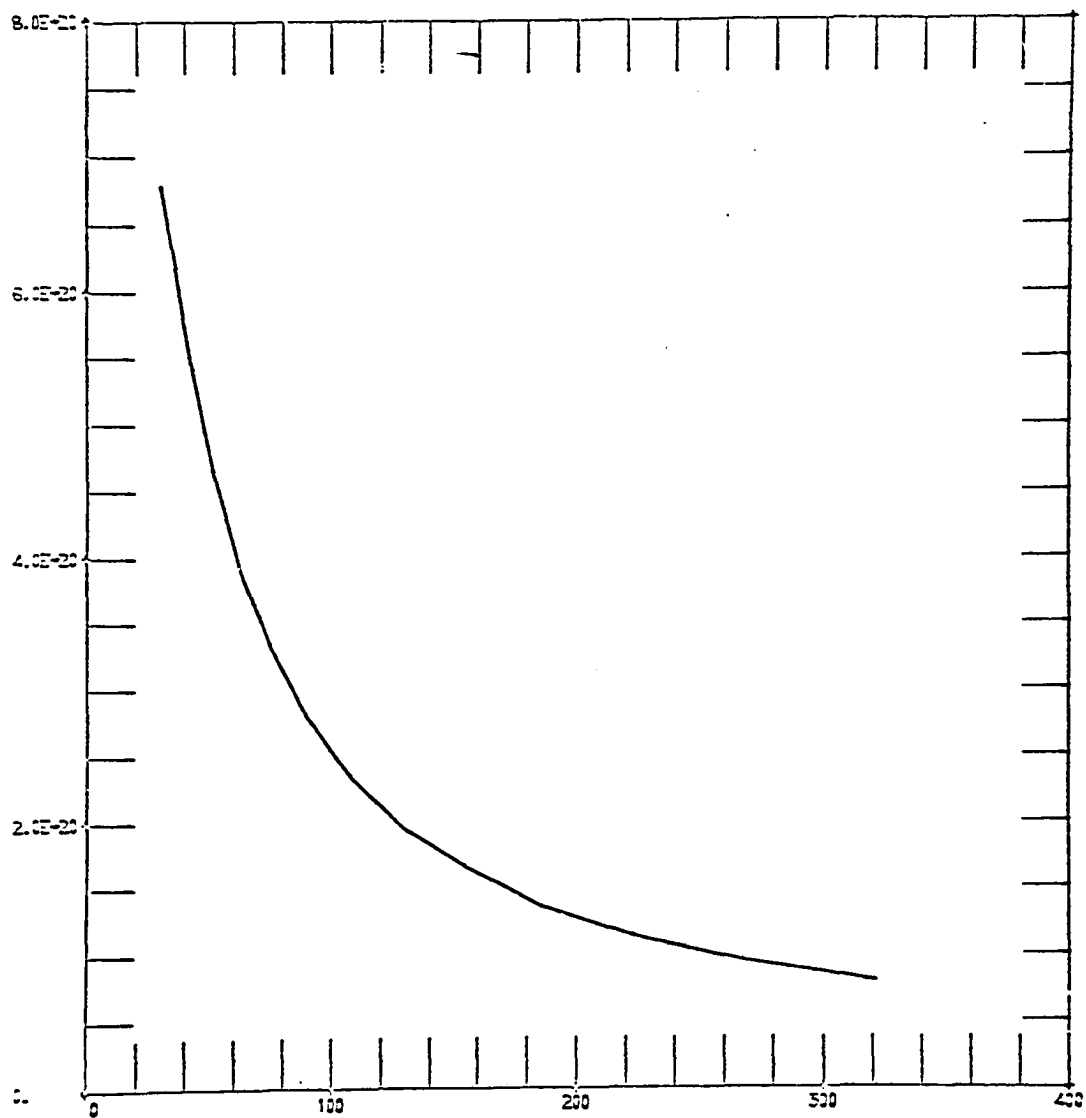


Figure A18. Cross section (cm²) vs Electron Energy (eV)
for the $3s_1''$ state.

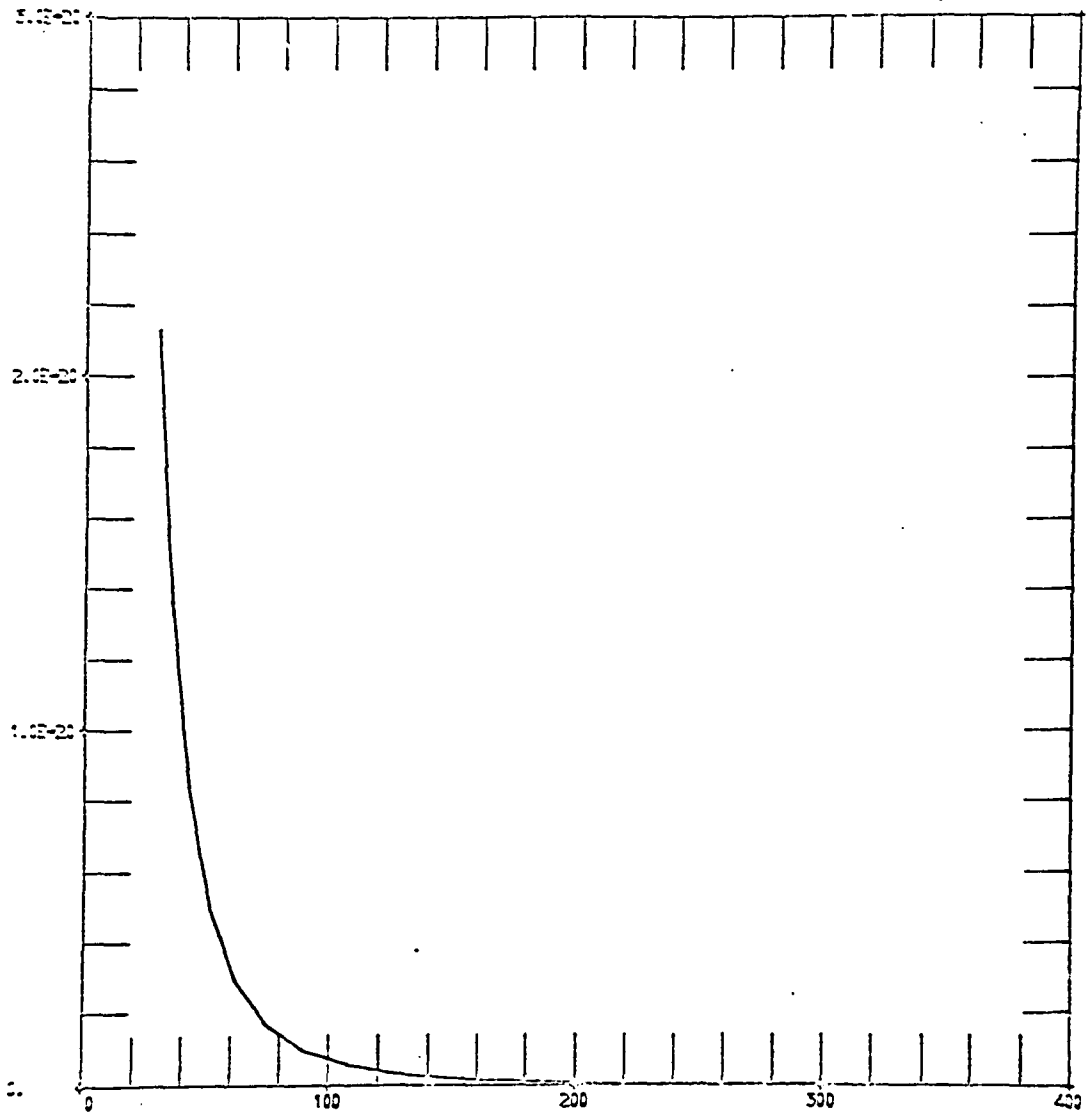


Figure A19. Cross section (cm²) vs Electron Energy (eV)
for the 3d₃ state.

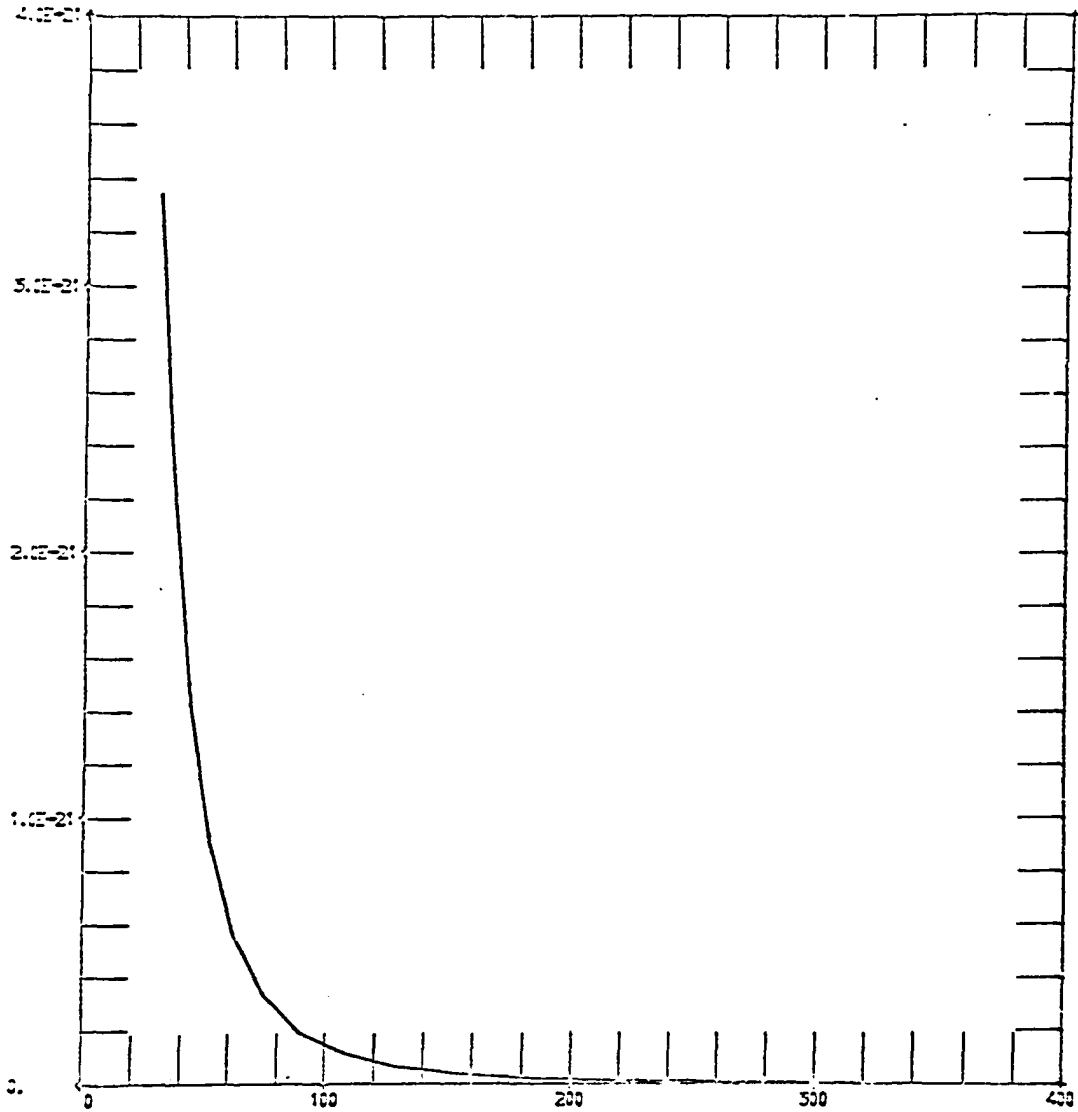


Figure A20. Cross section (cm²) vs Electron Energy (eV)
for the 3d₁'' state.

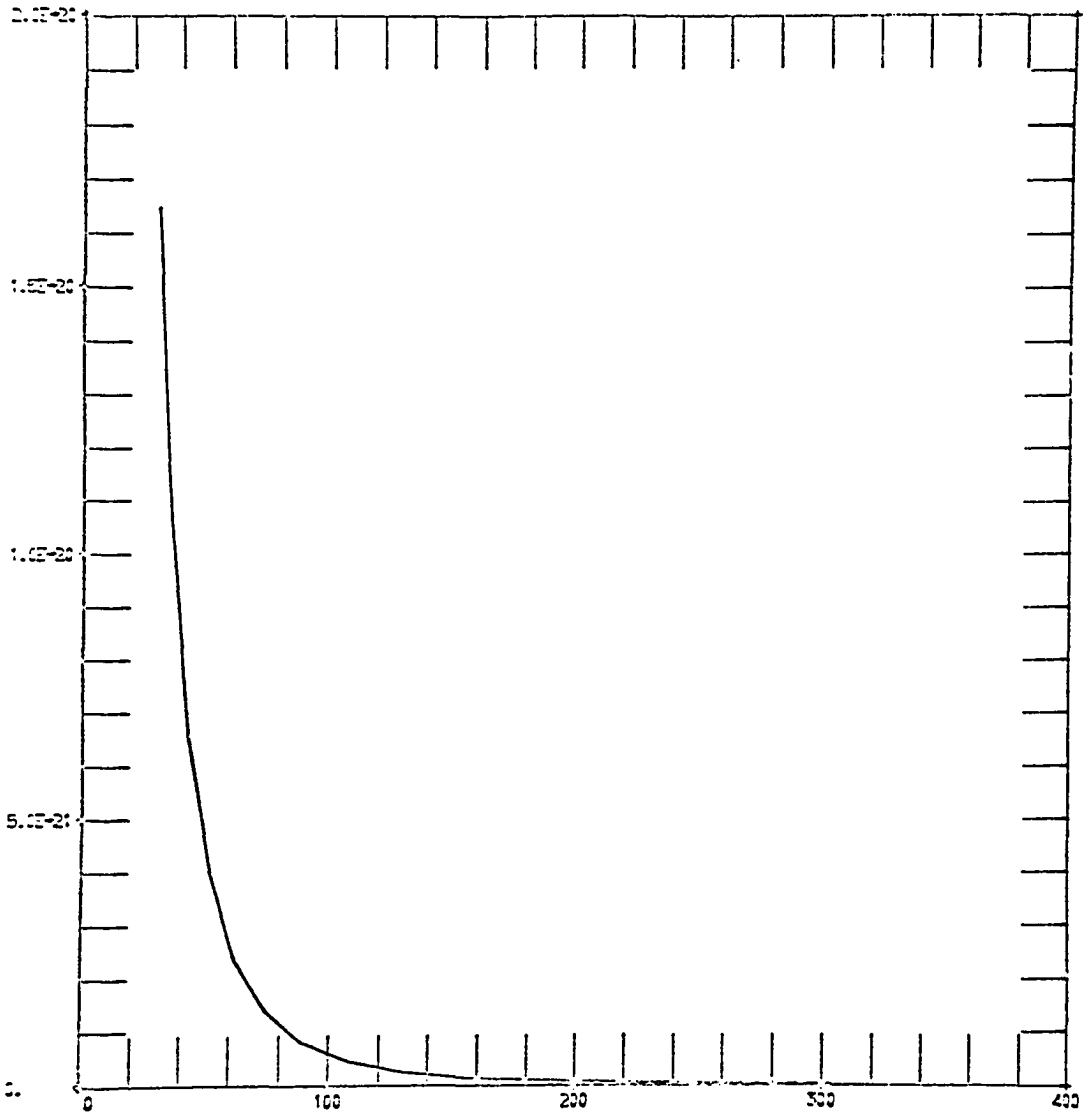


Figure A21. Cross section (cm^2) vs Electron Energy (eV)
for the $3s_1'''$ state.

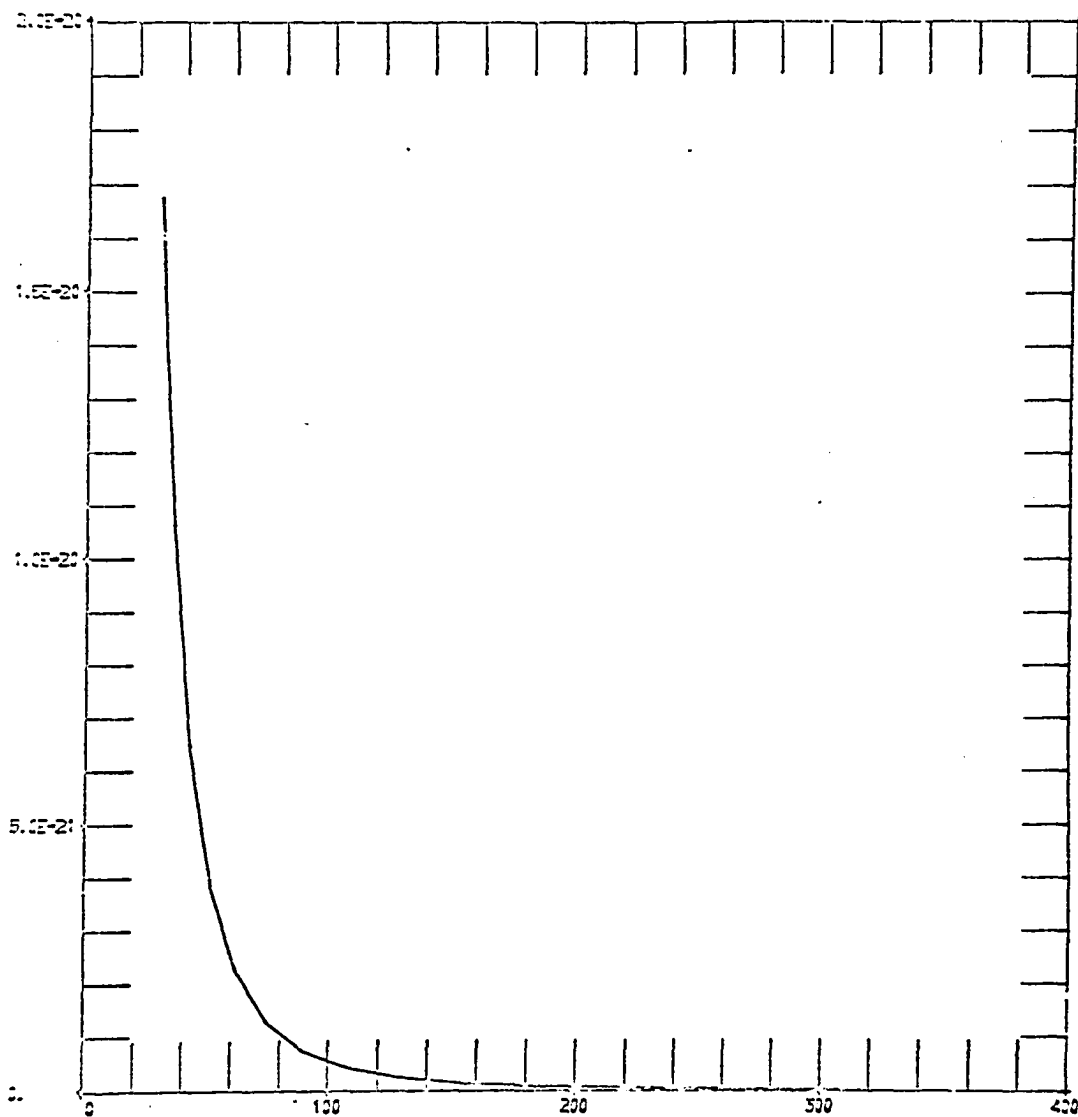


Figure A22. Cross section (cm^2) vs Electron Energy (eV)
for the $3s_1''$ state.

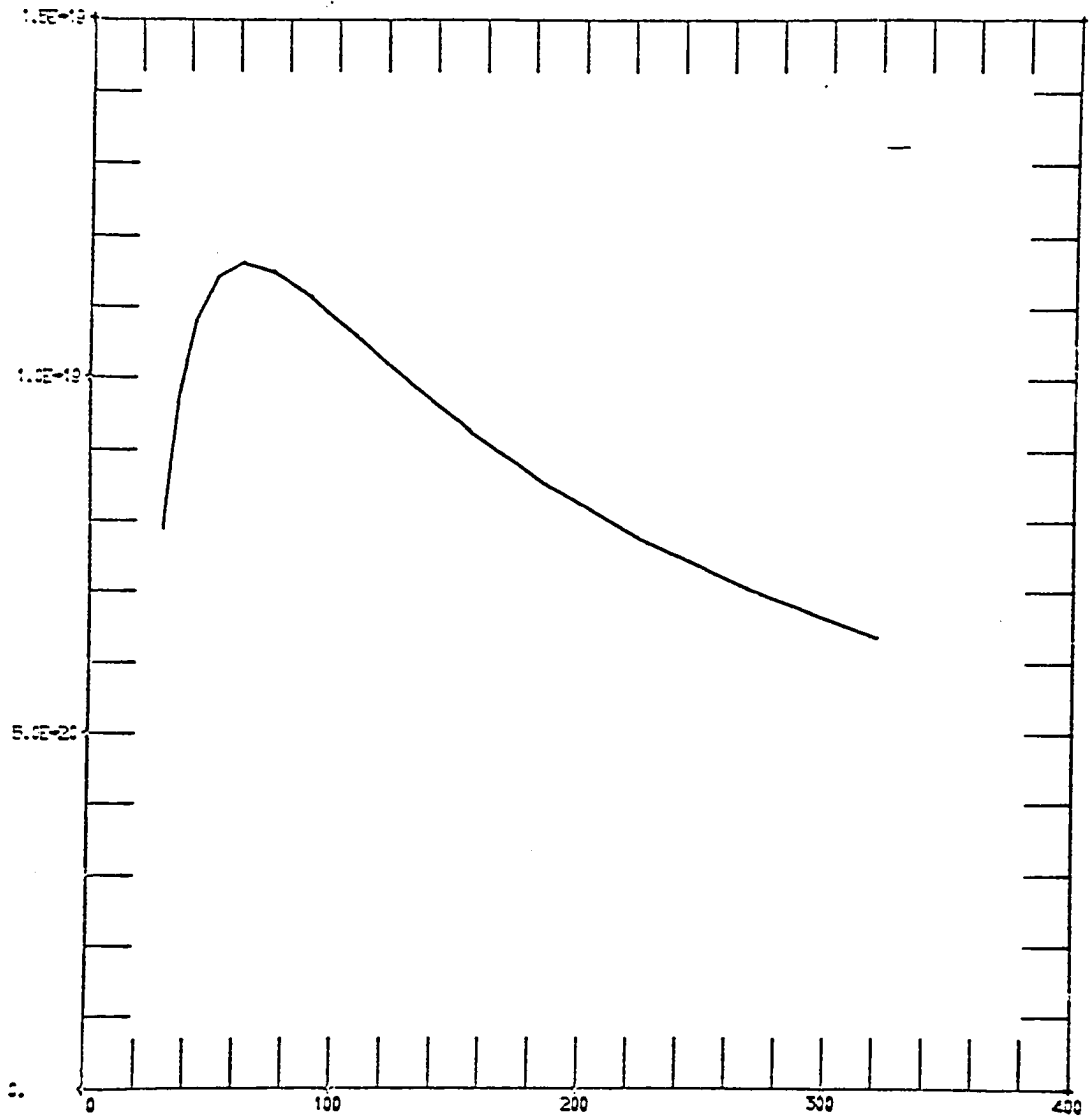


Figure A23. Cross section (cm²) vs Electron Energy (eV)
for the 3d₅ state.

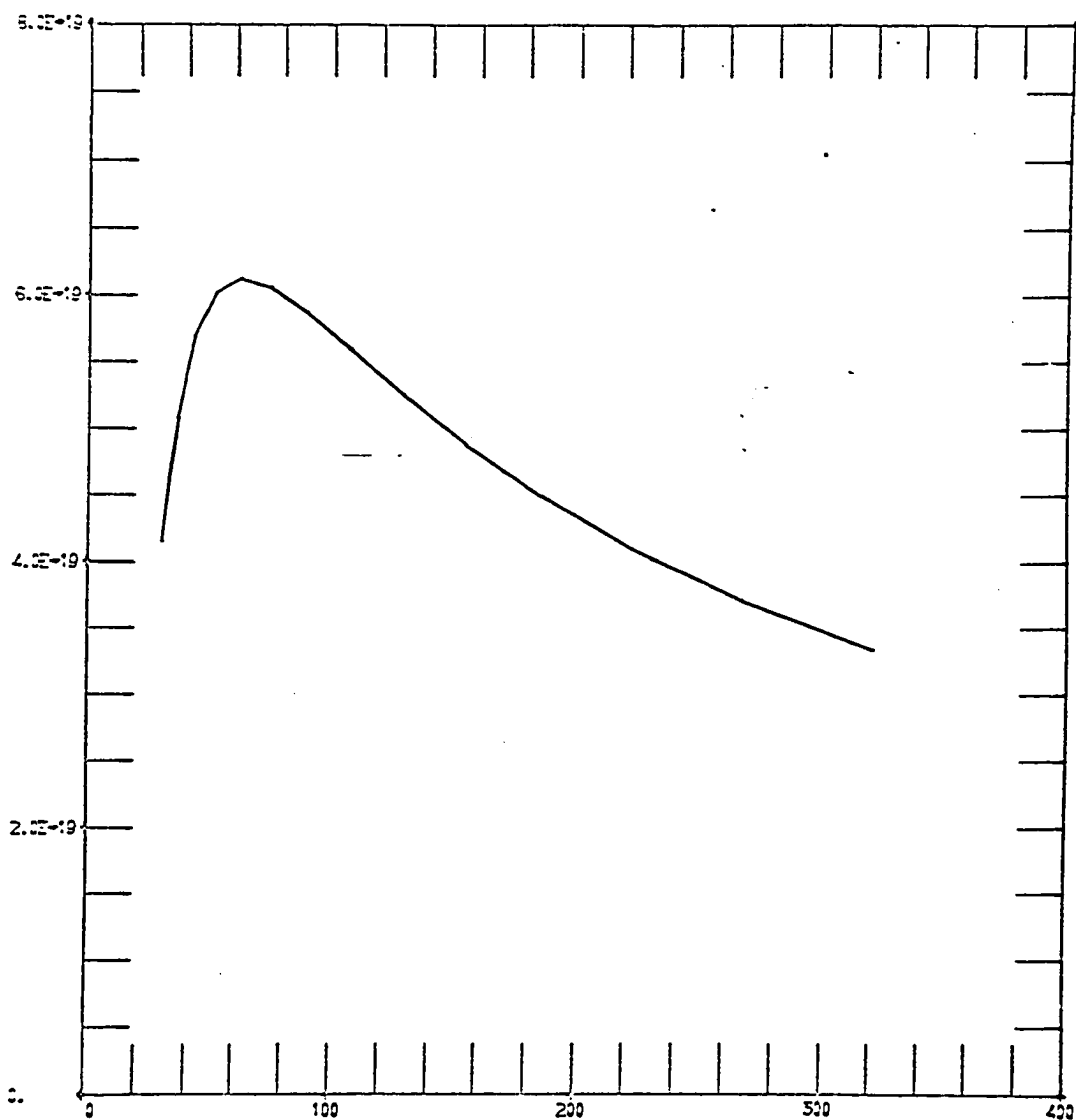


Figure A24. Cross section (cm²) vs Electron Energy (eV)
for the $3d_2$ state.

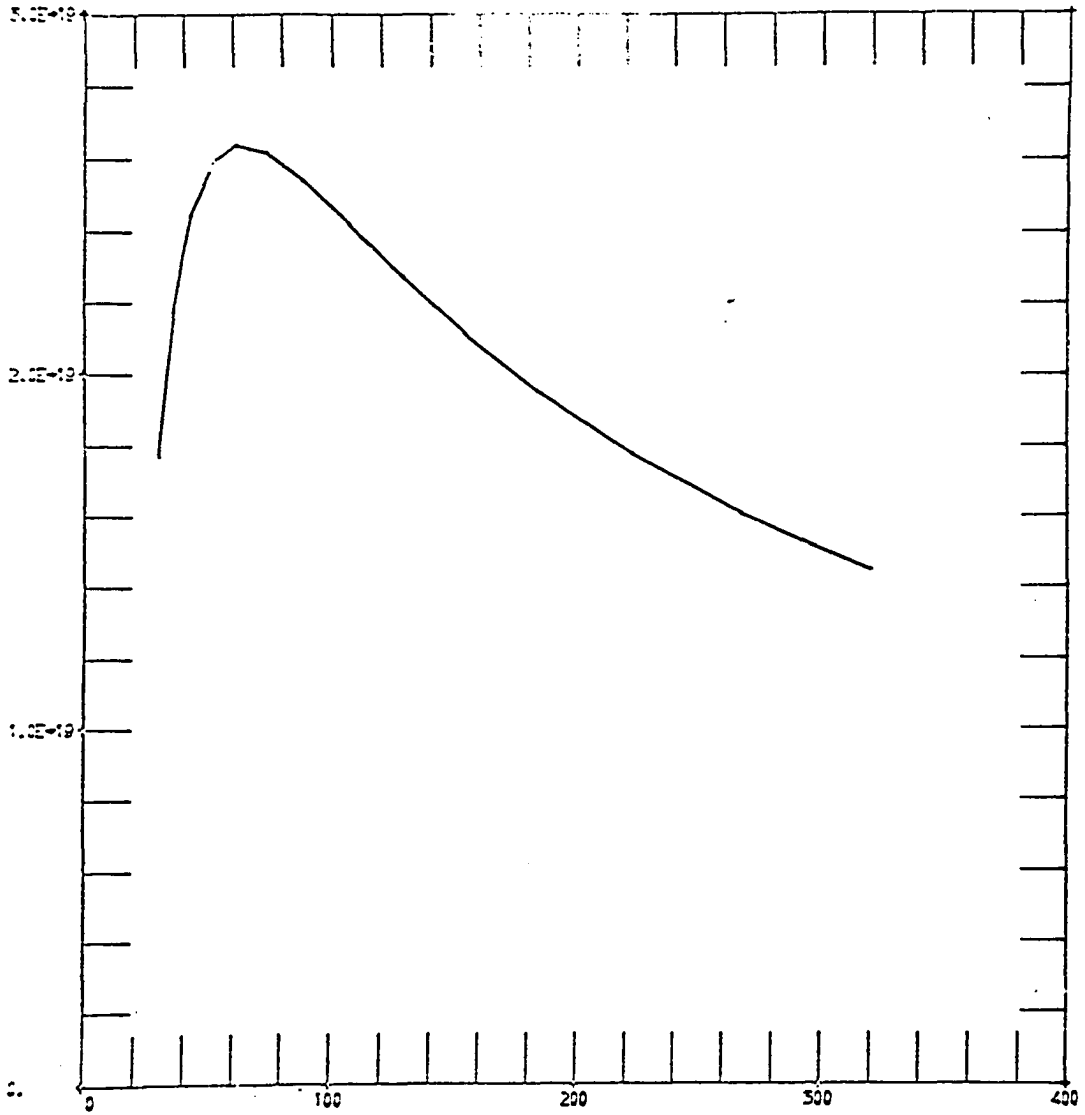


Figure A25. Cross section (cm²) vs Electron Energy (eV)
for the 3s₁ state.

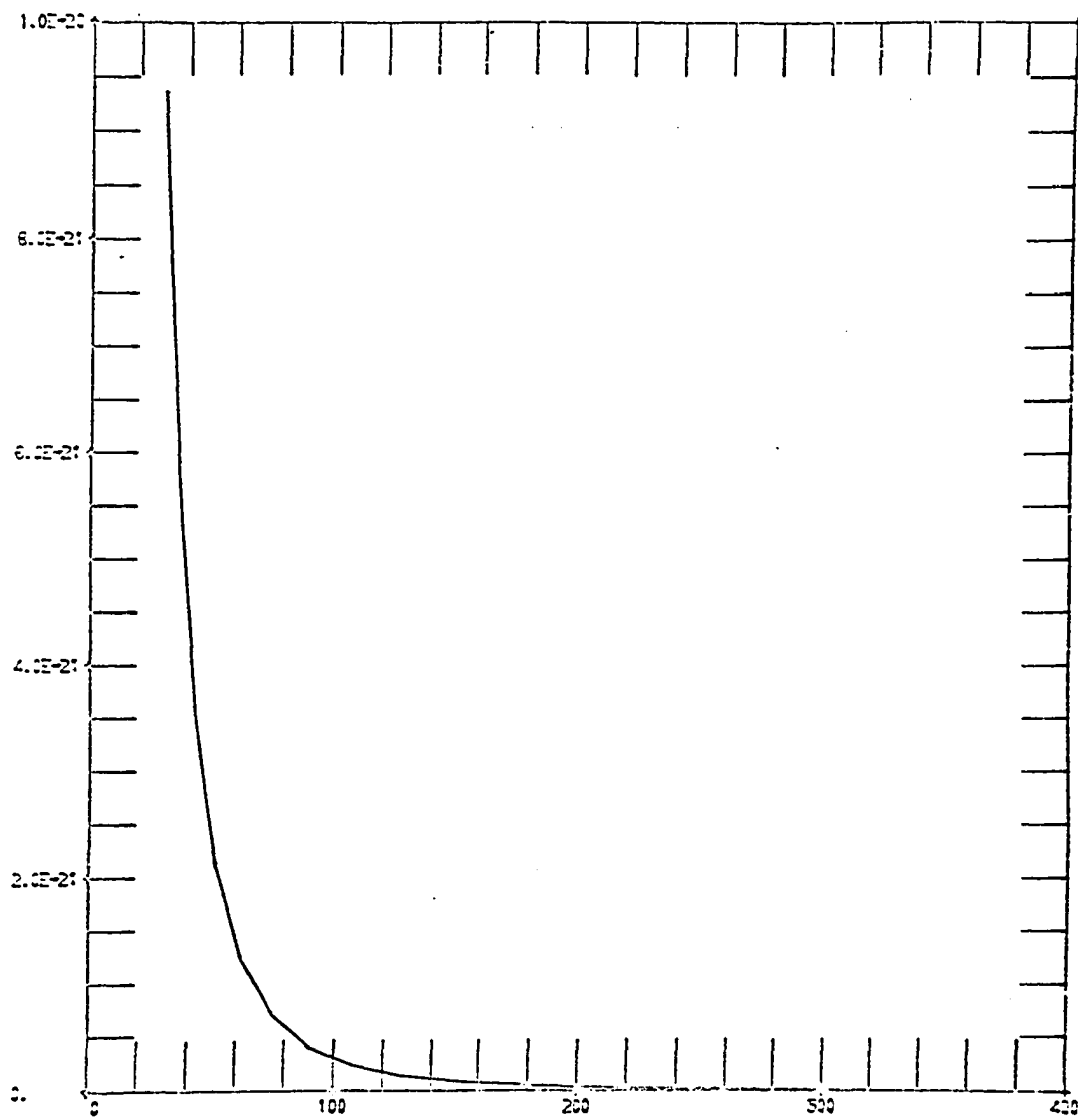


Figure A26. Cross section (cm²) vs Electron Energy (eV)
for the 3d₆ state.

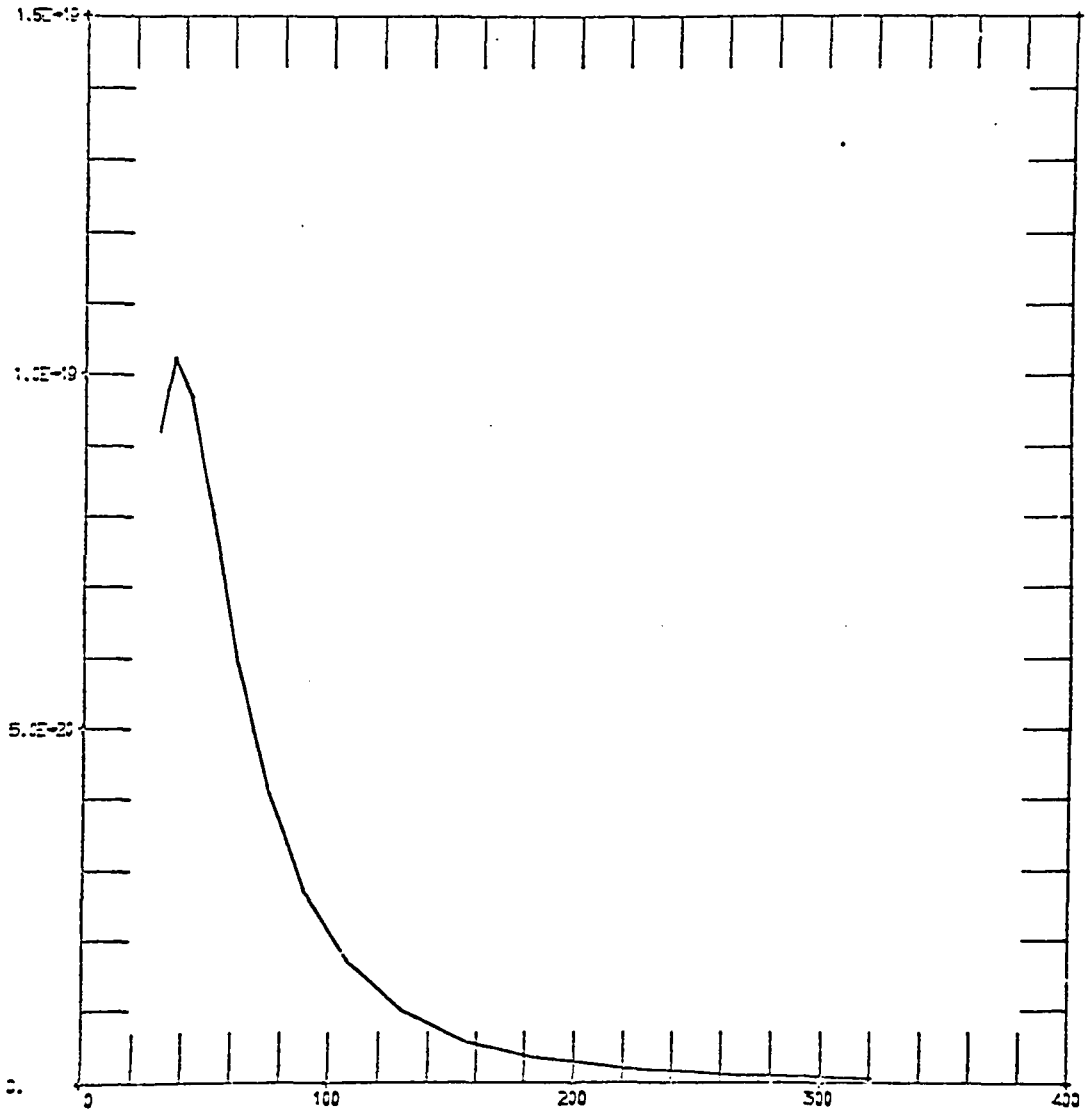


Figure A27. Cross section (cm²) vs Electron Energy (eV)
for the 2s₅ state.

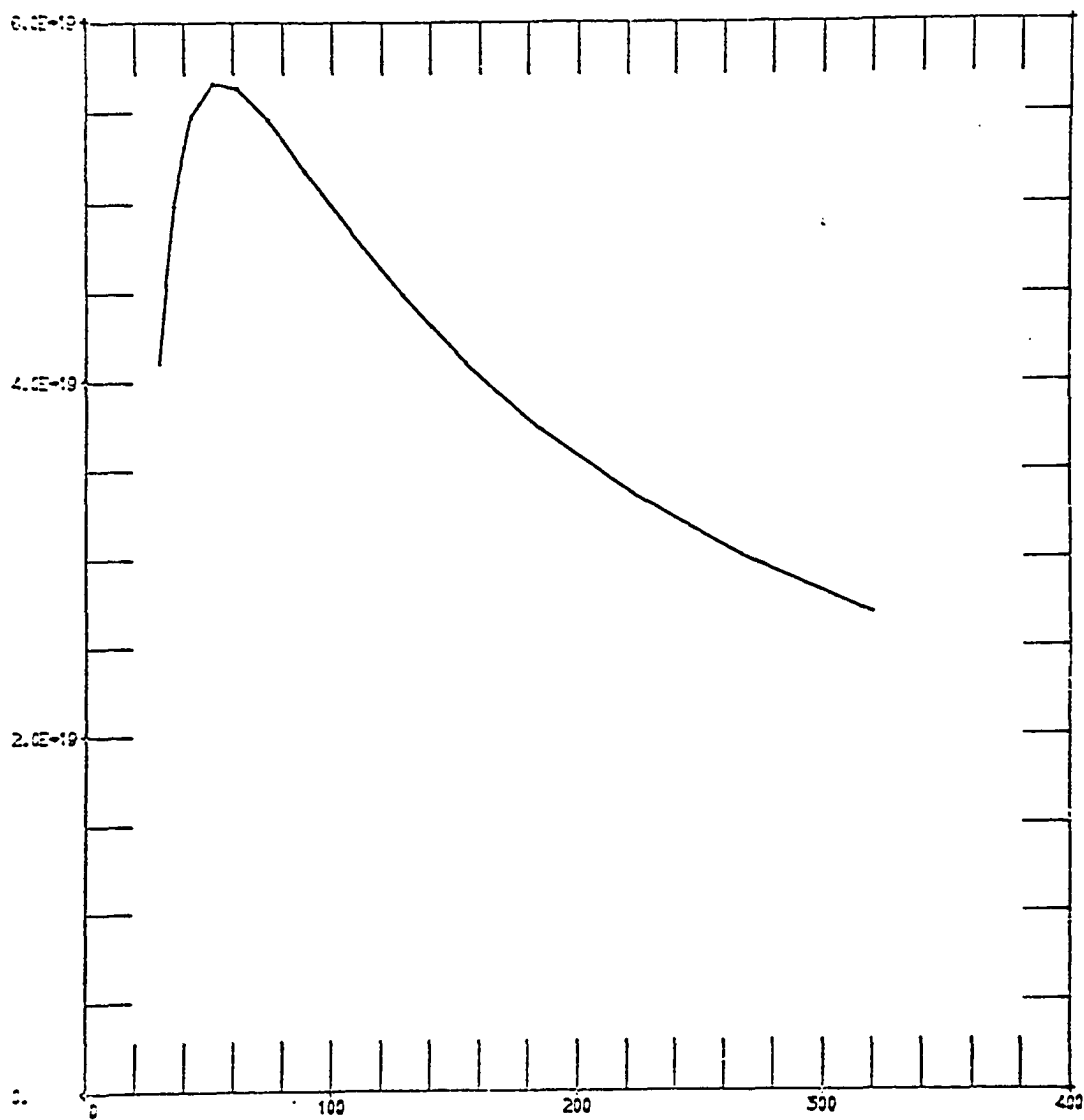


Figure A28. Cross section (cm²) vs Electron Energy (eV)
for the 2s₄ state.

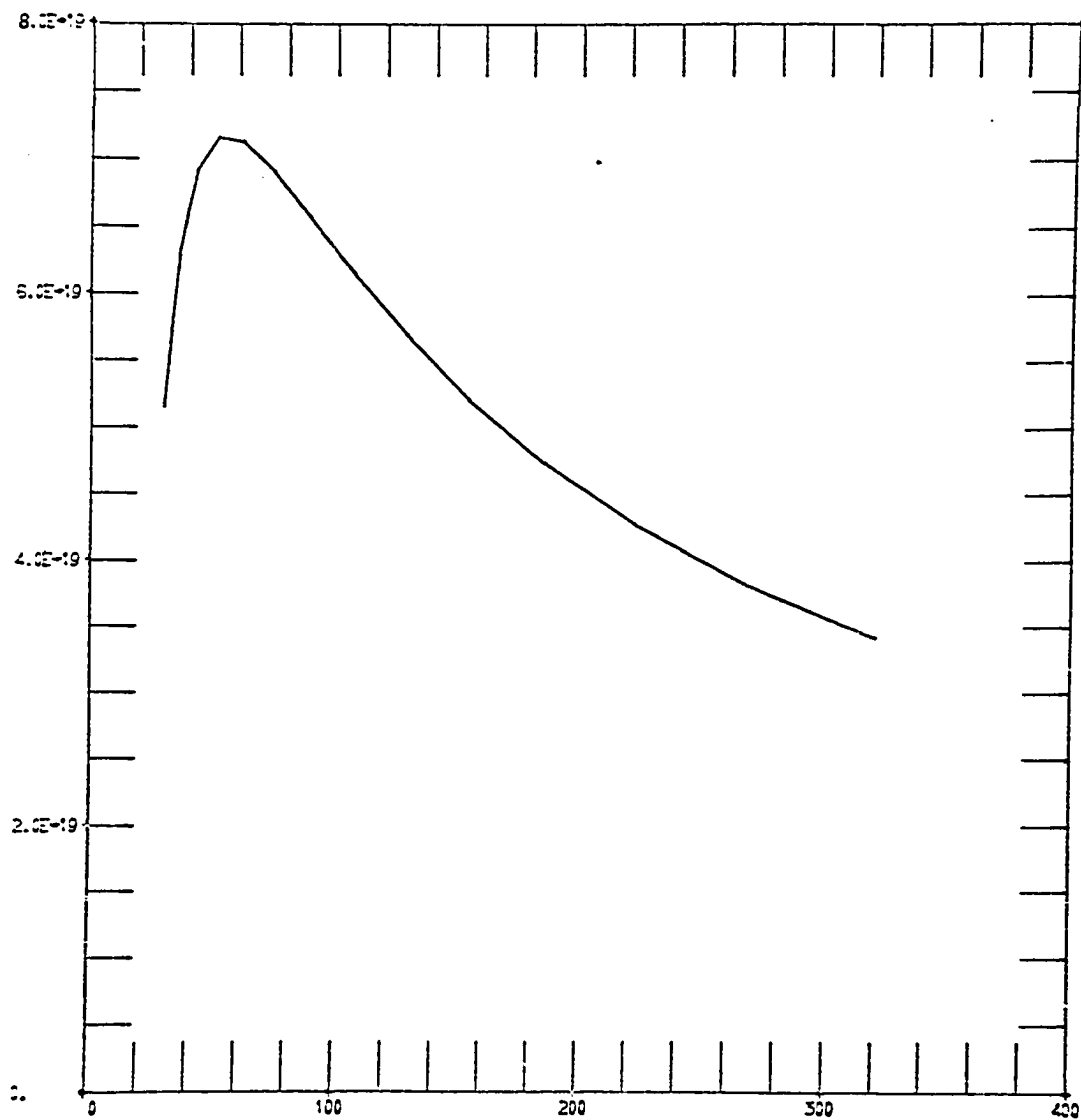


Figure A29. Cross section (cm²) vs Electron Energy (eV)
for the 2s₂ state.

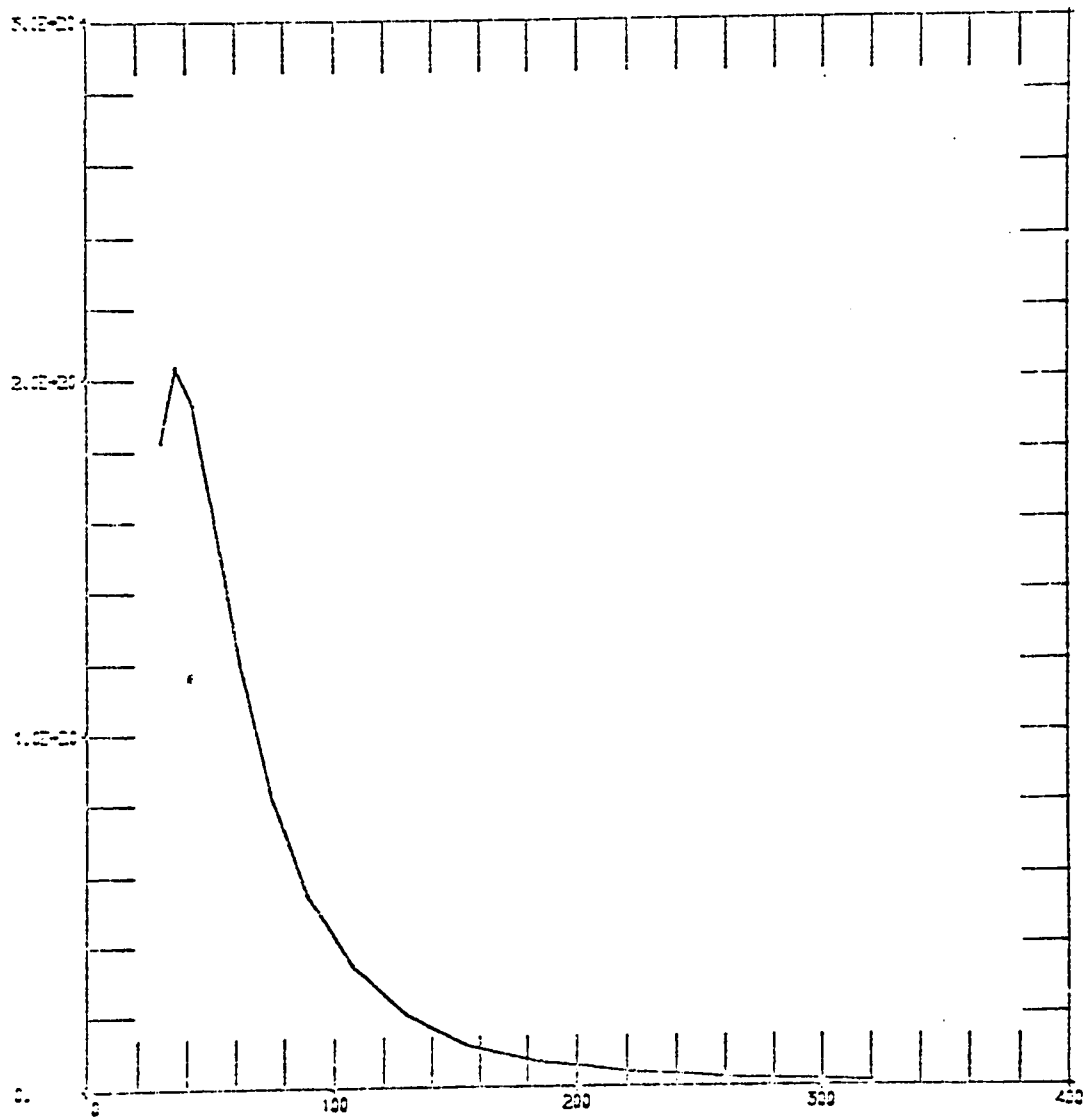


Figure A30. Cross section (cm²) vs Electron Energy (eV)
for the 2s₃ state.